18.354 Nonlinear Dynamics II: Continuum Systems

Spring 2015 Lecture Notes

Instructor: Jörn Dunkel

Authors of Lecture Notes: Michael Brenner, Tom Peacock, Roman Stocker, Pedro Reis, Jörn Dunkel

Contents

1 Math basics

1.1 Derivatives and differential equations

In this course, we will mostly deal with ordinary differential equations (ODEs) and partial differential equations (PDEs) real-valued scalar or vector fields. Usually, non-bold symbols will be reserved for scalar objects f (e.g., mass density) and bold font $\boldsymbol{f} = (f_1, f_2, \ldots)$ for vector-valued objects, such as time-dependent position vectors $\boldsymbol{x}(t)$ or velocity fields $\boldsymbol{v}(t, \boldsymbol{x}) = (v_1(t, \boldsymbol{x}), v_2(t, \boldsymbol{x}), \ldots)$.

ODEs are equations that contain derivatives of scalar or vector-valued or, more generally, tensor-valued functions $f(x)$ of a single variable x. Depending on context, we will denote derivatives of such functions by

$$\frac{df}{dt} = \dot{f} = f' = f_x \tag{1}$$

PDEs are equations that contain derivatives of scalar or vector-valued functions $f(x_1, x_2, \ldots)$ of more than one variable. Depending on context, we will denote partial derivatives by

$$\frac{\partial f}{\partial x_i} = \partial_{x_i} f = \partial_i f = f_{x_i} = f_{,i} \tag{2}$$

In standard 3D Cartesian coordinates (x_1, x_2, x_3) defined with respect to some global orthonormal frame Σ, spanned by the basis vectors $(\boldsymbol{e}_1, \boldsymbol{e}_2, \boldsymbol{e}_3)$, the gradient-operator ∇ is defined by

$$\nabla = \partial_x \boldsymbol{e}_1 + \partial_y \boldsymbol{e}_2 + \partial_z \boldsymbol{e}_3 = \sum_{i=1}^{3} \partial_i \boldsymbol{e}_i \equiv \partial_i \boldsymbol{e}_i, \tag{3}$$

where we have introduced the Einstein summation convention on the rhs. Applying ∇ to a scalar function f gives a vector

$$\nabla f = (\partial_1 f, \partial_2 f, \ldots) \tag{4}$$

whereas application of ∇ to a tensorial quantity depends on the choice of the product: For instance, in the case of a 3D vector field $\boldsymbol{v}(t, \boldsymbol{x})$, we can obtain a scalar field called *divergence*

$$\nabla \cdot \boldsymbol{v} \equiv \partial_i v_i, \tag{5a}$$

another (pseudo-)vector field called *curl*

$$\nabla \wedge \boldsymbol{v} \equiv (\epsilon_{ijk} \partial_j v_k) \tag{5b}$$

and the *gradient* matrix

$$\nabla \boldsymbol{v} \equiv (\partial_i v_j). \tag{5c}$$

The (scalar) Laplacian operator $\triangle$ in Cartesian coordinates is defined by

$$\triangle \equiv \nabla^2 \equiv \sum_i \partial_i \partial_i = \partial_{ii}. \tag{6}$$

Please recall how these operators look in cylindrical and spherical coordinates.

1.2 Linear and nonlinear objects

A mathematical operator - or, more generally, some property – $\mathcal{P}$ defined on vectors or functions f, g, is said to be *linear*, if it satisfies

$$\mathcal{P}(\alpha f + \beta g) = \alpha \mathcal{P}(f) + \beta \mathcal{P}(g) \tag{7}$$

Important examples are derivatives, integrals and expectation values.

A famous linear ODE, is the simple harmonic oscillator equation

$$\ddot{x}(t) = -\omega^2 x(t) \tag{8}$$

which has fundamental sin- and cos-solutions, that can be used to construct more general solutions by superposition.

An important (homogeneous) linear PDE, is Laplace's equation

$$\nabla^2 f(t, \boldsymbol{x}) = 0. \tag{9}$$

Functions f satisfying this equation are called *harmonic*.

Later on, we will often try to approximate nonlinear PDEs through linear PDEs.

1.3 Complex numbers and functions

Although we will mostly deal with real fields in this course, it is sometimes helpful to rewrite equations in terms of complex quantities, especially, when dealing with 2D hydrodynamic problems. Complex numbers are 2D extensions of real numbers,

$$z = x + iy \in \mathbb{C}, \qquad i^2 = -1 \tag{10}$$

with real part $\Re z = x \in \mathbb{R}$ and imaginary part $\Im z = y \in \mathbb{R}$. The complex conjugate of a real number is given by

$$\bar{z} = x - iy \tag{11}$$

and corresponds to a reflection at the real axis or, equivalently, at the line $\Im(z) = 0$.

Addition of complex numbers is linear

$$z = z_1 + z_2 = (x_1 + iy_1) + (x_2 + iy_2) = (x_1 + x_2) + i(y_1 + y_2) = x + iy \tag{12}$$

corresponding to the addition of the two 2D vectors (x_1, y_1) and (x_2, y_2). In contrast, complex multiplication mixes real and imaginary parts

$$z = z_1 z_2 = (x_1 + iy_1)(x_2 + iy_2) = (x_1 x_2 - y_1 y_2) + i(x_1 y_2 + y_1 x_2) = x + iy \tag{13}$$

A complex function is a map

$$f : \mathbb{C} \to \mathbb{C}, \qquad f(z) = (u(x, y), v(x, y)) \tag{14}$$

that can be interpreted as a map from $\mathbb{R}^2 \to \mathbb{R}^2$. A function f is said to be complex differentiable (or *analytic* or *holomorphic*) if it satisfies the Cauchy-Riemann equations

$$\partial_x u = \partial_y v, \qquad \partial_y u = -\partial_x v \tag{15a}$$

By differentiating again, we find

$$\partial_x^2 u = \partial_x \partial_y v = -\partial_y^2 u = 0 \tag{15b}$$

$$\partial_y^2 v = \partial_y \partial_x u = -\partial_x^2 v = 0; \tag{15c}$$

$$\tag{15d}$$

this means that analytic functions $f = (u, v)$ are harmonic

$$\nabla^2 f = 0. \tag{15e}$$

An analytic function that we will frequently encounter is the exponential function

$$\exp(z) = \sum_{k=0}^{\infty} \frac{z^n}{k!} = 1 + z + \frac{z}{2!} + \dots \tag{16}$$

Euler's formula

$$e^{i\phi} = \cos\phi + i\sin\phi \,, \qquad \phi \in \mathbb{R} \tag{17}$$

relates exp to the trigonometric sin-and cos-functions.

When dealing with axisymmetric problems it is often advantageous to use the polar representation of a complex number

$$z = re^{i\phi} \,, \qquad r = |z| = \sqrt{z\bar{z}} \in \mathbb{R}_0^+ \,, \,, \qquad \phi = \arctan 2(y, x) \in [0, 2\pi) \tag{18}$$

From the properties of the exp-function, it follows that the multiplication of complex numbers

$$z = z_1 z_2 = r_1 e^{i\phi_1} r_2 e^{i\phi_2} = r_1 r_2 e^{i(\phi_1 + \phi_2)} \tag{19}$$

corresponds to a combined rotation and dilatation.

1.4   Fourier transforms

The Fourier transform of a function $f(t)$ is defined by

$$\hat{f}(\omega) = \frac{1}{\sqrt{2\pi}} \int_{-\infty}^{\infty} dt \, e^{i\omega t} \, f(t), \tag{20a}$$

its the inverse is given by

$$f(t) = \frac{1}{\sqrt{2\pi}} \int_{-\infty}^{\infty} d\omega \, e^{-i\omega t} \, \hat{f}(\omega) \tag{20b}$$

In particular, for the Dirac delta-function $\delta(t)$

$$\hat{\delta}(\omega) = \frac{1}{\sqrt{2\pi}} \int_{-\infty}^{\infty} dt \, e^{i\omega t} \, \delta(t) = \frac{1}{\sqrt{2\pi}}, \tag{21}$$

yielding the useful Fourier representation

$$\delta(t) = \frac{1}{2\pi} \int_{-\infty}^{\infty} d\omega \, e^{-i\omega t} \tag{22}$$

These definitions and properties extend directly to higher dimensions.

A main advantage of Fourier transformations is that they translate differential equations into simpler algebraic equations.

2   Dimensional analysis

Before moving on to more 'sophisticated things', let us think a little about dimensional analysis and scaling. On the one hand these are trivial, and on the other they give a simple method for getting answers to problems that might otherwise be intractable. The idea behind dimensional analysis is very simple: *Any physical law must be expressible in any system of units that you use.* There are two consequences of this:

- One can often guess the answer just by thinking about what the dimensions of the answer should be, and then expressing the answer in terms of quantities that are known to have those dimensions[1].

- The scientifically interesting results are *always* expressible in terms of quantities that are *dimensionless*, not depending on the system of units that you are using.

One example of a dimensionless number relevant for fluid dynamics that we have already encountered in the introductory class is the *Reynolds number*, which quantifies the relative strength of viscous and inertial forces. Another example of dimensional analysis that we will study in detail is the solution to the diffusion equation for the spreading of a point source. The only relevant physical parameter is the diffusion constant D, which has dimensions of $L^2 T^{-1}$. We denote this by writing $[D] = L^2 T^{-1}$. Therefore the characteristic scale over which the solution varies after time t must be $\sqrt{Dt}$. This might seem like a rather simple result, but it expresses the essence of solutions to the diffusion equation. Of course, we will be able to solve the diffusion equation exactly, so this argument wasn't really necessary. In practice, however, we will rarely find useful exact solutions to the Navier-Stokes equations, and so dimensional analysis will often give us insight before diving into the mathematics or numerical simulations. Before formalising our approach, let us consider a few examples where simple dimensional arguments intuitively lead to interesting results.

2.1   The pendulum

This is a trivial problem that you know quite well. Consider a pendulum with length L and mass m, hanging in a gravitational field of strength g. What is the period of the pendulum? We need a way to construct a quantity with units of time involving these numbers. The only possible way to do this is with the combination $\sqrt{L/g}$. Therefore, we know immediately that

$$\tau = c\sqrt{L/g}. \tag{23}$$

This result might seem trivial to you, as you will probably remember (e.g., from a previous course) that $c = 2\pi$, if one solves the full dynamical problem for for small amplitude oscillations. However, the above formula works even for large amplitude oscillations.

2.2   Pythagorean theorem

Now we try to prove the Pythagorean theorem by dimensional analysis. Suppose you are given a right triangle, with hypotenuse length L and smallest acute angle ϕ. The area of

---

[1]Be careful to distinguish between *dimensions* and *units*. For example mass (M), length (L) and time (T) are dimensions, and they can have different units of measurement (e. g. length may be in feet or meters)

the triangle is clearly

$$A = A(L, \phi). \tag{24}$$

Since ϕ is dimensionless, it must be that

$$A = L^2 f(\phi), \tag{25}$$

where f is some function we don't know.

Now the triangle can be divided into two little right triangles by dropping a line from the right angle which is perpendicular to the hypotenuse. The two right triangles have hypotenuses that happen to be the other two sides of our original right triangle, let's call them a and b. So we know that the areas of the two smaller triangles are $a^2 f(\phi)$ and $b^2 f(\phi)$ (where elementary geometry shows that the acute angle ϕ is the same for the two little triangles as the big triangle). Moreover, since these are all right triangles, the function f is the same for each. Therefore, since the area of the big triangle is just the sum of the areas of the little ones, we have

$$L^2 f = a^2 f + b^2 f,$$

or

$$L^2 = a^2 + b^2. \tag{26}$$

2.3   The gravitational oscillation of a star

It is known that the sun, and many other stars undergo some mode of oscillation. The question we might ask is how does the frequency of oscillation ω depend on the properties of that star? The first step is to identify the physically relevant variables. These are the density ρ, the radius R and the gravitational constant G (as the oscillations are due to gravitational forces). So we have

$$\omega = \omega(\rho, R, G). \tag{27}$$

The dimensions of the variables are $[\omega] = T^{-1}$, $[\rho] = ML^{-3}$, $[R] = L$ and $[G] = M^{-1}L^3T^{-2}$. The only way we can combine these to give as a quantity with the dimensions of time, is through the relation

$$\omega = c\sqrt{G\rho}. \tag{28}$$

Thus, we see that the frequency of oscillation is proportional to the square root of the density and independent of the radius. The determination of c requires a real stellar observation, but we have already determined a lot of interesting details from dimensional analysis alone. For the sun, $\rho = 1400 \text{kg/m}^3$, giving $\omega \sim 3 \times 10^{-4}\text{s}^{-1}$. The period of oscillation is approximately 1 hour, which is reasonable. However, for a neutron star ($\rho = 7 \times 10^{11}\text{kgm}^{-3}$) we predict $\omega \sim 7000\text{s}^{-1}$, corresponding to a period in the milli-second range.

2.4   The oscillation of a droplet

What happens if instead of considering a large body of fluid, such as a star, we consider a smaller body of fluid, such as a raindrop. Well, in this case we argue that surface tension γ

provides the relevant restoring force and we can neglect gravity. γ has dimensions of energy/area, so that $[\gamma] = MT^{-2}$. The only quantity we can now make with the dimensions of T^{-1} using our physical variables is

$$\omega = c\sqrt{\frac{\gamma}{\rho R^3}}, \tag{29}$$

which is not independent of the radius. For water $\gamma = 0.07\text{Nm}^{-1}$ giving us a characteristic frequency of 3Hz for a raindrop.

One final question we might ask ourselves before moving on is how big does the droplet have to be for gravity to have an effect? We reason that the crossover will occur when the two models give the same frequency of oscillation. Thus, when

$$\sqrt{\rho G} = \sqrt{\frac{\gamma}{\rho R^3}} \tag{30}$$

we find that

$$R_c \sim \left(\frac{\gamma}{\rho^2 G}\right)^{\frac{1}{3}} \tag{31}$$

This gives a crossover radius of about 10m for water.

2.5 Water waves

This is a subject we will deal with in greater detail towards the end of the course, but for now we look to obtain a basic understanding of the motion of waves on the surface of water. For example, how does the frequency of the wave depend on the wavelength λ? This is called the *dispersion relation*.

If the wavelength is long, we expect gravity to provide the restoring force, and the relevant physical variables in determining the frequency would appear to be the mass density ρ, the gravitational acceleration g and the wave number $k = 2\pi/\lambda$. The dimensions of these quantities are $[\rho] = ML^{-3}$, $[g] = LT^{-2}$ and $[k] = L^{-1}$. We can construct a quantity with the dimensions of T^{-1} through the relation

$$\omega = c\sqrt{gk}. \tag{32}$$

We see that the frequency of water waves is proportional to the square root of the wavenumber, in contrast to light waves for which the frequency is proportional to the wavenumber.

As with a droplet, we might worry about the effects of surface tension when the wavelength gets small. In this case we replace g with γ in our list of physically relevant variables. Given that $[\gamma] = MT^{-2}$, the dispersion relation must be of the form

$$\omega = c\sqrt{\gamma k^3/\rho}, \tag{33}$$

which is very different to that for gravity waves. If we look for a crossover, we find that the frequencies of *gravity waves* and *capillary waves* are equal when

$$k \sim \sqrt{\rho g/\gamma}. \tag{34}$$

This gives a wavelength of 1cm for water waves.

3 Dimensionless groups

A formal justification of the dimensional analysis approach in the previous section comes from Buckingham's Pi Theorem. Consider a physical problem in which the dependent parameter is a function of $n-1$ independent parameters, so that we may express the relationship among the variables in functional form as

$$q_1 = g(q_2, q_3, ..., q_n), \tag{35a}$$

where q_1 is the dependent parameter, and $q_2, ..., q_n$ are the $n-1$ independent parameters. Mathematically, we can rewrite the functional relationship in the equivalent form

$$0 = f(q_1, q_2, ..., q_n). \tag{35b}$$

where $f = q_1 - g(q_2, q_3, ..., q_n)$. For example, for the period of a pendulum we wrote $\tau = \tau(l, g, m)$, but we could just as well have written $f(\tau, l, g, m) = 0$. The Buckingham Pi theorem states that given a relation of the form (35), the n parameters may be grouped into $n-d$ *independent dimensionless* ratios, or dimensionless groups Π_i, expressible in functional form by

$$\Pi_1 = G(\Pi_2, \Pi_3, ..., \Pi_{n-d}), \tag{36a}$$

or, equivalently,

$$0 = F(\Pi_1, \Pi_2, ..., \Pi_{n-d}), \tag{36b}$$

where d is the number of independent dimensions (mass, length, time...). The formal proof can be found in the book *Scaling, Self Similarity and Intermediate Asymptotics* by Barenblatt. The Pi theorem does not predict the functional form of F or G, and this must be determined experimentally. The $n-d$ dimensionless groups Π_i are independent. A dimensionless group Π_i is *not* independent if it can be formed from a product or quotient of other dimensionless groups in the problem.

3.1 The pendulum

To develop an understanding of how to use Buckingham's Pi theorem, let's first apply it to the problem of a swinging pendulum, which we considered in the previous lecture. We argued that the period of the pendulum τ depends on the length l and gravity g. It cannot depend on the mass m since we cannot form a dimensionless parameter including m in our list of physical variables. Thus

$$\tau = \tau(l, g), \tag{37a}$$

or alternatively

$$0 = f(\tau, l, g). \tag{37b}$$

We have $n = 3$ and $d = 2$, so the problem has one dimensionless group

$$\Pi_1 = \tau l^\alpha g^\beta. \tag{38}$$

The relevant dimensions are $[\tau] = T, [l] = L, [g] = LT^{-2}$, so for Π_1 to be dimensionless equate the exponents of the dimension to find

$$
\begin{aligned}
1 - 2\beta &= 0, \\
\alpha + \beta &= 0,
\end{aligned}
$$

12

which are satisfied if $\alpha = -\frac{1}{2}$ and $\beta = \frac{1}{2}$. Thus

$$\Pi_1 = \tau\sqrt{g/l}. \tag{39}$$

We thus see Π_1 is just the constant of proportionality c from above. Thus we have

$$c = \tau\sqrt{g/l} \tag{40}$$

where c is a constant to be determined from an experiment.

3.2   Taylor's blast

This is a famous example, of some historical and fluid mechanical importance. The story goes something like this. In the early 1940's there appeared a picture of an atomic blast on the cover of Life magazine. GI Taylor, a fluid mechanician at Cambridge, wondered what the energy of the blast was. When he called his colleagues at Los Alamos and asked, they informed him that it was classified information, so he resorted to dimensional analysis. In a nuclear explosion there is an essentially instantaneous release of energy E in a small region of space. This produces a spherical shock wave, with the pressure inside the shock wave several thousands of times greater than the initial air pressure, that can be neglected. How does the radius R of this shock wave grow with time t? The relevant parameters are E, the density of air ρ and time t. Thus

$$R = R(E, \rho, t) \tag{41a}$$

or

$$0 = f(R, E, \rho, t). \tag{41b}$$

The dimensions of the physical variables are $[E] = ML^2T^{-2}, [t] = T, [R] = L$ and $[\rho] = ML^{-3}$. We have $n = 4$ physical variables and $d = 3$ dimensions, so the Pi theorem tells us there is one dimensionless group, Π_1. To form a dimensionless combination of parameters we assume

$$\Pi_1 = Et^\alpha \rho^\beta R^\gamma \tag{42}$$

and equating the exponents of dimensions in the problem requires that

$$\begin{aligned} 1 + \beta &= 0, \\ \alpha - 2 &= 0, \\ 2 - 3\beta + \gamma &= 0. \end{aligned}$$

It follows that $\alpha = 2, \beta = -1$ and $\gamma = -5$, giving

$$\Pi_1 = \frac{Et^2}{\rho R^5}. \tag{43}$$

Assuming that Π_1 is constant gives

$$R = c\left(\frac{E}{\rho}\right)^{\frac{1}{5}} t^{\frac{2}{5}}. \tag{44}$$

13

The relation shows that if one measures the radius of the shock wave at various instants in time, the slope of the line on a log-log plot should be 2/5. The intercept of the graph would provide information about the energy E released in the explosion, if the constant c could be determined. Since information about the development of blast with time was provided by the sequence of photos on the cover of Life magazine, Taylor was able to determine the energy of the blast to be 10^{14} Joules (he estimated c to be about 1 by solving a model shock-wave problem), causing much embarrassment.

3.3 The drag on a sphere

Now what happens if you have two dimensionless groups in a problem? Let's consider the problem of the drag on a sphere. We reason that the drag on a sphere D will depend on the relative velocity, U, the sphere radius, R, the fluid density ρ and the fluid viscosity μ. Thus

$$D = D(U, R, \rho, \mu) \tag{45a}$$

or

$$0 = f(D, U, R, \rho, \mu). \tag{45b}$$

Since the physical variables are all expressible in terms of dimensions M, L and T, we have $n = 5$ and $d = 3$, so there are two dimensionless groups. There is now a certain amount of arbitrariness in determining these, however we look for combinations that make some physical sense. For our first dimensionless group, we choose the Reynolds number

$$\Pi_1 = \frac{\rho U R}{\mu}, \tag{46}$$

as we know that it arises naturally when you nondimensionalise the Navier-Stokes equations. For the second we choose the combination

$$\Pi_2 = D \rho^\alpha U^\beta R^\gamma, \tag{47}$$

which, if we replaced D with μ, would just give the Reynolds number. Equating the exponents of mass length and time gives, $\alpha = -1$, $\beta = -2$ and $\gamma = -2$. Thus

$$\Pi_2 = \frac{D}{\rho U^2 R^2}, \tag{48}$$

and this is called the dimensionless drag force. Buckingham's Pi theorem tells us that we must have the functional relationship

$$\Pi_2 = G(\Pi_1) \tag{49}$$

or alternatively

$$\frac{D}{\rho U^2 R^2} = G(\text{Re}). \tag{50}$$

The functional dependence is determined by experiments. It is found that at high Reynolds numbers $G(\text{Re}) = 1$, so that

$$D = \rho U^2 R^2. \tag{51}$$

14

This is known as form drag, in which resistance to motion is created by inertial forces on the sphere. At low Reynolds numbers $G(\mathrm{Re}) \propto 1/\mathrm{Re}$ so that

$$D \propto \mu U R. \tag{52}$$

This is Stokes drag, caused by the viscosity of the fluid.

The power of taking this approach can now be seen. Without dimensional analysis, to determine the functional dependence of the drag on the relevant physical variables would have required four sets of experiments to determine the functional dependence of D on velocity, radius, viscosity and density. Now we need only perform one set of experiments using our dimensionless parameters and we have all the information we need.

4 Kepler's problem and Hamiltonian dynamics

Why do we study applied mathematics? Aside from the intellectual challenge, it is reasonable to argue that we do so to obtain an understanding of physical phenomena, and to be able to make predictions about them. Possibly the greatest example of this, and the origin of much of the mathematics we do, came from Newton's desire to understand the motion of the planets, which were known to obey Kepler's laws.

4.1 Kepler's laws of planetary motion

In the early seventeenth century (1609-1619) Kepler proposed three laws of planetary motion

(i) The orbits of the planets are ellipses, with the Sun's centre of mass at one focus of the ellipse.

(ii) The line joining a planet and the Sun describes equal areas in equal intervals of time.

(iii) The squares of the periods of the planets are proportional to the cubes of their semi-major axes.

These laws were based on detailed observations made by Tycho Brahe, and put to rest any notion that planets move in perfectly circular orbits. However, it wasn't until Newton proposed his law of gravitation in 1687 that the origins of this motion were understood. Newton proposed that

"Every object in the Universe attracts every other object with a force directed along a line of centres for the two objects that is proportional to the product of their masses and inversely proportional to the square of the separation of the two objects."

Based on this one statement, it is possible to derive Kepler's laws.

4.1.1 Second law

Keplers second law is the simplest to derive, and is a statement that the angular momentum of a particle moving under a central force, such as gravity, is constant. By definition, the angular momentum $\boldsymbol{L}$ of a particle with mass m and velocity $\boldsymbol{u}$ is

$$\boldsymbol{L} = \boldsymbol{r} \wedge m\frac{d\boldsymbol{r}}{dt}, \tag{53}$$

15

where r is the vector position of the particle. The rate of change of angular momentum is given by

$$\frac{d\boldsymbol{L}}{dt} = \boldsymbol{r} \wedge \boldsymbol{f} = \boldsymbol{r} \wedge f(r)\hat{\boldsymbol{r}} = 0, \tag{54}$$

where $f(r)\hat{\boldsymbol{r}}$ is the central force, depending only on the distance $r = |\boldsymbol{r}|$ and pointing in the direction $\hat{\boldsymbol{r}} = \boldsymbol{r}/r$. It can therefore be seen that the angular momentum of a particle moving under a central force is constant, a consequence of this being that motion takes place in a plane. The area swept out by the line joining a planet and the sun is half the area of the parallelogram formed by $\boldsymbol{r}$ and $d\boldsymbol{r}$. Thus

$$dA = \frac{1}{2}|\boldsymbol{r} \wedge d\boldsymbol{r}| = \frac{1}{2}\left|\boldsymbol{r} \wedge \frac{d\boldsymbol{r}}{dt}dt\right| = \frac{L}{2m}dt, \tag{55}$$

where $L = |\boldsymbol{L}|$ is a constant. The area swept out is therefore also constant.

4.1.2 First law

To prove Keplers first law consider the sun as being stationary (i.e., infinitely heavy), and the planets in orbit around it. The equation of motion for a planet is

$$m\frac{d^2\boldsymbol{r}}{dt^2} = f(r)\hat{\boldsymbol{r}}. \tag{56}$$

In plane polar coordinates

$$\frac{d\boldsymbol{r}}{dt} = \dot{r}\hat{\boldsymbol{r}} + r\dot{\theta}\hat{\boldsymbol{\theta}}, \tag{57a}$$

$$\frac{d^2\boldsymbol{r}}{dt^2} = (\ddot{r} - r\dot{\theta}^2)\hat{\boldsymbol{r}} + (r\ddot{\theta} + 2\dot{r}\dot{\theta})\hat{\boldsymbol{\theta}}. \tag{57b}$$

In component form, equation (56) therefore becomes

$$m(\ddot{r} - r\dot{\theta}^2) = f(r), \tag{58a}$$

$$m(r\ddot{\theta} + 2\dot{r}\dot{\theta}) = 0. \tag{58b}$$

Putting (57a) into (53) gives

$$L = \left|\boldsymbol{r} \wedge m\frac{d\boldsymbol{r}}{dt}\right| = |mr^2\dot{\theta}|. \tag{59}$$

Thus

$$r^2\dot{\theta} = l, \tag{60}$$

where $l = L/m$ is the angular momentum per unit mass. Given a radial force $f(r)$, equations (58a) and (58b) can now be solved to obtain r and θ as functions of t. A more practical result is to solve for $r(\theta)$, however, and this requires the definition of a new variable

$$r = \frac{1}{u}. \tag{61}$$

16

Rewriting the equations of motion in terms of the new variable requires the identities

$$\dot{r} = -\frac{1}{u^2}\dot{u} = -\frac{1}{u^2}\frac{d\theta}{dt}\frac{du}{d\theta} = -l\frac{du}{d\theta}, \tag{62a}$$

$$\ddot{r} = -l\frac{d}{dt}\frac{du}{d\theta} = -l\dot{\theta}\frac{d^2u}{d\theta^2} = -l^2u^2\frac{d^2u}{d\theta^2}. \tag{62b}$$

Equation (58a) becomes

$$\frac{d^2u}{d\theta^2} + u = -\frac{1}{ml^2u^2}f\left(\frac{1}{u}\right). \tag{63}$$

This is the differential equation governing the motion of a particle under a central force. Conversely, if one is given the polar equation of the orbit $r = r(\theta)$, the force function can be derived by differentiating and putting the result into the differential equation. According to Newtons law of gravitation $f(r) = -k/r^2$, so that

$$\frac{d^2u}{d\theta^2} + u = \frac{k}{ml^2}. \tag{64}$$

This has the general solution

$$u = A\cos(\theta - \theta_0) + \frac{k}{ml^2}, \tag{65}$$

where A and θ_0 are constants of integration that encode information about the initial conditions. Choosing $\theta_0=0$ and replacing u by the original radial coordinate $r = 1/u$,

$$r = \left(A\cos\theta + \frac{k}{ml^2}\right)^{-1} \tag{66}$$

which is the equation of a conic section with the origin at the focus. This can be rewritten in standard form

$$r = r_0\frac{1 + \epsilon}{1 + \epsilon\cos\theta}, \tag{67}$$

where

$$\epsilon = \frac{Aml^2}{k}, \qquad r_0 = \frac{ml^2}{k(1 + \epsilon)}. \tag{68}$$

ϵ is called the eccentricity of the orbit:

- $\epsilon = 0$ is a circle,

- $\epsilon < 1$ is an ellipse,

- $\epsilon = 1$ is a parabola and

- $\epsilon > 1$ is a hyperbola.

For an elliptical orbit, r_0 is the distance of closest approach to the sun, and is called the *perihelion*. Similarly,

$$r_1 = r_0(1 + \epsilon)/(1 - \epsilon) \tag{69}$$

is the furthest distance from the sun and is called the *aphelion*. Orbital eccentricities are small for planets, whereas comets have parabolic or hyperbolic orbits. Interestingly though, Halley's comet has a very eccentric orbit but, according to the definition just given, is not a comet!

4.1.3 Third law

To prove Keplers third law go back to equation (55). Integrating this area law over time gives

$$A(\tau) = \int_0^\tau dA = \frac{l\tau}{2}, \tag{70}$$

where τ is the period of the orbit. The area A of an ellipse can also be written as $A = \pi a b$ where a and b are the semi-major and semi-minor axes, yielding

$$\frac{l\tau}{2} = \pi a b \tag{71}$$

The ratio of a and b can be expressed in terms of the eccentricity

$$\frac{b}{a} = \sqrt{1 - \epsilon^2}. \tag{72}$$

Using this expression to substitute b in (71)

$$\tau = \frac{2\pi a^2}{l}\sqrt{1 - \epsilon^2} \tag{73}$$

The length of the major axis is

$$2a = r_0 + r_1 = \frac{2ml^2}{k(1 - \epsilon^2)}. \tag{74}$$

Squaring (71) and replacing gives

$$\tau^2 = \frac{4\pi^2 m}{k} a^3, \tag{75}$$

confirming Kepler's 3rd law.

4.2 Hamiltonian dynamics of many-body systems

The Kepler problem is essentially a two-body problem. In the remainder of this course, we will be interested in classical (non-quantum) systems that consist of $N \gg 2$ particles. The complete microscopic dynamics of such systems is encoded in their Hamiltonian

$$H = \sum_{n=1}^N \frac{\boldsymbol{p}_n^2}{2m_n} + U(\boldsymbol{x}_1, \ldots, \boldsymbol{x}_N), \tag{76a}$$

where m_n, $\boldsymbol{p}_n(t)$ and $\boldsymbol{x}_n(t)$ denote the mass, momentum and position of the nth particle. The first contribution on the rhs. of Eq. (76a) is the kinetic energy, and U is the potential energy. For our purposes, it is sufficient to assume that we can decompose (76a) into a sum of pair interactions

$$U(\boldsymbol{x}_1, \ldots, \boldsymbol{x}_N) = \frac{1}{2} \sum_{n,k:n\neq k} \Phi(\boldsymbol{x}_n, \boldsymbol{x}_k). \tag{76b}$$

Given H, Newton's equations can be compactly rewritten as

$$\dot{\boldsymbol{x}}_n = \nabla_{\boldsymbol{p}_n} H \, , \qquad \dot{\boldsymbol{p}}_n = -\nabla_{\boldsymbol{x}_n} H. \qquad (77)$$

That this so-called Hamiltonian dynamics is indeed equivalent to Newton's laws of motion can be seen by direct insertion, which yields

$$\dot{\boldsymbol{x}}_n = \frac{\boldsymbol{p}_n}{m_n} \, , \qquad \dot{\boldsymbol{p}}_n = m_n \ddot{\boldsymbol{x}}_n = -\nabla_{\boldsymbol{x}_n} U. \qquad (78)$$

An important observation is that many physical systems obey certain conservation laws. For instance, the Hamiltonian (76a) itself remains conserved under the time-evolution (77)

$$\begin{aligned} \frac{d}{dt} H &= \sum_n \left[(\nabla_{\boldsymbol{p}_n} H) \cdot \dot{\boldsymbol{p}}_n + (\nabla_{\boldsymbol{x}_n} H) \cdot \dot{\boldsymbol{x}}_n \right] \\ &= \sum_n \left[(\nabla_{\boldsymbol{p}_n} H) \cdot (-\nabla_{\boldsymbol{x}_n} H) + (\nabla_{\boldsymbol{x}_n} H) \cdot \nabla_{\boldsymbol{p}_n} H \right] \equiv 0. \end{aligned} \qquad (79)$$

which is just the statement of energy conservation. Other important examples of conserved quantities are total linear momentum and angular momentum,

$$\boldsymbol{P} = \sum_n \boldsymbol{p}_n \, , \qquad \boldsymbol{L} = \sum_n \boldsymbol{x}_n \wedge \boldsymbol{p}_n \qquad (80)$$

if the pair potentials Φ only depend on the distance between particles.

There exists a deep mathematical connection between such invariants and symmetries of the underlying Hamiltonian, known as Noether's theorem. For example, energy conservation is a consequence of the fact that the Hamiltonian (76a) is note explicitly time-dependent and, hence, invariant under time translations. Similarly, conservation of linear momentum is linked to spatial translation invariance and conservation of angular momentum to rotational invariance.

For the remainder of this course, it will be important to keep in mind that microscopic symmetries and conservation laws must be preserved in coarse-grained macroscopic continuum descriptions.

4.3   Practical limitations

Deriving Kepler's laws required us to solve a second-order linear ordinary differential equation, which was obtained by considering the idealised case in which a single planet is orbiting the sun. If we consider a more realistic problem in which several planets orbit the sun, all interacting with each other via gravity, the problem becomes analytically intractable. Indeed, for just two planets orbiting the sun one encounters the celebrated 'three-body problem', for which there is no general analytical solution. Lagrange showed that there are some solutions to this problem if we restrict the planets to move in the same plane, and assume that the mass of one of them is so small as to be negligible. In the absence of an explicit solution to the 'three body problem' one must use ideas from 18.03 to calculate fixed points of the equations and investigate their stability. However, now you see the problem. The critical number of equations for complicated things to happen is three (for ODE's), and yet any

relevant problem in the world contains many more than three degrees of freedom. Indeed a physical problem typically contains 10^{23} interacting particles (Avogadro's number), which is so great a number that it is unclear if the mathematical techniques described above are of any use. The central aim of this course is to make theoretical progress towards understanding systems with many degrees of freedom. To do so we shall invoke the "continuum hypothesis", imagining that the discrete variable (e.g. the velocity of a particular molecule of fluid) can be replaced with a continuum (e.g. the velocity field $\boldsymbol{v}(\boldsymbol{x}, t)$). There are many subtleties that arise in trying to implement this idea, among them;

(i) How does one write down macroscopic descriptions in terms of microscopic constants in a systematic way? It would be terrible to have to solve 10^{23} coupled differential equations!

(ii) Forces and effects that *a priori* appear to be small are not always negligible. This turns out to be of fundamental importance, but was not recognised universally until the 1920's.

(iii) The mathematics of how to solve 'macroscopic equations', which are nonlinear partial differential equations, is non-trivial. We will need to introduce many new ideas.

In tackling these problems we will spend a lot of time doing fluid mechanics, the reason being that it is by far the most developed field for the study of these questions. Experiments are readily available and the equations of motion are very well known (and not really debated!). Furthermore, fluid dynamics is an important subject in its own right, being relevant to many different scientific disciplines (e.g. aerospace engineering, meteorology, coffee cups). We will also introduce other examples (e.g. elasticity) to show the generality of the ideas.

4.4 Suggestions

For more details on Kepler's laws, and a java applet to let you play with them, go to

$$\text{http://csep10.phys.utk.edu/astr161/lect/history/kepler.html}$$

5 Random walkers and diffusion

The most important (and obvious) problem when introducing the continuum hypothesis is to figure out how to treat Avogadro's number of particles obeying Schrödinger's equation or Newton's laws. This a little ambitious for us to start with, so we begin by trying to understand how the simplest microscopic model for the motion of particles can lead to macroscopic laws. We will see that the simplest model, that of a randomly moving particle, leads to a nice derivation of the diffusion equation, whose properties will be investigated in the next lecture.

Consider the motion of particles along one axis. The particles start at time $t = 0$ at position $x = 0$ and execute a random walk according to the following rules:

(i) Each particle steps to the right or the left once every τ seconds, moving a distance $dx_i = \pm\delta$.

(ii) The probability of going to the right at each step is $1/2$, and the probability of going to the left is $1/2$, independently of the previous history.

(iii) Each particle moves independently of all the other particles, i.e. the particles do not interact with one another.

There are two striking consequences of these rules. Let N be the total number of particles and $x_i(n)$ be the position of the ith particle after n steps, and denote the average position of all particles by

$$X(n) = \frac{1}{N} \sum_{i=1}^{N} x_i(n). \tag{81}$$

The mean displacement of the particles after n steps is

$$
\begin{aligned}
\langle X(n) \rangle &= \frac{1}{N} \sum_{i=1}^{N} \langle x_i(n) \rangle \\
&= \frac{1}{N} \sum_{i=1}^{N} [\langle x_i(n-1) \rangle + \langle dx_i \rangle] \\
&= \frac{1}{N} \sum_{i=1}^{N} \left[\langle x_i(n-1) \rangle + \delta \cdot \frac{1}{2} + (-\delta) \cdot \frac{1}{2} \right] \\
&= \frac{1}{N} \sum_{i=1}^{N} \langle x_i(n-1) \rangle \\
&= \langle X(n-1) \rangle. \tag{82}
\end{aligned}
$$

Thus particles go nowhere on average.

Secondly, assuming that the all particles start at $x_i(0) = 0$, the root-mean-square displacement of the particles, which is a good measure of spreading, is obtained as follows:

$$
\begin{aligned}
\langle [X(n) - X(0)]^2 \rangle &= \langle X(n)^2 \rangle \\
&= \left\langle \left[\frac{1}{N} \sum_{i=1}^{N} x_i(n) \right] \left[\frac{1}{N} \sum_{k=1}^{N} x_k(n) \right] \right\rangle \\
&= \frac{1}{N^2} \sum_{i=1}^{N} \sum_{k=1}^{N} \langle x_i(n) x_k(n) \rangle \\
&= \frac{1}{N^2} \sum_{i=1}^{N} \langle x_i(n)^2 \rangle, \tag{83}
\end{aligned}
$$

where we have used that, by virtue of assumption (iii),

$$\langle x_i(n) x_k(n) \rangle = \langle x_i(n) \rangle \langle x_k(n) \rangle = 0 \qquad \text{for } i \neq k.$$

The mean-square displacement per particle can be calculated from

$$
\begin{aligned}
\langle x_i(n)^2 \rangle &= \langle [x_i(n-1) + dx_i]^2 \rangle \\
&= \langle x_i(n-1)^2 \rangle + 2\langle x_{i-1}(n)\, dx_i \rangle + \langle dx_i^2 \rangle \\
&= \langle x_i(n-1)^2 \rangle + 2\langle x_{i-1}(n) \rangle \langle dx_i \rangle + \delta^2 \\
&= \langle x_i(n-1)^2 \rangle + \delta^2.
\end{aligned}
\tag{84}
$$

Repeating this procedure n times and recalling that $x_i(0) = 0$, we find

$$
\langle x_i(n)^2 \rangle = \langle x_i(0)^2 \rangle + n\delta^2 = n\delta^2
\tag{85}
$$

and, hence, for the mean square displacement of the cloud's mean value

$$
\langle X(n)^2 \rangle = \frac{1}{N^2} \sum_{i=1}^{N} n\delta^2 = \frac{\delta^2}{N} n.
\tag{86}
$$

If we write n in terms of time such that $t = n\tau$, where τ is the time in between each step, then

$$
\sqrt{\langle x_i(n)^2 \rangle} = \left(\frac{t}{\tau} \right)^{\frac{1}{2}} \delta = \left(\frac{\delta^2 t}{\tau} \right)^{\frac{1}{2}} = \left(\frac{\delta^2}{\tau} \right)^{\frac{1}{2}} \sqrt{t}.
\tag{87}
$$

The root-mean-square displacement of each particle is proportional to the square-root of the time.

We now seek to derive a theory to predict the distribution of a cloud of random walkers at some time t given the distribution at $t = 0$. There are two ways to do so, one using particle fluxes and the other adopting a probabilistic approach.

5.1 Derivation of the diffusion equation using particle fluxes

Consider two neighbouring points on a line. At time t there are $N(x, t)$ particles at x and $N(x + \delta, t)$ particles at position $x + \delta$. At time $t + \tau$ half the particles at x will have stepped across the dashed line from left to right and half of the particles at $x + \delta$ will have stepped across the dashed line from right to left. The net number of particles crossing to the right is therefore

$$
-\frac{1}{2} \left[N(x + \delta, t) - N(x, t) \right].
\tag{88}
$$

To obtain the net flux, we divide by the area normal to the x-axis, A, and by the time interval τ,

$$
J_x = -\frac{[N(x + \delta, t) - N(x, t)]}{2A\tau}.
\tag{89}
$$

Multiplying by δ^2 / δ^2 gives

$$
J_x = -\frac{\delta^2}{2\tau} \frac{1}{\delta} \left[\frac{N(x + \delta, t) - N(x, t)}{A\delta} \right],
\tag{90}
$$

which can be rewritten

$$
J_x = -D \frac{n(x + \delta, t) - n(x, t)}{\delta},
\tag{91}
$$

where $D = \delta^2/2\tau$ is the diffusion coefficient and

$$n(x, t) = \frac{N(x, t)}{A\delta}$$

is the particle density (i.e., the number of particles per unit volume at position x at time t). If δ is assumed to be very small, then in the limit $\delta \to 0$, the flux becomes

$$J_x = -D\frac{\partial n}{\partial x}, \tag{92}$$

where we have ignored higher-order derivatives in making the approximation.

Now consider a single box with boundaries at $x - \delta/2$ and $x + \delta/2$. In a single time step, $J_x(x - \delta/2, t)A\tau$ particles will enter from the left and $J_x(x + \delta/2, t)A\tau$ particles will leave through the right boundary. The number of particles in the box increases as follows,

$$N(x, t + \tau) - N(x, t) = [J_x(x - \delta/2, t) - J_x(x + \delta/2, t)] A\tau.$$

By dividing both sides by $A\delta\tau$ the number of particles per unit volume in the box $n(x, t)$ is seen to increase at the rate[2]

$$\frac{n(x, t + \tau) - n(x, t)}{\tau} = -\frac{[J_x(x + \delta/2, t) - J_x(x - \delta/2, t)]}{\delta}. \tag{93}$$

In the limit $\tau \to 0$ and $\delta \to 0$, this becomes

$$\frac{\partial n}{\partial t} = -\frac{\partial J_x}{\partial x} = D\frac{\partial^2 n}{\partial x^2}, \tag{94}$$

which is Fick's law. This is commonly known as the *diffusion equation*. It tells us how a cloud of particles will redistribute itself in time. If we know the initial distribution and the boundary conditions, we can figure out all later distributions. It can be used to model many things, such as the spreading of dye in water, the transport of heat in solids, and the motion of bacteria.

5.2 Derivation using probabilities

Before going on to solve the diffusion equation, let us derive the diffusion equation using a different approach, involving probabilities. Assuming non-interacting particles, the number of particles in the interval $[x - \delta/2, x + \delta/2]$ at any given time is

$$N(x, t) = N_0 P(x, t) = N_0 p(x, t)\delta, \tag{95}$$

where N_0 is the total number of particles in the sample, $P(x, t) = p(x, t)\delta$ the probability of finding the particle at time t in $[x - \delta/2, x + \delta/2]$ and $p(x, t)$ the associated probability density. If we consider discrete changes in position and time, then for particles that move to the left or right with equal probability

$$P(x, t + \tau) = \frac{1}{2} [P(x + \delta, t) + P(x - \delta, t)], \tag{96}$$

---

[2]For strictly one-dimensional systems, the boundary area is just a point and, hence, $A = 1$ in this case.

where the size of the time step is τ and the spatial separation is δ. Upon dividing by δ, we can rewrite (96) in terms of the associated probability density

$$p(x, t + \tau) = \frac{1}{2} \left[p(x + \delta, t) + p(x - \delta, t) \right]. \tag{97}$$

Performing a Taylor expansion about the position x and time t in the limit $\delta, \tau \to 0$,

$$p(x, t) + \frac{\partial p}{\partial t} \tau \approx \frac{1}{2} \left[p(x, t) + \frac{\partial p}{\partial x} \delta + \frac{\partial^2 p}{\partial x^2} \frac{\delta^2}{2} + p(x, t) - \frac{\partial p}{\partial x} \delta + \frac{\partial^2 p}{\partial x^2} \frac{\delta^2}{2} \right]. \tag{98}$$

which simplifies to the diffusion equation for the probability density

$$\frac{\partial p}{\partial t} \approx D \frac{\partial^2 p}{\partial x^2}, \qquad D = \frac{\delta^2}{2\tau}. \tag{99}$$

To recover Eq. (94), we note that the number density of particles is given by $n = N_0 p$, and our derivation is complete.

Note that we have ignored higher-order terms in the Taylor expansion. Additional terms would give us

$$\frac{\partial p}{\partial t} + \frac{\tau}{2} \frac{\partial^2 p}{\partial t^2} \approx \frac{\delta^2}{2\tau} \frac{\partial^2 p}{\partial x^2} - \frac{\delta^4}{4!\tau} \frac{\partial^4 p}{\partial x^4}. \tag{100}$$

Are we allowed to ignore these extra terms? To see if we are, compare the ratio of the neglected terms on the right hand side

$$\frac{\delta^4}{\tau} \frac{\partial^4 p}{\partial x^4} \bigg/ \frac{\delta^2}{\tau} \frac{\partial^2 p}{\partial x^2}. \tag{101}$$

Now $\partial p / \partial x$ is essentially $\Delta p / \Delta x$, where Δp is a characteristic change in the value of p and Δx is the characteristic length over which it changes. Let $\Delta p = P$ and $\Delta x = L$; the ratio of the two terms is

$$\frac{\delta^4}{\tau} \frac{P}{L^4} \bigg/ \frac{\delta^2}{\tau} \frac{P}{L^2} \sim O \left(\frac{\delta}{L} \right)^2, \tag{102}$$

which is typically very small. This is an example of a scaling argument, which in this case implies that we are justified in neglecting the extra terms provided L is much greater than δ. You must be careful however, as this estimate is not correct everywhere. For example, in the tails of the distribution the characteristic lengthscale over which there is a change in p may become important. The argument of neglecting terms is therefore not always valid, and we shall discuss this point more when we encounter *singular perturbations* later in the course. The discovery of this issue and its resolution was probably the greatest achievement of applied mathematics in the twentieth century.

5.3   Suggestions

For an excellent read on random walkers and the diffusion equation, and their applications in biology, have a look at *Random Walks in Biology by Howard C. Berg* (a professor over at Harvard). In this book, the ideas we have discussed are applied to a number of biological phenomena, including the motion of bacteria (which would make a good course project).

6 Solving the diffusion equation

We have shown, through two different arguments, that the density of random walkers on a one dimensional lattice obeys the diffusion equation,

$$\frac{\partial n}{\partial t} = D\frac{\partial^2 n}{\partial x^2}. \tag{103}$$

This description is valid whenever examining the dynamics of large quantities of random walkers on scales much larger than the lattice spacing. As the next step, it is important to understand how to solve this equation, as the same mathematical problem will arise later on in our studies of fluid motion. For instance we would like to know the solution to the above equation, subject to the initial condition $n(x, t = 0) = n_0(x)$ and the boundary conditions that n vanishes at $\pm\infty$.

There are two basic techniques for solving this, each of which relies on a different method for representing the solution. In both cases, the central idea is that since the equation is *linear*, it is possible to "break down" any initial state into a linear combination of simpler problems. By solving the simpler problems explicitly it is then possible to reconstruct the general solution.

6.1 Fourier method

This method relies on the fact that it is possible to express $n(x, t)$ in a basis of plane waves[3], i.e.

$$n(x, t) = \frac{1}{2\pi}\int_{-\infty}^{\infty} e^{ikx}\hat{n}(k, t)dk. \tag{104}$$

As a complement to (104), the *Fourier coefficients* for a given distribution are found using the *Fourier transform*

$$\hat{n}(k, t) = \int_{-\infty}^{\infty} e^{-ikx}n(x, t)dx, \tag{105}$$

and we define $\hat{n}_0(k)$ to be the Fourier coefficients of the initial condition $n_0(x)$.

The strength of this approach is that it is simple to solve the diffusion equation for a single plane wave. For example, integrating the diffusion equation in the following manner

$$\int_{-\infty}^{\infty} \frac{\partial n}{\partial t}e^{-ikx}dx = \int_{-\infty}^{\infty} D\frac{\partial^2 n}{\partial x^2}e^{-ikx}dx \tag{106}$$

gives

$$\frac{\partial\hat{n}(k, t)}{\partial t} = (ik)^2 D\hat{n}(k, t) = -k^2 D\hat{n}(k, t). \tag{107}$$

Given the initial condition $n_0(x) \to \hat{n}_0(k)$ the solution of (107) is

$$\hat{n}(k, t) = \hat{n}_0(k)e^{-Dk^2 t}. \tag{108}$$

---

[3]An intuitive way of thinking is to note that a plane wave can be written as $e^{ikx} = \cos(kx) + i\sin(kx)$. The Fourier transform thus can be interpreted as expressing a (complex) function as a superposition of real and complex sinusoidal waves. The Fourier coefficient $\hat{n}(k, t)$ describes how large the contribution of a wave with wave vector $k \propto 1/\lambda$, with λ the wavelength, is in this superposition.

The solution of the original problem is therefore

$$n(x,t) = \frac{1}{2\pi} \int_{-\infty}^{\infty} \hat{n}_0(k) e^{ikx - Dk^2 t} dk. \tag{109}$$

We note that the high-wavenumber components (which correspond to sharp gradients) are rapidly damped, emphasising the smoothing property of diffusion.

Example Consider a distribution that is initially Gaussian (normal) about the point $x = 0$ at time $t = 0$, with standard deviation σ,

$$n(x,0) = \frac{1}{\sqrt{2\pi\sigma^2}} e^{-\frac{x^2}{2\sigma^2}}. \tag{110}$$

Note that in the limit where $\sigma \to 0$, this distribution corresponds to the Dirac delta-function $\delta(x)$, a function which is localized at zero. We come back to this limit again at the end of the example.

The Fourier transform of the above initial distribution is

$$\hat{n}_0(k) = \frac{1}{\sqrt{2\pi\sigma^2}} \int_{-\infty}^{\infty} e^{-ikx - \frac{x^2}{2\sigma^2}} dx = \frac{1}{\sqrt{2\pi\sigma^2}} \int_{-\infty}^{\infty} e^{-\left(\frac{x^2}{2\sigma^2} + ikx\right)} dx. \tag{111}$$

Completing the square for the exponent

$$\frac{x^2}{2\sigma^2} + ikx = \frac{1}{2\sigma^2} \left(x^2 + 2\sigma^2 ikx\right) = \frac{1}{2\sigma^2} \left[\left(x + ik\sigma^2\right)^2 + k^2\sigma^4\right]. \tag{112}$$

enables (111) to be rewritten as

$$\hat{n}_0(k) = \frac{e^{-\frac{k^2\sigma^2}{2}}}{\sqrt{2\pi\sigma^2}} \int_{-\infty}^{\infty} e^{-\frac{(x+ik\sigma^2)^2}{2\sigma^2}} dx. \tag{113}$$

To calculate the above integral, which involves a complex integrand, we use the Cauchy integral formula. It states that for a complex function $f(z) \in \mathbb{C}, z \in \mathbb{C}$, integration along a closed path in the complex plane is zero, provided that $f(z)$ has no poles inside the path:

$$\oint f(z) dz = 0 \tag{114}$$

Introducing the substitution $z = x + ik\sigma^2$, $dz = dx$, the integral (113) can be rewritten as

$$\hat{n}_0(k) = \frac{e^{-\frac{k^2\sigma^2}{2}}}{\sqrt{2\pi\sigma^2}} \lim_{R \to \infty} \int_{-R+ik\sigma^2}^{R+ik\sigma^2} e^{-\frac{z^2}{2\sigma^2}} dz \tag{115}$$

Let's keep R finite for the moment. We can then think of the integral as one segment of a closed curve with rectangular shape:

$$0 = \oint e^{-\frac{z^2}{2\sigma^2}} dz$$

$$= \int_{-R+ik\sigma^2}^{R+ik\sigma^2} e^{-\frac{z^2}{2\sigma^2}} dz + \int_{R+ik\sigma^2}^{R} e^{-\frac{z^2}{2\sigma^2}} dz + \int_{R}^{-R} e^{-\frac{z^2}{2\sigma^2}} dz + \int_{-R}^{-R+ik\sigma^2} e^{-\frac{z^2}{2\sigma^2}} dz \tag{116}$$

26

In the limit $R \to \infty$, the second as well as the last integral vanish due to the exponential damping with large R, leading to

$$\lim_{R \to \infty} \int_{-R+ik\sigma^2}^{R+ik\sigma^2} e^{-\frac{z^2}{2\sigma^2}} dz = \lim_{R \to \infty} \int_{-R}^{R} e^{-\frac{z^2}{2\sigma^2}} dz . \tag{117}$$

Inserting this into Eq. (115), we obtain

$$\hat{n}_0(k) = \frac{e^{-\frac{k^2\sigma^2}{2}}}{\sqrt{2\pi\sigma^2}} \int_{-\infty}^{\infty} e^{-\frac{x^2}{2\sigma^2}} dx. \tag{118}$$

This means that we can basically drop the imaginary part in the original integral, Eq. (113).

From 18.01 we know that

$$\int_{-\infty}^{\infty} e^{-x^2} = \sqrt{\pi},$$

so by making a change of variable $y = x/\sqrt{2\sigma^2}$ we have that

$$\hat{n}_0(k) = e^{-\frac{k^2\sigma^2}{2}}. \tag{119}$$

This result is worth keeping in mind: The Fourier transform of a Gaussian is a Gaussian.

To obtain the full solution of the diffusion equation in real space, we have to insert $\hat{n}_0(k)$ into (104),

$$n(x,t) = \frac{1}{2\pi} \int_{-\infty}^{\infty} e^{ikx - Dk^2t - k^2\sigma^2/2} dk. \tag{120}$$

We can do a bit of rearranging to get

$$n(x,t) = \frac{1}{2\pi} \int_{-\infty}^{\infty} e^{ikx - k^2\left(Dt + \sigma^2/2\right)} dk . \tag{121}$$

As before we complete the square for the exponent,

$$k^2 \left(Dt + \frac{\sigma^2}{2}\right) - ikx = \left(Dt + \frac{\sigma^2}{2}\right) \left\{ \left[k - \frac{ix}{2(Dt + \sigma^2/2)}\right]^2 + \frac{x^2}{4\left(Dt + \sigma^2/2\right)^2} \right\}, \tag{122}$$

so that the integral becomes

$$n(x,t) = \frac{e^{-\frac{x^2}{4(Dt+\sigma^2/2)}}}{2\pi} \int_{-\infty}^{\infty} e^{-(Dt+\sigma^2/2)\left[k - \frac{ix}{2(Dt+\sigma^2/2)}\right]^2} dk. \tag{123}$$

This is essentially the same integral that we had before, so we drop the imaginary part and change the integration variable, giving the result

$$n(x,t) = \frac{e^{-\frac{x^2}{4(Dt+\sigma^2/2)}}}{\sqrt{4\pi\left(Dt + \sigma^2/2\right)}}. \tag{124}$$

This is the solution of the diffusion equation starting from a Gaussian distribution at time $t = 0$.

Note:

- Introducing $\tilde{\sigma}^2 = 2(Dt + \sigma^2/2)$, the solution is a Gaussian with a standard deviation $\tilde{\sigma}$, i.e. the width of the solution grows like $\sqrt{Dt}$ in time. Similarly, the amplitude decreases like $\frac{1}{\sqrt{Dt}}$.

- Let us substitute $t_d = \sigma^2/(2D)$. The solution then can be written as

$$n(x,t) = \frac{e^{-\frac{x^2}{4D(t+t_d)}}}{\sqrt{4\pi D(t + t_d)}}. \tag{125}$$

Remember that in the limit $t_d = \frac{\sigma^2}{2D} \to 0$ the initial condition (110) corresponds to a Dirac delta function. Thus an initially Gaussian distribution of particles that is diffusing may be viewed as having originated from a delta function a time t_d ago. Indeed, it can be shown that diffusion will cause any form of particle distribution initially localised about zero to eventually look like a Gaussian.

6.2 Green's function method

This method relies on another trick for representing the solution, that is somewhat more intuitive. Now, instead of representing n in a basis of plane wave states, we will express it as a basis of states which are localised in *position*. This is done by using the so-called Dirac delta function, denoted $\delta(x - x_0)$. You should think of this of a large spike of unit area that is centered exactly at the position x_0. The definition of δ is that given any function[4] $f(x)$,

$$\int_{-\infty}^{\infty} f(x')\,\delta(x - x')dx' = f(x). \tag{126}$$

We can represent the initial distribution of particles $n(x,0) = n_0(x)$ as a superposition of δ-functions

$$n_0(x) = \int_{-\infty}^{\infty} n_0(x')\,\delta(x - x')\,dx'. \tag{127}$$

This formula decomposes n_0 into a continuous series of "spikes". The idea is to then understand how each spike individually evolves and then superimpose the evolution of each

---

[4]Intuitively, one can obtain the Dirac δ-function from the normalized Gaussian (110) by letting $\sigma \to 0$. Derivatives of order n of the δ-function, denoted by $\delta^{(n)}$, can be defined by partial integration

$$\int_{-\infty}^{\infty} f(x')\,\delta^{(n)}(x - x')\,dx' = (-1)^n \int_{-\infty}^{\infty} f^{(n)}(x')\,\delta(x - x')\,dx'.$$

The Fourier transformation of the δ-function is given by

$$\hat{\delta}(k) = \int_{-\infty}^{\infty} e^{-ikx}\delta(x)\,dx = 1.$$

Applying the inverse transformation yields a useful integral representation of the Dirac δ-function

$$\delta(x) = \frac{1}{2\pi}\int_{-\infty}^{\infty} e^{ikx}\hat{\delta}(k)\,dk = \frac{1}{2\pi}\int_{-\infty}^{\infty} e^{ikx}\,dk.$$

spike to find the final density distribution. We define the Green's function $G(x - x', t)$ so that $G(x - x', 0) = \delta(x - x')$, and

$$n(x, t) = \int_{-\infty}^{\infty} G(x - x', t) \, n_0(x') \, dx'. \tag{128}$$

Plugging this into the diffusion equation we see that

$$\int_{-\infty}^{\infty} n_0(x') \frac{\partial G(x - x', t)}{\partial t} \, dx' = D \int_{-\infty}^{\infty} n_0(x') \frac{\partial^2 G(x - x', t)}{\partial x^2} \, dx'. \tag{129}$$

Thus $G(x - x', t)$ *obeys the diffusion equation* and we have reduced the problem to the mathematics of solving the diffusion equation for the localised initial condition $\delta(x - x')$.

There are many ways of solving this problem. The one in most textbooks is to actually use the Fourier decomposition of $\delta(x - x')$ and solve the equation in Fourier space, and then transform back into real space. This is an advisable procedure as the Fourier transform of δ is very simple[5]. We will advocate another procedure however, that is more elegant and uses an idea that we will return to later in our studies of fluids. The idea is to use dimensional analysis to determine the solution. If we look at the diffusion equation

$$\frac{\partial n}{\partial t} = D \frac{\partial^2 n}{\partial x^2} \tag{130}$$

we see that roughly '$\partial/\partial t$' $\sim$ '$\partial^2/\partial x^2$'. (I've written this in quotes because there is a sense in which this equality is meaningless.) What I mean by it is that if you have a function n which obeys a diffusion equation, taking a single time derivative of the function gives a number of about the same size as when you take two spatial derivatives. This means that the characteristic length scale over which n varies is of order $\sqrt{t}$. Now, since the initial distribution δ is perfectly localised, we expect that at time t, $G(x - x')$ will have a characteristic width $\sqrt{t}$. Thus, we guess a (so-called) similarity solution

$$G(x - x', t) = A(t) \, F\left(\frac{x - x'}{\sqrt{t}}\right). \tag{131}$$

The time dependence of $A(t)$ is determined by the conservation of particles. Since

$$\int_{-\infty}^{\infty} n \, dx = \int_{-\infty}^{\infty} A(t) \, F\left(\frac{x}{\sqrt{t}}\right) dx = A(t)\sqrt{t} \int_{-\infty}^{\infty} F(y) dy \tag{132}$$

must be constant in time (we have changed variables from x to $y = x/\sqrt{t}$), we see that

$$A(t) = \frac{A_0}{\sqrt{t}} \tag{133}$$

for some constant A_0. Now let's just plug in

$$G(x, t) = \frac{A_0}{\sqrt{t}} F(x/\sqrt{t})$$

---

[5]Note that in the limit $t_d = \sigma^2/(2D) \to 0$ the initial condition (110) approaches a Dirac delta function, so we have already 'solved'the problem: equation (125) tells us that an initially Gaussian distribution of particles that is diffusing may be viewed as having originated from a delta function a time t_d ago.

into the diffusion equation. This gives us the following ordinary differential equation for $F(y)$

$$\frac{1}{t^{\frac{3}{2}}}\left(-\frac{1}{2}F - \frac{1}{2}yF'\right) = \frac{1}{t^{\frac{3}{2}}}DF''. \tag{134}$$

Cancelling out the time factors and integrating this equation once gives

$$-\frac{1}{2}Fy = DF'. \tag{135}$$

This equation can be immediately integrated to give $F(y) = F_0 e^{-y^2/4D}$, and thus

$$G(x - x', t) = \frac{F_0}{\sqrt{t}} e^{-\frac{(x-x')^2}{4Dt}}, \tag{136}$$

where the constant $F_0 = 1/\sqrt{4\pi D}$ is determined by requiring that $\int dx\, G = 1$.

Mean square displacement   We would like to determine $\langle x(t)^2 \rangle$ for a collection of particles starting at $x_0 = 0$. Since $G(x - x_0, t)$ is the solution of the diffusion equation with initial condition $\delta(x - x_0)$, we can compute the mean square displacement from

$$\begin{aligned}
\langle x(t)^2 \rangle &= \int_{-\infty}^{\infty} dx\, x^2\, G(x, t) \\
&= \int_{-\infty}^{\infty} dx\, \frac{x^2}{\sqrt{4\pi Dt}} e^{-\frac{x^2}{4Dt}} \\
&= \frac{\sqrt{\alpha}}{\sqrt{\pi}} \int_{-\infty}^{\infty} dx\, x^2 e^{-\alpha x^2}
\end{aligned} \tag{137}$$

where $\alpha = 1/(4Dt)$. To evaluate the integral, note that

$$\int_{-\infty}^{\infty} dx\, x^2 e^{-\alpha x^2} = -\frac{d}{d\alpha} \int_{-\infty}^{\infty} dx\, e^{-\alpha x^2} = -\frac{d}{d\alpha} \sqrt{\frac{\pi}{\alpha}} = \frac{\pi}{2\alpha^{3/2}}. \tag{138}$$

which then gives

$$\langle x(t)^2 \rangle = \frac{1}{2\alpha} = 2Dt. \tag{139}$$

We have thus recovered the fundamental result that the mean square displacement of Brownian particles grows linearly in time.

6.3   Zero-flux solution: Sedimentation

Consider spherical particles diffusing under the effect of a constant drift velocity u in one dimension, described by the conservation law

$$\frac{\partial n}{\partial t} = -\frac{\partial}{\partial x} J_x \tag{140}$$

with current

$$J_x = un - D\frac{\partial}{\partial x} n. \tag{141}$$

Interpreting $x > 0$ as the distance from the bottom of a vessel and assuming reflective boundaries at $x = 0$, we may think of u arising from the effects of gravity

$$u = \frac{-gm_*}{6\pi\eta a} \tag{142}$$

where g is the gravitational acceleration, a and $m_* > 0$ denote radius and effective bouyant mass[6] of the particles, and η the viscosity of the fluid. The stationary zero-current solution, satisfying $J_x = 0$, is obtained by integrating

$$un - D\frac{\partial}{\partial x}n = 0, \tag{143}$$

yielding an exponentially decaying density profile

$$n(x) = Ce^{-x/\lambda} \tag{144}$$

with characteristic sedimentation length

$$\lambda = -\frac{D}{u} = \frac{6\pi\eta aD}{gm_*} > 0. \tag{145}$$

Sutherland and Einstein showed in 1905 that the diffusion constant D of a small particle moving in a fluid is given by

$$D = \frac{kT}{6\pi\eta a}, \tag{146}$$

where k is the Boltzmann's constant and T the temperature (measured on a Kelvin scale), implying that

$$\lambda = \frac{kT}{gm_*}. \tag{147}$$

Note that particle shape (and mass density) enter through the buoyant mass m_*.

7 Linear stability analysis and pattern formation

7.1 Linear stability analysis of fixed points for ODEs

Consider a particle (e.g., bacterium) moving in one-dimension with velocity $v(t)$, governed by the nonlinear ODE

$$\frac{d}{dt}v(t) = -(\alpha + \beta v^2)v =: f(v). \tag{148}$$

We assume that the parameter β is strictly positive, but allow α to be either positive or negative. The fixed points of Eq. (148) are, by definition, velocity values v_* that satisfy the condition $f(v_*) = 0$. For $\alpha > 0$, there exists only one fixed points $v_0 = 0$. For $\alpha < 0$, we find the three fixed points $v_0 = 0$ and $v_\pm = \pm\sqrt{-\alpha/\beta}$. That is, the system undergoes pitchfork bifurcation at the critical parameter value $\alpha = 0$.

---

[6]The buoyant mass m_* is defined as the difference between the particle mass and the mass of the liquid that is displaced by the particle. Particles heavier than water have $m_* > 0$ whereas $m_* < 0$ for gas bubbles.

To evaluate the stability of a fixed points v_*, we can linearize the nonlinear equation (148) in the vicinity of the fixed points by considering small perturbations

$$v(t) = v_* + \delta v(t). \tag{149}$$

By inserting this perturbation ansatz into (148) and noting that, to leading order,

$$f(v_* + \delta v) \quad f(v_*) + f'(v_*)\,\delta v = f'(v_*)\,\delta v, \tag{150}$$

we find that the growth of the perturbation $\delta v(t)$ is governed by the linear ODE

$$\frac{d}{dt}\delta v(t) = f'(v_*)\,\delta v(t), \tag{151}$$

which has the solution

$$\delta v(t) = \delta v(0)\,e^{f'(v_*)t}. \tag{152}$$

If $f'(v_*) > 0$, then the perturbation will grow and the fixed point is said to be linearly unstable. whereas for $f'(v_*) < 0$ the perturbation will decay implying that the fixed point is stable.

For our specific example, we find

$$f'(v_0) = -\alpha\,, \qquad f'(v_\pm) = -(\alpha + 3\beta v_\pm^2) = 2\alpha \tag{153}$$

This means that for $\alpha > 0$, the fixed point $v_0 = 0$ is stable, indicating that the particle will be damped to rest in this case. By contrast, for $\alpha < 0$, the fixed point v_0 becomes unstable and the new fixed points $v_\pm = \pm\sqrt{-\alpha/\beta}$ become stable; that is, for $\alpha < 0$ the particle will be driven to a non-vanishing stationary speed. Equation (148) with $\alpha < 0$ defines one of the simplest models of active particle motion.

7.2 Stability analysis for PDEs

The above ideas can be readily extended to PDEs. To illustrate this, consider a scalar density $n(x,t)$ on the interval $[0, L]$, governed by the diffusion equation

$$\frac{\partial n}{\partial t} = D\frac{\partial^2 n}{\partial x^2} \tag{154a}$$

with reflecting boundary conditions,

$$\frac{\partial n}{\partial x}(0, t) = \frac{\partial n}{\partial t}(L, t) = 0. \tag{154b}$$

This dynamics defined by Eqs. (154) conserves the total 'mass'

$$N(t) = \int_0^L dx\, n(x, t) \equiv N_0, \tag{155}$$

and a spatially homogeneous stationary solution is given by

$$n_0 = N_0/L. \tag{156}$$

To evaluate its stability, we can consider wave-like perturbations

$$n(x,t) = n_0 + \delta n(x,t) , \qquad \delta n = \epsilon \, e^{\sigma t - ikx}. \tag{157}$$

Inserting this perturbation ansatz into (154) gives the dispersion relation

$$\sigma(k) = -Dk^2 \geq 0, \tag{158}$$

signaling that n_0 is a stable solution, because all modes with $k > 0$ become exponentially damped.

7.3 Swift-Hohenberg theory of pattern formation

As a simple generalization of (154), we consider the simplest isotropic fourth-order PDE model for a non-conserved real-valued order-parameter $\psi(\mathbf{x}, t)$ in two space dimensions $\mathbf{x} = (x, y)$, given by

$$\partial_t \psi = F(\psi) + \gamma_0 \nabla^2 \psi - \gamma_2 (\nabla^2)^2 \psi, \tag{159}$$

where $\partial_t = \partial/\partial t$ denotes the time derivative, and $\nabla = (\partial/\partial x, \partial/\partial y)$ is the two-dimensional Laplacian. The force F is derived from a Landau-potential $U(\psi)$

$$F = -\frac{\partial U}{\partial \psi}, \qquad U(\psi) = \frac{a}{2}\psi^2 + \frac{b}{3}\psi^3 + \frac{c}{4}\psi^4, \tag{160}$$

where $c > 0$ to ensure stability. The appearance of higher-order spatial derivatives means that this model accounts for longer-range effects than the diffusion equation. This becomes immediately clear when one writes a (159) in a discretized form as necessary, for example, when trying to solve this equation numerically on a space-time grid: second-order spatial derivatives require information about field values at nearest neighbors, whereas fourth-order derivatives involves field values at next-to-nearest neighbors. In this sense, higher-than-second-order PDE models, such as the Swift-Hohenberg model (159), are more 'nonlocal' than the diffusion equation (154).

The field ψ could, for example, quantify local energy fluctuations, local alignment, phase differences, or vorticity. In general, it is very challenging to derive the exact functional dependence between macroscopic transport coefficients $(a, b, c, \gamma_1, \gamma_2)$ and microscopic interaction parameters. With regard to practical applications, however, it is often sufficient to view transport coefficients as purely phenomenological parameters that can be determined by matching the solutions of continuum models, such as the one defined by Eqs. (159) and (160), to experimental data. This is analogous to treating the viscosity in the classical Navier-Stokes equations as a phenomenological fit parameter. The actual predictive strength of a continuum model lies in the fact that, once the parameter values have been determined for a given set-up, the theory can be used to obtain predictions for how the system should behave in different geometries or under changes of the boundary conditions (externally imposed shear, etc.). In some cases, it may also be possible to deduce qualitative parameter dependencies from physical or biological considerations. For instance, if ψ describes vorticity or local angular momentum in an isolated 'active' fluid, say a bacterial suspension, then transitions from $a > 0$ to $a < 0$ or $\gamma_0 > 0$ to $\gamma_0 < 0$, which both lead to non-zero flow patterns, must be connected to the microscopic self-swimming speed v_0 of the

bacteria. Assuming a linear relation, this suggests that, to leading order, $a_0 = \delta - \alpha v_0$ where $\delta > 0$ is a passive damping contribution and $\alpha v_0 > 0$ the active part, and similarly for γ_0. It may be worthwhile to stress at this point that higher-than-second-order spatial derivatives can also be present in passive systems, but their effects on the dynamics will usually be small as long as $\gamma_0 > 0$. If, however, physical or biological mechanisms can cause γ_0 to become negative, then higher-order damping terms, such as the γ_2-term in (159), cannot be neglected any longer as they are essential for ensuring stability at large wave-numbers, as we shall see next.

Linear stability analysis   The fixed points of (159) are determined by the zeros of the force $F(\psi)$, corresponding to the minima of the potential U, yielding

$$\psi_0 = 0 \tag{161a}$$

and

$$\psi_\pm = -\frac{b}{2c} \pm \sqrt{\frac{b^2}{4c^2} - \frac{a}{c}}, \qquad \text{if} \quad b^2 > 4ac. \tag{161b}$$

Linearization of (159) near ψ_0 for small perturbations

$$\delta\psi = \epsilon_0 \exp(\sigma_0 t - i\mathbf{k} \cdot \mathbf{x}) \tag{162}$$

gives

$$\sigma_0(\mathbf{k}) = -(a + \gamma_0 \, \mathbf{k}^{\,2} + \gamma_2 \, \mathbf{k}^{\,4}). \tag{163}$$

Similarly, one finds for

$$\psi = \psi_\pm + \epsilon_\pm \exp(\sigma_\pm t - i\mathbf{k} \cdot \mathbf{x}) \tag{164}$$

the dispersion relation

$$\sigma_\pm(\mathbf{k}) = -\left[-(2a + b\psi_\pm) + \gamma_0 |\mathbf{k}|^2 + \gamma_2 |\mathbf{k}|^4\right]. \tag{165}$$

In both cases, k-modes with $\sigma > 0$ are unstable. From Eqs. (163) and (165), we see immediately that $\gamma_2 > 0$ is required to ensure small-wavelength stability of the theory and, furthermore, that non-trivial dynamics can be expected if a and/or γ_0 take negative values. In particular, all three fixed points can become simultaneously unstable if $\gamma_0 < 0$.

Symmetry breaking   In the context biological systems, the minimal model (159) is useful for illustrating how microscopic symmetry-breaking mechanisms that affect the motion of individual microorganisms or cells can be implemented into macroscopic field equations that describe large collections of such cells. To demonstrate this, we interpret ψ as a vorticity-like 2D pseudo-scalar field that quantifies local angular momentum in a dense microbial suspension, assumed to be confined to a thin quasi-2D layer of fluid. If the confinement mechanism is top-bottom symmetric, as for example in a thin free-standing bacterial film, then one would expect that vortices of either handedness are equally likely. In this case,
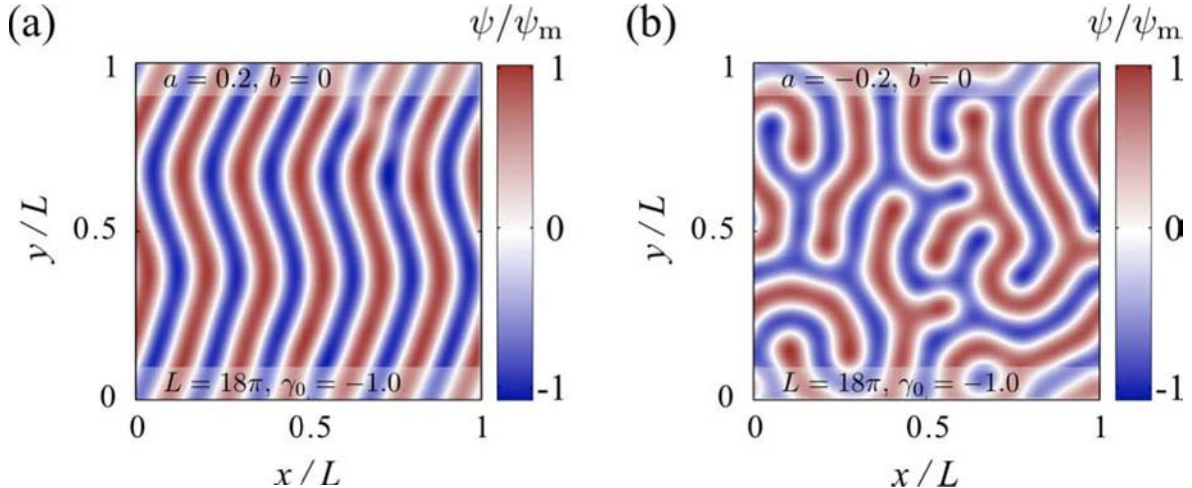
Figure 1: Numerical illustration of structural transitions in the order-parameter ψ for symmetric (a) mono-stable and (b) bi-stable potentials $U(\psi)$ with $b = 0$. (c) Snapshots of the order-parameter field ψ at $t = 500$, scaled by the maximum value ψ_m, for a mono-stable potential $U(\psi)$ and homogeneous random initial conditions. (b) Snapshots of the order-parameter at $t = 500$ for a bi-stable potential. For $\gamma_0 \ll -(2\pi)^2 \gamma_2 / L^2$, increasingly more complex quasi-stationary structures arise; qualitatively similar patterns have been observed in excited granular media and chemical reaction systems.

(159) must be invariant under $\psi \to -\psi$, implying that $U(\psi) = U(-\psi)$ and, therefore, $b = 0$ in (160). Intuitively, the transformation $\psi \to -\psi$ corresponds to a reflection of the observer position at the midplane of the film (watching the 2D layer from above *vs.* watching it from below).

The situation can be rather different, however, if we consider the dynamics of microorganisms close to a liquid-solid interface, such as the motion of bacteria or sperms cells in the vicinity of a glass slide (Fig. 2). In this case, it is known that the trajectory of a swimming cell can exhibit a preferred handedness. For example, the bacteria *Escherichia coli* and *Caulobacter* have been observed to swim in circles when confined near to a solid surface. More precisely, due to an intrinsic chirality in their swimming apparatus, these organisms move on circular orbits in clockwise (anticlockwise) direction when viewed from inside the bulk fluid (glass surface). Qualitatively similar behavior has also been reported for sea urchin sperm swimming close to solid surfaces.

Hence, for various types of swimming microorganisms, the presence of the near-by no-slip boundary breaks the reflection symmetry, $\psi \not\to -\psi$. The simplest way of accounting for this in a macroscopic continuum model is to adapt the potential $U(\psi)$ by permitting values $b \neq 0$ in (160). The result of a simulation with $b > 0$ is shown in Fig. 2a. In contrast to the symmetric case $b = 0$ (compare Fig. 1c), an asymmetric potential favors the formation of stable hexagonal patterns (Fig. 2a) – such self-assembled hexagonal vortex lattices have indeed been observed experimentally for highly concentrated spermatozoa of sea urchins (*Strongylocentrotus droebachiensis*) near a glass surface (Fig. 2b).
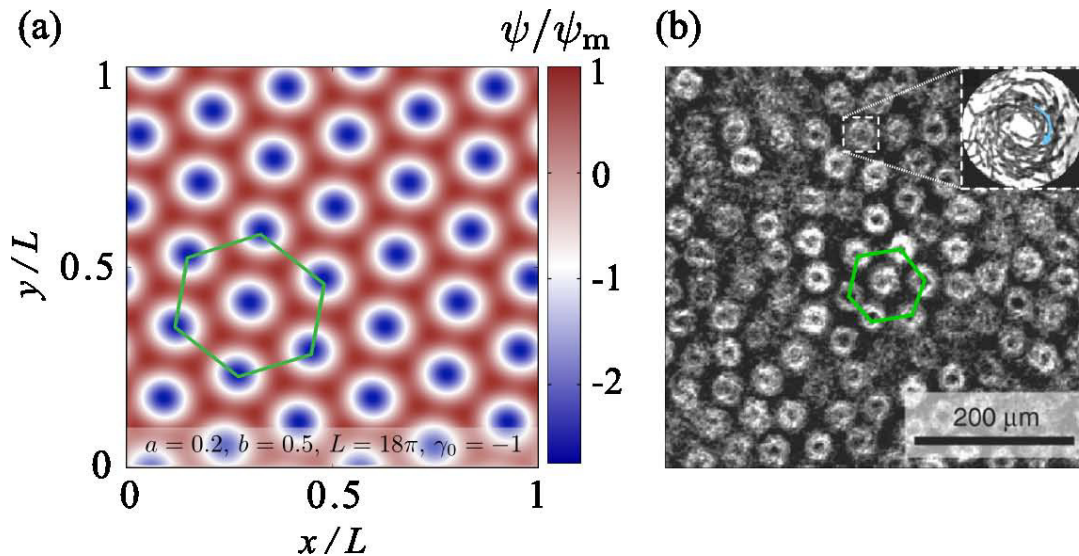
Figure 2: Effect of symmetry-breaking in the Swift-Hohenberg model. (a) Stationary hexagonal lattice of the pseudo-scalar angular momentum order-parameter ψ, scaled by the maximum value $\psi_{\rm m}$, as obtained in simulationsof Eqs. (159) and (160) with $b > 0$, corresponding to a broken reflection symmetry $\psi \not\to -\psi$. Blue regions correspond to clockwise motions. (b) Hexagonal vortex lattice formed spermatozoa of sea urchins (*Strongylocentrotus droebachiensis*) near a glass surface. At high densities, the spermatozoa assemble into vortices that rotate in clockwise direction (inset) when viewed from the bulk fluid.

7.4 Reaction-diffusion (RD) systems

RD systems provide another generic way of modeling structure formation in chemical and biological systems. The idea that RD processes could be responsible for morphogenesis goes back to a 1952 paper by Alan Turing (see class slides), and it seems fair to say that this paper is the most important one ever written in mathematical biology.

RD system can represented in the form

$$\partial_t \boldsymbol{q}(t, \boldsymbol{x}) = D\nabla^2 \boldsymbol{q} + \boldsymbol{R}(\boldsymbol{q}), \tag{166}$$

where

- $\boldsymbol{q}(t, \boldsymbol{x})$ as an n-dimensional vector field describing the concentrations of n chemical substances, species etc.

- D is a *diagonal* $n \times n$-diffusion matrix, and

- the n-dimensional vector $\boldsymbol{R}(\boldsymbol{q})$ accounts for all *local* reactions.

7.4.1 Two species in one space dimension

As a specific example, let us consider $\boldsymbol{q}(t, \boldsymbol{x}) = (u(t,x), v(t,x))$, $D = \mathrm{diag}(D_u, D_v)$ and $\boldsymbol{R} = (F(u,v), G(u,v))$, then

$$u_t = D_u u_{xx} + F(u,v) \tag{167a}$$

$$v_t = D_v v_{xx} + G(u,v) \tag{167b}$$

In general, (F, G) can be derived from the reaction/reproduction kinetics, and conservation laws may impose restrictions on permissible functions (F, G). The fixed points (u_*, v_*) of (167) are determined by the condition

$$\boldsymbol{R}(u_*, v_*) = \begin{pmatrix} F(u_*, v_*) \\ G(u_*, v_*) \end{pmatrix} = \boldsymbol{0}. \tag{168}$$

Expanding (167) for small plane-wave perturbations

$$\begin{pmatrix} u(t,x) \\ v(t,x) \end{pmatrix} = \begin{pmatrix} u_* \\ v_* \end{pmatrix} + \boldsymbol{\epsilon}(t,x) \tag{169a}$$

with

$$\boldsymbol{\epsilon} = \hat{\boldsymbol{\epsilon}}\, e^{\sigma t - ikx} = \begin{pmatrix} \hat{\epsilon} \\ \hat{\eta} \end{pmatrix} e^{\sigma t - ikx}, \tag{169b}$$

we find the linear equation

$$\sigma \hat{\boldsymbol{\epsilon}} = - \begin{pmatrix} k^2 D_u & 0 \\ 0 & k^2 D_v \end{pmatrix} \hat{\boldsymbol{\epsilon}} + \begin{pmatrix} F_u^* & F_v^* \\ G_u^* & G_v^* \end{pmatrix} \hat{\boldsymbol{\epsilon}} \equiv M\hat{\boldsymbol{\epsilon}}, \tag{170}$$

where

$$F_u^* = \partial_u F(u_*, v_*)\,, \qquad F_v^* = \partial_v F(u_*, v_*)\,, \qquad G_u^* = \partial_u G(u_*, v_*)\,, \qquad G_v^* = \partial_v G(u_*, v_*).$$

Solving this eigenvalue equation for σ, we obtain

$$\sigma_\pm = \frac{1}{2}\left\{ -(D_u + D_v)k^2 + (F_u^* + G_v^*) \pm \sqrt{4 F_v^* G_u^* + [F_u^* - G_v^* + (D_v - D_u)k^2]^2} \right\}. \tag{171}$$

In order to have an instability for some finite value k, at least one of the two eigenvalues must have a positive real part. This criterion can be easily tested for a given reaction kinetics (F, G). We still consider a popular example.

7.4.2 Lotka-Volterra model

This model describes a simple predator-prey dynamics, defined by

$$F(u,v) = Au - Buv, \tag{172a}$$

$$G(u,v) = -Cv + Euv \tag{172b}$$

with positive rate parameters $A, B, C, E > 0$. The field $u(t, x)$ measures the concentration of prey and $v(t, x)$ that of the predators. The model has two fixed points

$$(u_0, v_0) = (0, 0), \qquad (u_*, v_*) = (C/E, A/B), \tag{173}$$

with Jacobians

$$\begin{pmatrix} F_u(u_0, v_0) & F_v(u_0, v_0) \\ G_u(u_0, v_0) & G_v(u_0, v_0) \end{pmatrix} = \begin{pmatrix} A & 0 \\ 0 & -C \end{pmatrix} \tag{174a}$$

and

$$\begin{pmatrix} F_u(u_*, v_*) & F_v(u_*, v_*) \\ G_u(u_*, v_*) & G_v(u_*, v_*) \end{pmatrix} = \begin{pmatrix} A - \frac{BC}{E} & -A \\ C & -C + \frac{AE}{B} \end{pmatrix}. \tag{174b}$$

It is straightforward to verify that, for suitable choices of A, B, C, D, the model exhibits a range of unstable k-modes.

8 Variational Calculus

In this part of the course, we consider the energetics governing the shape of water droplets, soap films, bending beams etc. For systems with a few degrees of freedom (e.g., particle mechanics) you are used to the idea of solving equations of the form

$$\frac{d^2 x}{dt^2} = -\frac{dU(x)}{dx}, \tag{175}$$

where $U(x)$ is an energy function. You will recall that the basic idea to understanding this type of equation is to first find the fixed points (the places where the force on the particle is zero) and then understand their stability. By piecing the trajectories that go into and out of the fixed points together you arrive at a complete description of how the system works, even if you can't calculate everything.

We now want to figure out how to think about solving such problems in continuous systems. In this case the state of the system is described not by discrete variables x_i but by functions $f_i(x)$. A good example of the difference is to consider a mass-spring system. If there are n masses connected by springs then we would want to know $x_i(t)$, the position of the ith mass. The limit of infinitely many small masses connected by small springs is an elastic rod, in which case we would want to know $h(x, t)$, the displacement of the rod at a given position x and time t. To develop techniques for continuous systems we consider an energy functional $U[f(x)]$, which is a function of a function. Several sorts of difficulties arise (mathematical and otherwise) when one tries to think about physical problems described by this energy using the same notions as those for finite dimensional dynamical systems. We will start by considering some simple problems.

8.1 What is the shortest path between two points?

It will come as no great surprise that it is a straight line, but lets show this to be the case. In 2D there is some function $h(x)$ that is the path between two points x_1 and x_2 (think of

$h(x)$ as the height above the x-axis). The length of the path is given by the functional

$$L[h] = \int_{x_1}^{x_2} dx \sqrt{1 + \left(\frac{dh}{dx}\right)^2}. \tag{176}$$

Now consider an alternate path $h(x) + \delta h(x)$ which is only slightly different from the previous path considered. The length of this path is

$$L[h + \delta h] = \int_{x_1}^{x_2} dx \sqrt{1 + \left(\frac{d}{dx}(h + \delta h)\right)^2}. \tag{177}$$

Taylor-expanding the integrand for small δh and keeping only terms of linear order in $\delta h' = d\delta h/dx$, we find

$$L[h + \delta h] - L[h] \simeq \int_{x_1}^{x_2} dx \frac{h' \delta h'}{\sqrt{1 + h'^2}}. \tag{178}$$

Integrating by parts gives

$$L[h + \delta h] - L[h] \simeq \left[\frac{h'}{\sqrt{1 + h'^2}} \delta h\right]_{x_1}^{x_2} - \int_{x_1}^{x_2} dx \left(\frac{h'}{\sqrt{1 + h'^2}}\right)' \delta h. \tag{179}$$

The first term on the right hand side is identically zero, as we require δh to be zero at either end (since we know our starting and ending point). Otherwise, for our path to be a minimum we require δL to be zero for arbitrary δh. If this were not the case we could always choose a δh and $-\delta h$ to increase or decrease the path length. Thus $h(x)$ must satisfy

$$\left(\frac{h'}{\sqrt{1 + h'^2}}\right)' = 0, \tag{180}$$

the solution of which is a straight line (check this for yourself). By analogy with systems containing few degrees of freedom we say that this solution satisfies the condition $\delta L/\delta h = 0$.

8.2 Functional differentiation

We now generalize the example from the previous section by defining a formal functional derivative. To this end consider a general functional $I[f]$ of some function $f(x)$. A functionals is, by definition, a map that assigns a number to a function $f(x)$. Basic examples are the delta-functional $\Delta_{x_0}[f] := f(x_0)$, which is related to the delta function by

$$\Delta_{x_0}[f] = \int_{-\infty}^{\infty} dx\, \delta(x - x_0) f(x) = f(x_0), \tag{181a}$$

or integrals

$$J[f] = \int_{-\infty}^{\infty} dx\, f(x)\, c(x). \tag{181b}$$

A functional I is called *linear*, if it satisfies

$$I[af + bg] = aI[f] + bI[g] \tag{182}$$

39

for arbitrary numbers a, b and functions f, g. Obviously, both examples in Eq. (181) are linear. Typical examples of nonlinear functionals are action functionals, such as

$$S[x, \dot{x}] = \int_0^t ds \, \left[\frac{m}{2} \dot{x}(s)^2 - V(x(s)) \right],$$ (183)

where, for example, $V(x) = kx^2/2$ for the harmonic oscillator.

Given some functional $I[f]$, we can define its point-wise *functional derivative* by

$$\frac{\delta I[f]}{\delta f(y)} = \lim_{\epsilon \to 0} \frac{1}{\epsilon} \{ I[f(x) + \epsilon \delta(x - y)] - I[f(x)] \}$$ (184)

If I is linear, this simplifies to

$$\frac{\delta I[f]}{\delta f(y)} = I[\delta(x - y)],$$ (185)

yielding, for example,

$$\frac{\delta \Delta_{x_0}[f]}{\delta f(y)} = \int dx \, \delta(x - x_0)\delta(x - y) = \delta(x_0 - y_0)$$ (186a)

and

$$\frac{\delta J[f]}{\delta f(y)} = \int dx \, \delta(x - y)c(x) = c(y).$$ (186b)

Similar to ordinary derivatives, functional derivatives are linear[7]

$$\frac{\delta}{\delta f} \{ aF[f] + bG[f] \} = a \frac{\delta F}{\delta f} + b \frac{\delta G}{\delta f}, \qquad a, b \in \mathbb{R},$$ (187a)

satisfy the product rule

$$\frac{\delta}{\delta f} \{ F[f]G[f] \} = \frac{\delta F}{\delta f} G[f] + F \frac{\delta G}{\delta f}$$ (187b)

as well as *two* chain rules

$$\frac{\delta}{\delta f}(F[g(f)]) = \frac{\delta(F[g(f)])}{\delta g} \frac{dg(x)}{df(x)}$$ (187c)

$$\frac{\delta}{\delta f} g(F[f]) = \frac{dg(F[f])}{dF} \frac{\delta(F[f])}{\delta f}$$ (187d)

As a nice little exercise, you can use the above properties to prove that the exponential functional

$$F[f] = e^{\int dx \, f(x)c(x)}$$ (188)

satisfies the *functional differential equation*

$$\frac{\delta F[f]}{\delta f(y)} = c(y) \, F[f].$$ (189)

---

[7]See, e.g., Appendix A in Parr & Young, *Density-Functional Theory of Atoms and Molecules* (1989, Oxford University Press)

8.3 Euler-Lagrange equations

In practice, relevant functionals typically not just depend on a function but also on its derivatives, see Eq. (183). For instance, let us assume we are looking for a twice differentiable function $Y(x)$, satisfying the boundary conditions $Y(x_1) = y_1$, $Y(x_2) = y_2$ and minimizing the integral

$$I[Y] = \int_{x_1}^{x_2} f(x, Y, Y')dx. \tag{190}$$

What is the differential equation satisfied by $Y(x)$? To answer this question, we compute the functional derivative

$$
\begin{aligned}
\frac{\delta I[Y]}{\delta Y} &= \lim_{\epsilon \to 0} \frac{1}{\epsilon} \{ I[Y(x) + \epsilon\delta(x - y)] - I[Y(x)] \} \\
&= \int_{x_1}^{x_2} \left[\frac{\partial f}{\partial Y}\delta(x - y) + \frac{\partial f}{\partial Y'}\delta'(x - y) \right] dx \\
&= \int_{x_1}^{x_2} \left[\frac{\partial f}{\partial Y} - \frac{d}{dx}\frac{\partial f}{\partial Y'} \right] \delta(x - y)dx. \tag{191}
\end{aligned}
$$

Equating this to zero, yields the Euler-Lagrange equations

$$0 = \frac{\partial f}{\partial Y} - \frac{d}{dx}\frac{\partial f}{\partial Y'} \tag{192}$$

It should be noted that the condition $\delta I/\delta Y = 0$ alone is not a sufficient condition for a minimum. In fact, the relation might even indicate a maximum. It is often possible, however, to convince oneself that no maximum exists for the integral (e.g., the distance along a smooth path can be made as long as we like), and that our solution is a minimum. To be rigorous, however, one should also consider the possibility that the minimum is merely a local minimum, or perhaps the relation $\delta I/\delta Y = 0$ indicates a point of inflexion.

It is easy to check that Eq. (192) yields the Newton equations

$$m\ddot{x} = -V'(x), \tag{193}$$

when applied to the action functional (183). Similarly, the Euler-Lagrange equations for the shortest-path integral (176) just give the ODE (180).

8.4 Brachistrochrone

In June 1696, Johann Bernoulli set the following problem: Given two points A and B in a vertical plane, find the path from A to B that takes the shortest time for a particle moving under gravity without friction. This proposal marked the real beginning of general interest in the calculus of variations. (The term 'brachistochrone' derives from the Greek *brachistos* meaning shortest and *chronos* meaning time.)

If the particle starts with zero initial speed at height h_0, energy conservation requires $mv^2/2 = mg(h_0 - h(x))$, where v is particle speed, h_0 is the original height of the particle and $h(x)$ is the height of the particle at position x. Thus

$$v = \sqrt{2g(h_0 - h(x))}. \tag{194}$$

By definition $v = ds/dt$ so that the time taken to go from A to B is

$$\int_A^B dt = \int_A^B \frac{ds}{\sqrt{2g[h_0 - h(x)]}}. \tag{195}$$

We know that $ds = \sqrt{1 + h'^2}$, so that the time taken is

$$T[h] = \int_A^B dx \sqrt{\frac{1 + h'^2}{2g(h_0 - h)}}. \tag{196}$$

The integrand

$$f = \sqrt{\frac{1 + h'^2}{2g(h_0 - h)}} \tag{197}$$

determines the time of descent. We can insert f directly into the Euler-Lagrange equation (192) to obtain the ODE that governs the shortest-time solution. Here, we shall pursue a slightly different approach by starting from the readily verifiable identity

$$\frac{d}{dx}\left(h' \frac{\partial f}{\partial h'} - f\right) = 0, \tag{198}$$

which integrates to

$$h' \frac{\partial f}{\partial h'} - f = C, \tag{199}$$

with some constant C. Substituting for f we obtain explicitly

$$\frac{h'^2}{\sqrt{(h_0 - h)(1 + h'^2)}} - \sqrt{\frac{1 + h'^2}{h_0 - h}} = C. \tag{200}$$

Solving this for h' and integrating both sides of the expression, we obtain

$$x = \int dh \frac{\sqrt{h_0 - h}}{\sqrt{2a - (h_0 - h)}}, \tag{201}$$

where $C = (2a)^{-\frac{1}{2}}$. To evaluate this integral we substitute $h_0 - h = 2a \sin^2 \frac{\theta}{2}$ and obtain

$$x = 2a \int \sin^2 \frac{\theta}{2} d\theta + x_0 = a(\theta - \sin \theta) + x_0. \tag{202}$$

We have thus found a parametric representation for the desired curve of most rapid descent:

$$x = x_0 + a(\theta - \sin \theta), \quad h = h_0 - a(1 - \cos \theta). \tag{203}$$

These are the equations of a cycloid generated by the motion of a fixed point on the circumference of a circle of radius a, which rolls on the negative side of the given line $h = h_0$. By adjustments of the arbitrary constants, a and x_0 it is always possible to construct one and only one cycloid of which one arch contains the two points between which the brachistochrone is required to extend. Moreover, this arc renders the time of descent an absolute minimum compared with all other arcs.

42

9 Surface Tension

Moving on, we shall now use our knowledge of variational principles to investigate the shape of water droplets and soap films. The surface S of a droplet has energy

$$E[S] = \gamma \int dS \tag{204}$$

with the coefficient of proportionality γ being the *surface tension*. The questions we now want to answer are: What are the equilibrium shapes predicted by this energy? How can we incorporate constraints, such as fixed volume, into the problem? Is the solution stable? First we will look at the problem in one dimension, and then extend our analysis to many dimensions.

9.1 Two-dimensional bubble

Consider a two-dimensional bubble, corresponding to an area B confined by a non-intersecting closed path ∂B in the plane. Let's assume we can describe parameterize path by $y(x)$. The surface energy is

$$E[y] = \gamma \int_{\partial B} ds = \gamma \int_{\partial B} dx \sqrt{1 + y'^2}. \tag{205}$$

We have already solved the problem to determine the curve that connects two points while satisfying $\delta E/\delta y = 0$, the solution being a straight line. Now we need to introduce the constraint of a fixed volume, and this is done by adding a Lagrange multiplier. Thus we consider the functional

$$E[y] = \gamma \int_{\partial B} dx \sqrt{1 + y'^2} - \lambda \int_B dx \, y \tag{206}$$

the second integral being the volume of the bubble. We combine this into

$$E[y] = \int dx \left[\gamma \sqrt{1 + y'^2} - \lambda y \right] \tag{207}$$

Inserting the integrand into the Euler-Lagrange equations gives

$$\gamma \left(\frac{y'}{\sqrt{1 + y'^2}} \right)' = \lambda. \tag{208}$$

The term on the left hand side is called the *mean curvature* of the surface, and the solution is readily shown to be a circle (as we expect). You can test this yourself since you know the equation of a circle is just $x^2 + y^2 = r^2$.

9.2 Soap film between two hoops

Now lets be a little more ambitious and consider a cylindrically symmetric two dimensional surface, confined by two parallel rings located at $x = -a$ and $x = a$. Given the axi-symmetry of the problem, we may express the surface energy is

$$E = \gamma \int_A dA = \gamma \int_A 2\pi r \, ds. \tag{209}$$

The arclength ds is simply $\sqrt{1+r'^2}dx$, and we see that through symmetry we have reduced this to a one dimensional problem. The problem to be solved is now

$$E[r] = 2\pi\gamma \int_{-a}^{a} dx\, r\sqrt{1+r'^2} \overset{!}{=} \min. \tag{210}$$

Putting the integrand into the Euler-Lagrange equation gives

$$\sqrt{1+r'^2} - \frac{d}{dx}\left(\frac{rr'}{\sqrt{1+r'^2}}\right) = 0 \tag{211}$$

which can be simplified to

$$rr'' - r'^2 = 1 \tag{212}$$

We can see immediately that a particular solution of this equation is given by the *catenoid*[8]

$$r = a\cosh(x/a), \tag{213}$$

which corresponds to the special case $R/a = \cosh(1)$. For other ratios, we need to solve (212) numerically.

9.3 Rayleigh-Plateau Instability

In the previous section, we considered the shape of a soap film, stretched between two hoops. We know, however, that the film breaks after a certain extension, but it is not clear that there is anything in our problem to account for this. What is wrong? To answer this question we must analyze the stability of the solution we have found. This is a topic that we will address in more detail later on in the course, but shall touch upon now.

In one-dimensional calculus we check if our extremum is a maximum or a minimum, and if it is the former it is unstable. We now adopt the same approach in variational calculus, and consider the instability of a thin cylinder of fluid. This was studied by Plateau in the 1870's, who was interested in the formation of droplets from a jet. In cylindrical coordinates $y(x) = r_0$ for the perfect cylinder. The cylinder has surface energy and we look for an extremum by considering the functional

$$E[r] = \gamma \int dx\, 2\pi r\sqrt{1+r'^2} - \lambda \int dx\, \pi r^2, \tag{214}$$

where the second part is just the volume constraint.

We shall perturb the shape and show that if the wavelength of disturbance is greater than $2\pi r_0$, the energy of the system decreases. Using the analysis from above, we know that an extremum is required to satisfy the Euler-Lagrange equations

$$\gamma\left[\frac{1}{\sqrt{1+r'^2}} - \frac{r\,r''}{(1+r'^2)^{3/2}}\right] = \lambda r. \tag{215}$$

---

[8]You can find more soap film solutions at http://www.susqu.edu/brakke/evolver/evolver.html. There, you will also download a surface evolver code to investigate minimal surfaces in more detail.

For the perfect cylinder $y(x) = r_0$ is a solution with $\lambda = \gamma/r_0$. Note that λ has dimensions of force/area, and is in fact the pressure. We now consider a perturbation such that

$$r(x) = r_0 + \epsilon \cos kx. \tag{216}$$

This perturbation is in some sense arbitrary, because any perturbation can be decomposed into sines and cosines. Thus

$$E[r] = \gamma \int \left[2\pi(r_0 + \epsilon \cos kx)\sqrt{1 + \epsilon^2 k^2 \sin^2 kx} - \frac{\pi}{r_0}(r_0 + \epsilon \cos kx)^2 \right] dx. \tag{217}$$

Assuming that ϵ is small, we can expand the square root, yielding

$$E[r] = \gamma \int \left[2\pi(r_0 + \epsilon \cos kx)\left(1 + \frac{1}{2}\epsilon^2 k^2 \sin^2 kx\right) - \frac{\pi}{r_0}(r_0 + \epsilon \cos kx)^2 \right] dx. \tag{218}$$

Expanding everything out, we find that terms linear in ϵ cancel out, and we are left with

$$E[r] = \gamma \int \pi r_0 dx + \epsilon^2 \gamma \pi \int \left[r_0 k^2 \sin^2 kx - \frac{\cos^2 kx}{r_0} \right] dx. \tag{219}$$

The first term corresponds to the energy E_0 of the undeformed problem, so we are really interested in the sign of the second integral ΔE. If it is positive then the energy is increased as a result of the perturbation, and the system will be stable. However, if the integral is negative, then by perturbing the system the energy is decreased, and the system must be unstable.

Since the disturbance is periodic, we integrate over one wavelength, $2\pi/k$, to determine the energy per wavelength. We know that

$$\int_0^{2\pi} dx \, \sin^2 kx = \int_0^{2\pi} dx \, \cos^2 kx = \frac{\pi}{k}, \tag{220}$$

so that the energy change, ΔE, is

$$\Delta E = \epsilon^2 \gamma \pi^2 \left(r_0 k - \frac{1}{r_0 k} \right). \tag{221}$$

So now we see that if $r_0 k > 1$ the system is stable, because ΔE is positive. However, if $r_0 k < 1$ then ΔE is negative and the system is unstable. Since $k = 2\pi/\lambda$ this can be rearranged to say that the system is unstable to wavelengths λ greater $2\pi r_0$, the circumference of the cylinder. This was Plateau's results, which Rayleigh found to be wrong by a factor of $\sqrt{2}$, due to hydrodynamic effects within the cylinder (i.e., $\lambda = 2\sqrt{2}\pi r_0$ is the correct answer). The physical reasoning arises from the fact that by perturbing the cylinder you may be increasing the length of the surface along the cylinder, but you are reducing the cross sectional area. It is the trade off between these two that determines the stability.

So does this answer our question of why the soap film breaks? Perhaps. You see, if the distance between the two hoops is less than the $2\pi/r_0$, then the system is not open to long wavelength perturbations, and is therefore stable. As soon as the separation exceeds the critical wavelength, instability sets in and the bubble breaks. Note, however, that a

critical part of our stability analysis relied on the constraint of constant volume to determine instability. With the soap film this is not present, so perhaps an alternative mechanism is responsible (e.g., possibly the shape of the soap film between the two hoops becomes so eccentric that surfaces in the middle touch, and there is a pinch off?). What would happen if the ends of the two hoops were closed, so that the volume constraint did then apply? Our stability analysis would now seem more relevant. The only way to check is to now go do some experiments (a good course project!).

10 Some basic differential geometry

In the next section, we will look more closely at the the mathematical description of elastic materials. To prepare this discussion, it is useful to briefly recall a few basics of differential geometry.

10.1 Differential geometry of curves

Consider a continuous curve $\boldsymbol{r}(t) \in \mathbb{R}^3$, where $t \in [0, T]$. The length of the curve is given by

$$L = \int_0^T dt \, ||\dot{\boldsymbol{r}}(t)|| \tag{222}$$

where $\dot{\boldsymbol{r}}(t) = d\boldsymbol{r}/dt$ and $|| \cdot ||$ denotes the Euclidean norm. The local unit tangent vector is defined by

$$\boldsymbol{t} = \frac{\dot{\boldsymbol{r}}}{||\dot{\boldsymbol{r}}||}. \tag{223}$$

The unit normal vector, or unit curvature vector, is

$$\boldsymbol{n} = \frac{(\boldsymbol{I} - \boldsymbol{t}\boldsymbol{t}) \cdot \ddot{\boldsymbol{r}}}{||(\boldsymbol{I} - \boldsymbol{t}\boldsymbol{t}) \cdot \ddot{\boldsymbol{r}}||}. \tag{224}$$

Unit tangent vector $\hat{\boldsymbol{t}}(t)$ and unit normal vector $\hat{\boldsymbol{n}}(t)$ span the *osculating* ('kissing') plane at point t. The unit binormal vector is defined by

$$\boldsymbol{b} = \frac{(\boldsymbol{I} - \boldsymbol{t}\boldsymbol{t}) \cdot (\boldsymbol{I} - \boldsymbol{n}\boldsymbol{n}) \cdot \dddot{\boldsymbol{r}}}{||(\boldsymbol{I} - \boldsymbol{t}\boldsymbol{t}) \cdot (\boldsymbol{I} - \boldsymbol{n}\boldsymbol{n}) \cdot \dddot{\boldsymbol{r}}||}. \tag{225}$$

The orthonormal basis $\{\boldsymbol{t}(t), \boldsymbol{n}(t), \boldsymbol{b}(t)\}$ spans the local Frenet frame.

The local curvature $\kappa(t)$ and the associated radius of curvature $\rho(t) = 1/\kappa$ are defined by

$$\kappa(t) = \frac{\dot{\boldsymbol{t}} \cdot \boldsymbol{n}}{||\dot{\boldsymbol{r}}||}, \tag{226}$$

and the local torsion $\tau(t)$ by

$$\tau(t) = \frac{\dot{\boldsymbol{n}} \cdot \boldsymbol{b}}{||\dot{\boldsymbol{r}}||}. \tag{227}$$

Plane curves satisfy, by definition, $\boldsymbol{b} = const.$ or, equivalently, $\tau = 0$.

Given $||\dot{\boldsymbol{r}}||$, $\kappa(t)$, $\tau(t)$ and the initial values $\{\boldsymbol{t}(0), \boldsymbol{n}(0), \boldsymbol{b}(0)\}$, the Frenet frames along the curve can be obtained by solving the Frenet-Serret system

$$\frac{1}{||\dot{\boldsymbol{r}}||} \begin{pmatrix} \dot{\boldsymbol{t}} \\ \dot{\boldsymbol{n}} \\ \dot{\boldsymbol{b}} \end{pmatrix} = \begin{pmatrix} 0 & \kappa & 0 \\ -\kappa & 0 & \tau \\ 0 & -\tau & 0 \end{pmatrix} \begin{pmatrix} \boldsymbol{t} \\ \boldsymbol{n} \\ \boldsymbol{b} \end{pmatrix}. \tag{228a}$$

The above formulas simplify if t is the arc length, for in this case $||\dot{\boldsymbol{r}}|| = 1$.

As a simple example (which is equivalent to our shortest path problem) consider a polymer confined in a plane. Assume the polymer's end-points are fixed at $(x, y) = (0, 0)$ and $(x, y) = (0, L)$, respectively, and that the ground-state configuration corresponds to a straight line connecting these two points. Denoting the tension[9] by γ, adopting the parameterization $y = h(x)$ for the polymer and assuming that the bending energy is negligible, the energy relative to the ground-state is given by

$$E = \gamma \left[\int_0^L dx \sqrt{1 + h_x^2} - L \right], \tag{229}$$

where $h_x = h'(x)$. Restricting ourselves to small deformations, $|h_x| \ll 1$, we may approximate

$$E \simeq \frac{\gamma}{2} \int_0^L dx \, h_x^2. \tag{230}$$

Minimizing this expression with respect to the polymer shape h yields the Euler-Lagrange equation

$$h_{xx} = 0. \tag{231}$$

10.2 Two-dimensional surfaces

We now consider an orientable surface in $\mathbb{R}^3$. Possible local parameterizations are

$$\boldsymbol{F}(s_1, s_2) \in \mathbb{R}^3 \tag{232}$$

where $(s_1, s_2) \in U \subseteq \mathbb{R}^2$. Alternatively, if one chooses Cartesian coordinates $(s_1, s_2) = (x, y)$, then it suffices to specify

$$z = f(x, y) \tag{233a}$$

or, equivalently, the implicit representation

$$\Phi(x, y, z) = z - f(x, y). \tag{233b}$$

The vector representation (232) can be related to the 'height' representation (233a) by

$$\boldsymbol{F}(x, y) = \begin{pmatrix} x \\ y \\ f(x, y) \end{pmatrix} \tag{234}$$

---

[9]γ carries units of energy/length.

Denoting derivatives by $\boldsymbol{F}_i = \partial_{s_i}\boldsymbol{F}$, we introduce the surface metric tensor $g = (g_{ij})$ by

$$g_{ij} = \boldsymbol{F}_i \cdot \boldsymbol{F}_j, \tag{235a}$$

abbreviate its determinant by

$$|g| := \det g, \tag{235b}$$

and define the associated Laplace-Beltrami operator ∇^2 by

$$\nabla^2 h = \frac{1}{\sqrt{|g|}} \partial_i(g_{ij}^{-1}\sqrt{|g|}\partial_j h), \tag{235c}$$

for some function $h(s_1, s_2)$. For the Cartesian parameterization (234), one finds explicitly

$$\boldsymbol{F}_x(x, y) = \begin{pmatrix} 1 \\ 0 \\ f_x \end{pmatrix}, \qquad \boldsymbol{F}_y(x, y) = \begin{pmatrix} 0 \\ 1 \\ f_y \end{pmatrix} \tag{236}$$

and, hence, the metric tensor

$$g = (g_{ij}) = \begin{pmatrix} \boldsymbol{F}_x \cdot \boldsymbol{F}_x & \boldsymbol{F}_x \cdot \boldsymbol{F}_y \\ \boldsymbol{F}_y \cdot \boldsymbol{F}_x & \boldsymbol{F}_y \cdot \boldsymbol{F}_y \end{pmatrix} = \begin{pmatrix} 1 + f_x^2 & f_x f_y \\ f_y f_x & 1 + f_y^2 \end{pmatrix} \tag{237a}$$

and its determinant

$$|g| = 1 + f_x^2 + f_y^2, \tag{237b}$$

where $f_x = \partial_x f$ and $f_y = \partial_y f$. For later use, we still note that the inverse of the metric tensor is given by

$$g^{-1} = (g_{ij}^{-1}) = \frac{1}{1 + f_x^2 + f_y^2} \begin{pmatrix} 1 + f_y^2 & -f_x f_y \\ -f_y f_x & 1 + f_x^2 \end{pmatrix}. \tag{237c}$$

Assuming the surface is regular at (s_1, s_2), which just means that the tangent vectors $\boldsymbol{F}_1$ and $\boldsymbol{F}_2$ are linearly independent, the local unit normal vector is defined by

$$\boldsymbol{N} = \frac{\boldsymbol{F}_1 \wedge \boldsymbol{F}_2}{||\boldsymbol{F}_1 \wedge \boldsymbol{F}_2||}. \tag{238}$$

In terms of the Cartesian parameterization, this can also be rewritten as

$$\boldsymbol{N} = \frac{\nabla\Phi}{||\nabla\Phi||} = \frac{1}{\sqrt{1 + f_x^2 + f_y^2}} \begin{pmatrix} -f_x \\ -f_y \\ 1 \end{pmatrix}. \tag{239}$$

Here, we have adopted the convention that $\{\boldsymbol{F}_1, \boldsymbol{F}_2, \boldsymbol{N}\}$ form a right-handed system.

To formulate 'geometric' energy functionals for membranes, we still require the concept of curvature, which quantifies the local bending of the membrane. We define a 2×2-curvature tensor $R = (R_{ij})$ by

$$R_{ij} = \boldsymbol{N} \cdot (\boldsymbol{F}_{ij}) \tag{240}$$

48

and local *mean curvature* H and local *Gauss curvature* K by

$$H = \frac{1}{2}\operatorname{tr}(g^{-1} \cdot R), \qquad K = \det(g^{-1} \cdot R). \tag{241}$$

Adopting the Cartesian representation (233a), we have

$$\boldsymbol{F}_{xx} = \begin{pmatrix} 0 \\ 0 \\ f_{xx} \end{pmatrix}, \qquad \boldsymbol{F}_{xy} = \boldsymbol{F}_{yx} = \begin{pmatrix} 0 \\ 0 \\ f_{xy} \end{pmatrix}, \qquad \boldsymbol{F}_{yy} = \begin{pmatrix} 0 \\ 0 \\ f_{yy} \end{pmatrix} \tag{242a}$$

yielding the curvature tensor

$$(R_{ij}) = \begin{pmatrix} \boldsymbol{N} \cdot \boldsymbol{F}_{xx} & \boldsymbol{N} \cdot \boldsymbol{F}_{xy} \\ \boldsymbol{N} \cdot \boldsymbol{F}_{yx} & \boldsymbol{N} \cdot \boldsymbol{F}_{yy} \end{pmatrix} = \frac{1}{\sqrt{1 + f_x^2 + f_y^2}} \begin{pmatrix} f_{xx} & f_{xy} \\ f_{yx} & f_{yy} \end{pmatrix} \tag{242b}$$

Denoting the eigenvalues of the matrix $g^{-1} \cdot R$ by κ_1 and κ_2, we obtain for the mean curvature

$$H = \frac{1}{2}(\kappa_1 + \kappa_2) = \frac{(1 + f_y^2)f_{xx} - 2f_x f_y f_{xy} + (1 + f_x^2)f_{yy}}{2(1 + f_x^2 + f_y^2)^{3/2}} \tag{243}$$

and for the Gauss curvature

$$K = \kappa_1 \cdot \kappa_2 = \frac{f_{xx} f_{yy} - f_{xy}^2}{(1 + f_x^2 + f_y^2)^2}. \tag{244}$$

An important result that relates curvature and topology is the Gauss-Bonnet theorem, which states that any compact two-dimensional Riemannian manifold M with smooth boundary ∂M, Gauss curvature K and geodesic curvature k_g of ∂M satisfies the integral equation

$$\int_M K \, dA + \oint_{\partial M} k_g \, ds = 2\pi \, \chi(M). \tag{245}$$

Here, dA is the area element on M, ds the line element along ∂M, and $\chi(M)$ the Euler characteristic of M. The latter is given by $\chi(M) = 2 - 2g$, where g is the *genus* (number of handles) of M. For example, the 2-sphere $M = \mathbb{S}^2$ has $g = 0$ handles and hence $\chi(\mathbb{S}^2) = 2$, whereas a two-dimensional torus $M = \mathbb{T}^2$ has $g = 1$ handle and therefore $\chi(\mathbb{T}^2) = 0$.

Equation (245) implies that, for any closed surface, the integral over K is always a constant. That is, for closed membranes, the first integral in Eq. (245) represents just a trivial (constant) energetic contribution.

10.3 Minimal surfaces

Minimal surfaces are surfaces that minimize the area within a given contour ∂M,

$$A(M|\partial M) = \int_M dA = \min! \tag{246}$$

Assuming a Cartesian parameterization $z = f(x, y)$ and abbreviating $f_i = \partial_i f$ as before, we have

$$dA = \sqrt{|g|}\, dxdy = \sqrt{1 + f_x^2 + f_y^2}\, dxdy =: \mathcal{L}\, dxdy, \tag{247}$$

and the minimum condition (246) can be expressed in terms of the Euler-Lagrange equations

$$0 = \frac{\delta A}{\delta f} = -\partial_i \frac{\partial \mathcal{L}}{\partial f_i}. \tag{248}$$

Inserting the Lagrangian $\mathcal{L} = \sqrt{|g|}$, one finds

$$0 = -\left[\partial_x \left(\frac{f_x}{\sqrt{1 + f_x^2 + f_y^2}} \right) + \partial_y \left(\frac{f_y}{\sqrt{1 + f_x^2 + f_y^2}} \right) \right] \tag{249}$$

which may be recast in the form

$$0 = \frac{(1 + f_y^2)f_{xx} - 2f_x f_y f_{xy} + (1 + f_x^2)f_{yy}}{(1 + f_x^2 + f_y^2)^{3/2}} = -2H. \tag{250}$$

Thus, minimal surfaces satisfy

$$H = 0 \qquad \Leftrightarrow \qquad \kappa_1 = -\kappa_2, \tag{251}$$

implying that each point of a minimal surface is a saddle point.

10.4   Helfrich's model

Assuming that lipid bilayer membranes can be viewed as two-dimensional surfaces, Helfrich proposed in 1973 the following geometric curvature energy per unit area for a closed membrane

$$\epsilon = \frac{k_c}{2}(2H - c_0)^2 + k_G K, \tag{252}$$

where constants k_c, k_G are bending rigidities and c_0 is the spontaneous curvature of the membrane. The full free energy for a closed membrane can then be written as

$$E_c = \int dA\, \epsilon + \sigma \int dA + \Delta p \int dV, \tag{253}$$

where σ is the surface tension and Δp the osmotic pressure (outer pressure minus inner pressure). Minimizing F with respect to the surface shape, one finds after some heroic manipulations the shape equation[10]

$$\Delta p - 2\sigma H + k_c(2H - c_0)(2H^2 + c_0 H - 2K) + k_c \nabla^2(2H - c_0) = 0, \tag{254}$$

---

[10]The full derivation can be found in Chapter 3 of Z.-C. Ou-Yang, *Geometric Methods in the Elastic Theory of Membranes in Liquid Crystal Phases* (World Scientific, Singapore, 1999).

where ∇^2 is the Laplace-Beltrami operator on the surface. The derivation of Eq. (254) uses our earlier result

$$\frac{\delta A}{\delta f} = -2H, \tag{255}$$

and the fact that the volume integral may be rewritten as[11]

$$V = \int dV = \int dA \, \frac{1}{3} \mathbf{F} \cdot \mathbf{N} \,, \tag{256}$$

which gives

$$\frac{\delta V}{\delta f} = 1, \tag{257}$$

corresponding to the first term on the rhs. of Eq. (254).

For open membranes with boundary ∂M, there is no volume constraint and a plausible energy functional reads

$$E_o = \int dA \, \epsilon + \sigma \int dA + \gamma \oint_{\partial M} ds, \tag{258}$$

where γ is the line tension of the boundary. In this case, variation yields not only the corresponding shape equation but also a non-trivial set of boundary conditions.

11 Elasticity

What shape does a piece of paper take when we push it in at the ends? To answer this question let's acquaint ourselves with another continuum approximation, used to describe the deformation of elastic solids (we might actually have studied this before our work on fluids, as it is conceptually simpler). We first need to find a way to describe stress and strain within the solid, and then determine the relation between the two. Then we can derive the equations of elasticity and apply them to the buckling of a thin plate.

11.1 Strain

If a solid is deformed, then points within the solid will move. We fix our attention on a single point, whose coordinates are (x_1, x_2, x_3), and the close neighborhood of this point. We suppose that in the strained state the Cartesian coordinates of the same point have become (x'_1, x'_2, x'_3). The displacement of this point due to the deformation is denoted by $\boldsymbol{u} = \boldsymbol{u}(x_1, x_2, x_3)$, where

$$u_i = x'_i - x_i. \tag{259}$$

The vector $\boldsymbol{u}$ is called the *displacement vector*.

When a body is deformed the distance between its points change. Let's consider two points very close together. If the vector joining them before is dx_i, the vector joining them in

---

[11]Here, we made use of the volume formula $dV = \frac{1}{3} h \, dA$ for a cone or pyramid of height $h = \mathbf{F} \cdot \mathbf{N}$.

the deformed body is $dx'_i = dx_i + du_i$. This distance between the points was originally $dl = \sqrt{dx_1^2 + dx_2^2 + dx_3^2}$ and is now $dl' = \sqrt{dx_1'^2 + dx_2'^2 + dx_3'^2}$. Using the summation convention, which tells us to sum over repeated indices (i.e., $a_i b_i = a_1 b_1 + a_2 b_2 + a_3 b_3$), and substituting in that $du_i = (\partial u_i/\partial x_k)dx_k$, we get

$$dl'^2 = dl^2 + 2\frac{\partial u_i}{\partial x_k}dx_i dx_k + \frac{\partial u_i}{\partial x_k}\frac{\partial u_i}{\partial x_l}dx_k dx_l. \tag{260}$$

We shall neglect the last of these terms, as we consider the u_i to be small, so that

$$dl'^2 = dl^2 + 2e_{ij}dx_i dx_j \tag{261}$$

where

$$e_{ij} = \frac{1}{2}\left(\frac{\partial u_i}{\partial x_j} + \frac{\partial u_j}{\partial x_i}\right) \tag{262}$$

are the components of the *strain tensor* $\mathbf{e}$. This is called linear elasticity (even though it is not really linear). It is often very useful to separate *pure shear* from *pure compression* effects, which can be achieved by rewriting[12]

$$e_{ij} = \left(e_{ij} - \frac{\delta_{ij}}{3}e_{ll}\right) + \frac{\delta_{ij}}{3}e_{ll} = \left(e_{ij} - \frac{\delta_{ij}}{3}\nabla\cdot\mathbf{u}\right) + \frac{\delta_{ij}}{3}\nabla\cdot\mathbf{u}. \tag{263}$$

The first part in parentheses has a vanishing trace and therefore represents pure shear.

11.2   Stress tensor

When a body is deformed, the arrangement of molecules within is changed, and forces arise that want to restore the body to its equilibrium configuration. These are called *internal stresses*, represented by a stress tensor $\sigma = (\sigma_{ij})$, and when there is no deformation the stress is zero

$$\sigma_{ik} = 0. \tag{264}$$

The three components of a force on a volume element V can be obtained from stresses by transforming a surface integral into a volume integral

$$\int_{\partial V}\sigma_{ik}dA_k = \int_V (\partial_k \sigma_{ik})dV = \int_V f_i dV \tag{265}$$

Hence, the vector f_i must be given by the divergence of the *stress tensor* σ_{ik}.

$$f_i = \frac{\partial \sigma_{ik}}{\partial x_k}. \tag{266}$$

We recognize that $\sigma_{ik}dA_k$ is the force per unit area in the i-direction on the surface element with outward normal $d\mathbf{A}$. One thing we know about the stress tensor is that it is symmetric

---

[12]In d dimensions one would simply replace $\delta_{ij}/3$ by δ_{ij}/d everywhere.

$(\sigma_{ij} = \sigma_{ji})$. If, for example, the body is in a gravitational field then the internal stresses must everywhere balance gravity, in which case the equilibrium equations are

$$\frac{\partial \sigma_{ik}}{\partial x_k} + \rho g_i = 0. \tag{267}$$

Additional external forces applied to the surface of the body will enters as boundary conditions that complement the equilibrium conditions (267). For instance, if there is an external force per unit area, $\hat{\boldsymbol{f}}$, acting over the surface, then we require

$$\sigma_{ik} n_k = \hat{f}_i, \tag{268}$$

where $\boldsymbol{n}$ is the outward unit normal on the surface.

11.3 Hooke's law

In general, we would like to use Eqs. (267) to predict the deformation of a solid body under a given force distribution. That is, we have to express the stress tensor σ_{ij} in terms of the displacement field $\boldsymbol{u}$. The main body of the mathematical theory of elasticity rests on the *assumption of a linear homogeneous relation between the elements of the stress tensor and the strain tensor*. This is just the continuum version of *Hooke's Law*. To simplify matters, let's focus on materials that are *isotropic* (i.e., the elastic properties are independent of direction). In this case

$$\sigma_{ij} = \lambda \delta_{ij}(e_{11} + e_{22} + e_{33}) + 2\mu e_{ij} = \lambda \delta_{ij} \mathrm{Tr} \boldsymbol{e} + 2\mu e_{ij} \tag{269}$$

where δ_{ij} is the Kronecker delta and λ and μ are positive elastic constants of the material, called *Lame coefficients*. The corresponding *(free) energy density E* of the body associated with deformation, obtained from the relation

$$\sigma_{ij} = \frac{\partial E}{\partial e_{ij}}, \tag{270}$$

is therefore

$$E = \frac{1}{2}\lambda e_{ii}^2 + \mu e_{ij}^2. \tag{271}$$

As stated above, the sum $e_{ii} = \mathrm{Tr} \boldsymbol{e}$ is related to the change in volume associated with a deformation. If this is zero, only the shape of the body is altered, corresponding to pure shear. Recalling our above decomposition

$$e_{ij} = (e_{ij} - \frac{1}{3}\delta_{ij}e_{ll}) + \frac{1}{3}\delta_{ij}e_{ll}. \tag{272}$$

we can obtain a general expression for the energy density of a deformed isotropic body, by replacing (271) with

$$E = \frac{1}{2}Ke_{ll}^2 + \mu(e_{ik} - \frac{1}{3}\delta_{ik}e_{ll})^2 \tag{273}$$

where K and μ positive constants, respectively called the *modulus of compression* and the *modulus of rigidity*. In 3D, K is related to the Lame coefficients by[13]

$$K = \lambda + \frac{2}{3}\mu \tag{274}$$

---

[13]In 2D, this relation becomes $K = \lambda + \mu$.

11.4 A simple problem

Consider the simple case of a beam. Let the beam be along the z-axis, and let us pull it a both ends to stretch it. The force per unit area p is uniform over each end. The resulting deformation is uniform throughout the body and, hence, so is the stress tensor. It therefore follows that all components σ_{ik} are zero except for σ_{zz}, and from the forcing condition at the end we have that $\sigma_{zz} = p$.

From the general expression that relates the components of the stress and strain tensors, we see that all components e_{ik} with $i \neq k$ are zero. The equilibrium equations are therefore

$$e_{xx} = e_{yy} = -\frac{1}{3}\left(\frac{1}{2\mu} - \frac{1}{3K}\right)p \tag{275}$$

and

$$e_{zz} = \frac{1}{3}\left(\frac{1}{\mu} + \frac{1}{3K}\right)p. \tag{276}$$

The component e_{zz} gives the lengthening of the rod, and the coefficient of p is the *coefficient of extension*. Its reciprocal is *Young's modulus*

$$Y = \frac{9K\mu}{3K + \mu}. \tag{277}$$

The components e_{xx} and e_{yy} give the relative compression of the rod in the transverse direction. The ratio of the transverse compression to the longitudinal extension is called *Poisson's ratio*, ν:

$$e_{xx} = -\nu e_{zz}, \tag{278}$$

where

$$\nu = \frac{1}{2}\left(\frac{3K - 2\mu}{3K + \mu}\right). \tag{279}$$

Since K and μ are always positive, Poisson's ratio can vary between -1 and $\frac{1}{2}$. Note that a negative value corresponds to pulling on the beam and it getting thicker! Now we see why we use Y and ν; they are easier to measure. Inverting these formulae, we get

$$\mu = \frac{Y}{2(1 + \nu)}, \qquad K = \frac{Y}{3(1 - 2\nu)}. \tag{280}$$

The free energy then becomes

$$E = \frac{Y}{2(1 + \nu)}\left(e_{ik}^2 + \frac{\nu}{1 - 2\nu}e_{ll}^2\right). \tag{281}$$

The stress tensor is given in terms of the strain tensor by

$$\sigma_{ik} = \frac{Y}{1 + \nu}\left(e_{ik} + \frac{\nu}{1 - 2\nu}e_{ll}\delta_{ik}\right). \tag{282}$$

Conversely

$$e_{ik} = \frac{1}{Y}[(1 + \nu)\sigma_{ik} - \nu\sigma_{ll}\delta_{ik}]. \tag{283}$$

11.5   Bending of a thin beam

Now we are in a position to try and calculate the shape of a bent beam. Our analysis requires that the thickness be much smaller than the lateral dimension. The deformations must also be small, such that the displacements are small compared with the thickness. Although the general equilibrium equations are greatly simplified when considering thin plates, it is more convenient not to derive our result from these. Rather, we shall use our knowledge of variational calculus to calculate afresh the energy of a bent plate, and set about varying that energy.

When a plate is bent, it is stretched at some points and compressed at others: on the convex side there is evidently an extension and on the concave side there is compression. Somewhere in the middle there is a *neutral surface*, on which there is no extension or compression. The neutral surface lies midway through the plate.

We take a coordinate system with the origin on the neutral surface and the z-axis normal to the surface. The xy-plane is that of the undeformed surface. The displacement of the neutral surface is given by $u_z = w(x, y)$. For further calculations we note that since the plate is thin, comparatively small forces on the surface are needed to bend it. These forces are always considerably less than the internal stresses caused in the deformed beam by the extension and compression of its parts. Thus we have on both surfaces of the plate

$$\sigma_{xz} = \sigma_{yz} = \sigma_{zz} = 0. \tag{284}$$

Since the plate is small, these quantities must be small within the plate if they are zero on the surface. We therefore conclude that $\sigma_{xz} = \sigma_{yz} = \sigma_{zz}$ are small everywhere, and equate them to zero. From our general formulae relating stress and strain, we have

$$\sigma_{zx} = \frac{Y}{1+\nu} e_{zx}, \qquad \sigma_{zy} = \frac{Y}{1+\nu} e_{zy}, \tag{285}$$

$$\sigma_{zz} = \frac{Y}{(1+\nu)(1-2\nu)}[(1-\nu)e_{zz} + \nu(e_{xx} + e_{yy})]. \tag{286}$$

Substituting in our expression for the the strain tensor and equating to zero, we get

$$\frac{\partial u_x}{\partial z} = -\frac{\partial u_z}{\partial x}, \qquad \frac{\partial u_y}{\partial z} = -\frac{\partial u_z}{\partial y}, \tag{287}$$

$$e_{zz} = -\frac{\nu(e_{xx} + e_{yy})}{(1-\nu)}. \tag{288}$$

In the first two of these equations u_z can be replaced by $w(x, y)$. Thus, integrating the above relations gives

$$u_x = -z\frac{\partial w}{\partial x}, \qquad u_y = -z\frac{\partial w}{\partial y}, \tag{289}$$

where the constants of integration were chosen so as to make $u_x = u_y = 0$ for $z = 0$. Knowing u_x and u_y we can now determine all the components of the strain tensor:

$$e_{xx} = -z\frac{\partial^2 w}{\partial x^2}, \qquad e_{yy} = -z\frac{\partial^2 w}{\partial y^2} \qquad e_{xy} = -z\frac{\partial^2 w}{\partial x \partial y}, \tag{290}$$

$$e_{xz} = e_{yz} = 0, \qquad e_{zz} = \frac{z\nu}{1-\nu}\left(\frac{\partial^2 w}{\partial x^2} + \frac{\partial^2 w}{\partial y^2}\right). \tag{291}$$

We now calculate the free energy of the plate, using our general formula,

$$E = z^2 \frac{Y}{1+\nu}\left[\frac{1}{2(1-\nu)}\left(\frac{\partial^2 w}{\partial x^2} + \frac{\partial^2 w}{\partial y^2}\right)^2 + \left(\frac{\partial^2 w}{\partial x \partial y}\right)^2 - \frac{\partial^2 w}{\partial x^2}\frac{\partial^2 w}{\partial y^2}\right]. \tag{292}$$

Integrating from $-\frac{h}{2}$ to $\frac{h}{2}$, where h is the thickness of the plate, then integrating again over an area element gives the free energy per unit area

$$E_A = \frac{Yh^3}{24(1-\nu^2)}\int\int\left\{\left(\frac{\partial^2 w}{\partial x^2} + \frac{\partial^2 w}{\partial y^2}\right)^2 + 2(1-\nu)\left[\left(\frac{\partial^2 w}{\partial x \partial y}\right)^2 - \frac{\partial^2 w}{\partial x^2}\frac{\partial^2 w}{\partial y^2}\right]\right\}dxdy. \tag{293}$$

where the element of area can be written $dxdy$ since the deformation is small.

We now derive the equilibrium equation for a plate from the condition that it's free energy is a minimum. To simplify things, let's just ignore any y-dependence and consider a 2D problem. Using the calculus of variations we have that the energy of the distorted beam is

$$\frac{\delta E}{\delta w} = \frac{Yh^3}{12(1-\nu^2)}\frac{d^4 w}{dx^4}. \tag{294}$$

This expression must equal the force $f(x)$ applied to deform the plate:

$$\frac{Yh^3}{12(1-\nu^2)}\frac{d^4 w}{dx^4} = f(x). \tag{295}$$

The simplest boundary conditions are if the edges are clamped, in which case

$$w = 0, \qquad \frac{dw}{dx} = 0 \tag{296}$$

at the edges. The first of these expresses the fact that the edge of the plate undergoes no deformation, and the second that it remains horizontal. For more details, see chapter 2 in *Theory of Elasticity, Landau & Lifschitz.*

12 Towards hydrodynamic equations

The previous classes focussed on the continuum description of static (time-independent) elastic systems. We become more ambitious now and look to derive the hydrodynamic equations for a system of particles obeying Newton's laws. There are two ways we can go about this: by going from the microscopic to the macroscopic scale, or by adopting a *continuum approximation* and deriving the macro-equations from general considerations.

The general principle underlying this subject is that the *macroscopic variables are quantities that are microscopically conserved.* The reason for this is simply that the entire notion of a macroscopic equation relies on scale separation with the microscopic scale. Any quantity which is not conserved microscopically necessarily varies on a macroscopic scale. The only quantities that are candidate hydrodynamic variables are therefore those which are

conserved. This simple argument shows that what we really need to do is figure out how to generalise our random walkers to something that conserves momentum and energy.

To rigorously justify the macroscopic equations of motion for a fluid (i.e., a collection of particles interacting with each other by Newton's laws) it is necessary to find a way of passing in detail from the microscopic (quantum) mechanical description, to the macroscopic description. The ideas behind this are highly related to what we have already done for the random walker, albeit with another level of complexity.

12.1 Euler equations

Instead of obtaining macroscopic equations of fluid motion from microscopic principles (this will be done in Sec. 12.2 below), we shall first derive the equations of inviscid (frictionless) hydrodynamics purely from macro-considerations alone. This requires us to adopt a continuum approximation, which assumes a macroscopic scale large compared with the distance between molecules. We assume that the fluid is continuous in structure, and physical quantities such as the mass and momentum are spread uniformly over small volume elements.

The validity of the continuum hypothesis under everyday conditions is clear, as two of the more common fluids, air and water, are so obviously continuous and smoothly varying that no different hypothesis would seem natural. One or two numbers readily show the great difference between the lengthscale representative of the fluid as a whole and that representative of the particle structure. For most laboratory experiments, a characteristic linear dimension of the region occupied by the fluid is at least 1cm, and very little variation of the physical and dynamical properties of the fluid occurs over a distance of 10^{-3}cm. Thus an instrument with a sensitive volume of 10^{-9}cm^3 would give a *local* measurement. Small though this volume is, it contains about 10^{10} molecules of air at normal temperature and pressure (and an even larger number of molecules of water), which is large enough for an average of all the molecules to be independent of their number.

The continuum hypothesis implies that it is possible to attach a definite meaning to the notion of value 'at a point' of the various fluid properties such as density, velocity and temperature, and that in general values of these quantities are continuous functions of position and time. There is ample observational evidence that common real fluids move as if they were continuous, under normal conditions and indeed for considerable departures from normal conditions. However, some of the properties of the equivalent continuous media need to be determined empirically, and cannot be derived directly from microscopic principles.

12.1.1 The continuity equation

Let's suppose the fluid density is described by a function $\rho(\boldsymbol{r}, t)$. The total mass enclosed in a *fixed* volume V is

$$\int_V \rho dV. \tag{297}$$

The mass flux leaving this volume through the bounding surface $S = \partial V$ is

$$\int_S \rho \boldsymbol{u} \cdot \boldsymbol{n} dS, \tag{298}$$

57

where $\boldsymbol{u}(\boldsymbol{x},t)$ is the velocity of the fluid and $\boldsymbol{n}$ is the outward normal. Hence we have

$$\int_V \frac{\partial \rho}{\partial t} dV = -\int_S \rho\mathbf{u} \cdot \boldsymbol{n} dS = -\int_V \nabla \cdot (\rho\boldsymbol{u}) dV. \tag{299}$$

This must hold for any arbitrary fluid element dV, thus

$$\frac{\partial \rho}{\partial t} + \nabla \cdot (\rho\boldsymbol{u}) = 0. \tag{300}$$

This is called the *continuity equation.*

For fluids like water, the density does not change very much and we will often be tempted to neglect the density variations. If we make this approximation the continuity equation reduces to the *incompressibility condition*

$$\nabla \cdot \boldsymbol{u} = 0. \tag{301}$$

Like all approximations, this one is sometimes very good and sometimes not so good. We will have to figure out where it fails.

12.1.2 Momentum equations

So far we have more unknowns than equations (three velocity components but only one equation). We now consider the conservation of linear momentum and, adopting an alternative viewpoint to that used in deriving the continuity equation, consider Newton's laws for a particular *moving* element of fluid:

$$\frac{d}{dt} \int_{V(t)} \rho\boldsymbol{u} dV = -\int_{S(t)} p\boldsymbol{n} dS + \int_{V(t)} \boldsymbol{f} dV, \tag{302}$$

where $V(t)$ is the volume of the element enclosed by the surface $S(t)$, $\boldsymbol{f}$ is the density of body forces, such as gravity $\rho\boldsymbol{g}$, and p is a pressure force. The pressure force is a normal force per unit area (usually compressive) exerted across the surface of a fluid element, and is related to both intermolecular forces and momentum transfer across an interface. For any volume, the pressure force is

$$-\int p\boldsymbol{n} dS = -\int \nabla p dV. \tag{303}$$

Both $V(t)$ and $S(t)$ are being deformed by the motion of the fluid, so if we want to take the d/dt inside the integral sign we must take account of this. The *Reynolds transport theorem* does so, and it can be shown that for a deforming, *incompressible* fluid element

$$\frac{d}{dt} \int_{V(t)} \rho\boldsymbol{u} dV = \int_{V(t)} \rho\frac{D\boldsymbol{u}}{Dt} dV \tag{304}$$

Here

$$\frac{D}{Dt} = \frac{\partial}{\partial t} + (\boldsymbol{u} \cdot \nabla) \tag{305}$$

is called the *convective derivative*, and we shall discuss it's significance in a moment. Hence, assuming that $\boldsymbol{f}$ is solely given by gravity, $\boldsymbol{f} = \rho \boldsymbol{g}$, we find

$$\int_{V(t)} \rho \frac{D\boldsymbol{u}}{Dt} dV = \int_{V(t)} (-\nabla p + \rho \boldsymbol{g}) dV \tag{306}$$

Since this must hold for any arbitrary fluid element we arrive at

$$\frac{D\boldsymbol{u}}{Dt} = \frac{-\nabla p}{\rho} + \boldsymbol{g}. \tag{307}$$

This, combined with the the continuity equation (300), constitutes the *Euler equations*. Things can be tidied up a little if we realise that the gravitational force, being conservative, can be written as the gradient of a scalar potential $\nabla \psi$. It is therefore usual to redefine pressure as $p + \psi \rightarrow p$. This implies that gravity simply modifies the pressure distribution in the fluid and does nothing to change the velocity. However, we cannot do this if ρ is not constant or if we have a free surface (as we shall see later with water waves).

Assuming the density is constant means we now have four equations in four unknowns: three components of $\boldsymbol{u}$ and p. Note that if we do not demand constant density then the equations (continuity+momentum) only close with another relation, an equation of state $p(\rho)$.

12.2 From Newton's laws to hydrodynamic equations

To complement the purely macroscopic considerations from the previous section, we will now discuss how one can obtain hydrodynamic equations from the microscopic dynamics. To this end, we consider a many-particle system governed by Newton's equations

$$\frac{d\boldsymbol{x}_i}{dt} = \boldsymbol{v}_i , \qquad m\frac{d\boldsymbol{v}_i}{dt} = \boldsymbol{F}_i, \tag{308}$$

assuming that all particles have the same mass m, and that the forces $\boldsymbol{F}_i$ can be split into an external contribution $\boldsymbol{G}$ and pair interactions $\boldsymbol{H}(\boldsymbol{r}) = -\boldsymbol{H}(-\boldsymbol{r})$

$$\boldsymbol{F}(\boldsymbol{x}_1, \ldots, \boldsymbol{x}_n) = \boldsymbol{G}(\boldsymbol{x}_i) + \sum_{j \neq i} \boldsymbol{H}(\boldsymbol{x}_i - \boldsymbol{x}_j) = -\nabla_{\boldsymbol{x}_i} \Phi(\boldsymbol{x}_1, \ldots, \boldsymbol{x}_n) \tag{309}$$

We define the fine-grained phase-space density

$$f(t, \boldsymbol{x}, \boldsymbol{v}) = \sum_{i=1}^{N} \delta(\boldsymbol{x} - \boldsymbol{x}_i(t))\delta(\boldsymbol{v} - \boldsymbol{v}_i(t)) \tag{310}$$

where $\delta(\boldsymbol{x} - \boldsymbol{x}_i) = \delta(x - x_i)\delta(y - y_i)\delta(z - z_i)$ in three dimensions. Intuitively, the density f counts the number of particles that at time t are in the small volume $[\boldsymbol{x}, \boldsymbol{x} + d\boldsymbol{x}]$ while having velocities in $[\boldsymbol{v}, \boldsymbol{v} + d\boldsymbol{v}]$. By chain and product rule

$$
\begin{aligned}
\frac{\partial}{\partial t} f &= \sum_{i=1}^{N} \frac{d}{dt} [\delta(\boldsymbol{x} - \boldsymbol{x}_i)\delta(\boldsymbol{v} - \boldsymbol{v}_i)] \\
&= \sum_{i} \{\delta(\boldsymbol{v} - \boldsymbol{v}_i)\nabla_{\boldsymbol{x}_i}\delta(\boldsymbol{x} - \boldsymbol{x}_i) \cdot \dot{\boldsymbol{x}}_i + \delta(\boldsymbol{x} - \boldsymbol{x}_i)\nabla_{\boldsymbol{v}_i}\delta(\boldsymbol{v} - \boldsymbol{v}_i) \cdot \dot{\boldsymbol{v}}_i\} \\
&= -\nabla_{\boldsymbol{x}} \sum_{i=1}^{N} \delta(\boldsymbol{v} - \boldsymbol{v}_i)\delta(\boldsymbol{x} - \boldsymbol{x}_i) \cdot \boldsymbol{v}_i - \nabla_{\boldsymbol{v}} \sum_{i=1}^{N} \delta(\boldsymbol{x} - \boldsymbol{x}_i)\delta(\boldsymbol{v} - \boldsymbol{v}_i) \cdot \frac{\boldsymbol{F}_i}{m} \quad (311)
\end{aligned}
$$

where, in the last step, we inserted Newton's equations and used that

$$\frac{\partial}{\partial x_i}\delta(x - x_i) = -\frac{\partial}{\partial x}\delta(x - x_i) \tag{312}$$

Furthermore, making use of the defining properties of the delta-function

$$
\begin{aligned}
\frac{\partial}{\partial t}f &= -\boldsymbol{v}\cdot\nabla_{\boldsymbol{x}}\sum_{i=1}^N \delta(\boldsymbol{v}-\boldsymbol{v}_i)\delta(\boldsymbol{x}-\boldsymbol{x}_i) - \nabla_{\boldsymbol{v}}\sum_{i=1}^N \delta(\boldsymbol{x}-\boldsymbol{x}_i)\delta(\boldsymbol{v}-\boldsymbol{v}_i)\cdot\frac{\boldsymbol{F}_i}{m} \\
&= -\boldsymbol{v}\cdot\nabla_{\boldsymbol{x}}f - \frac{1}{m}\nabla_{\boldsymbol{v}}\sum_{i=1}^N \delta(\boldsymbol{x}-\boldsymbol{x}_i)\delta(\boldsymbol{v}-\boldsymbol{v}_i)\cdot\boldsymbol{F}_i.
\end{aligned}
\tag{313}
$$

Writing $\nabla = \nabla_{\boldsymbol{x}}$ and inserting (309) for the forces, we may rewrite

$$
\begin{aligned}
m\left(\frac{\partial}{\partial t} + \boldsymbol{v}\cdot\nabla\right)f &= -\nabla_{\boldsymbol{v}}\sum_{i=1}^N \delta(\boldsymbol{x}-\boldsymbol{x}_i)\delta(\boldsymbol{v}-\boldsymbol{v}_i)\cdot\left[\boldsymbol{G}(\boldsymbol{x}_i) + \sum_{j\neq i}\boldsymbol{H}(\boldsymbol{x}_i-\boldsymbol{x}_j)\right] \\
&= -\nabla_{\boldsymbol{v}}\sum_{i=1}^N \delta(\boldsymbol{x}-\boldsymbol{x}_i)\delta(\boldsymbol{v}-\boldsymbol{v}_i)\cdot\left[\boldsymbol{G}(\boldsymbol{x}) + \sum_{\boldsymbol{x}_j\neq\boldsymbol{x}}\boldsymbol{H}(\boldsymbol{x}-\boldsymbol{x}_j)\right] \\
&= -\left[\boldsymbol{G}(\boldsymbol{x}) + \sum_{\boldsymbol{x}_j\neq\boldsymbol{x}}\boldsymbol{H}(\boldsymbol{x}-\boldsymbol{x}_j)\right]\cdot\nabla_{\boldsymbol{v}}f
\end{aligned}
\tag{314}
$$

In the second line, we have again exploited the properties of the delta function which allow us to replace $\boldsymbol{x}_i$ by $\boldsymbol{x}$. Also note the appearance of the convective derivative on the lhs.; the above derivation shows that it results from Newton's first equation.

To obtain the hydrodynamic equations from (314), two additional reductions will be necessary:

- We need to replace the fine-grained density $f(t,\boldsymbol{x},\boldsymbol{v})$, which still depends implicitly on the (unknown) solutions $\boldsymbol{x}_j(t)$, by a *coarse-grained* density $\langle f(t,\boldsymbol{x},\boldsymbol{v})\rangle$.

- We have to construct the relevant field variables, the mass density $\rho(t,\boldsymbol{r})$ and velocity field $\boldsymbol{u}$, from the coarse-grained density $\bar{f}$.

To motivate the coarse-graining procedure, let us recall that the Newton equations (308) form a system of deterministic ODEs whose solutions are $\{\boldsymbol{x}_1(t),\ldots,\boldsymbol{x}_N(t)\}$ are uniquely determined by the initial conditions $\{\boldsymbol{x}_1(0),\ldots,\boldsymbol{x}_N(0);\boldsymbol{v}_1(0),\ldots,\boldsymbol{v}_N(0)\} =: \Gamma_0$. However, for any experimental realization of a macroscopic system (say, a glass of water), it is practically impossible to determine the initial conditions exactly. To account for this lack of knowledge, we may assume that the initial conditions are drawn from some probability distribution $\mathbb{P}(\Gamma_0)$. Without specifying the exact details of this distribution at this point, we may define the coarse-grained density $\langle f\rangle$ by averaging the fine-grained density f with respect to $\mathbb{P}(\Gamma_0)$, formally expressed as

$$\langle f(t,\boldsymbol{x},\boldsymbol{v})\rangle = \int \mathrm{d}\mathbb{P}(\Gamma_0)\, f(t,\boldsymbol{x},\boldsymbol{v}). \tag{315}$$

Averaging Eq. (314) and using the fact that integration over initial conditions commutes with the partial differentiations, we have

$$m \left(\frac{\partial}{\partial t} + \boldsymbol{v} \cdot \nabla \right) \langle f \rangle = -\nabla_{\boldsymbol{v}} \cdot [\boldsymbol{G}(\boldsymbol{x}) \langle f \rangle + \boldsymbol{C}] \tag{316}$$

where the collision-term

$$C(t, \boldsymbol{x}, \boldsymbol{v}) := \sum_{\boldsymbol{x}_j \neq \boldsymbol{x}} \langle \boldsymbol{H}(\boldsymbol{x} - \boldsymbol{x}_j) f(t, \boldsymbol{x}, \boldsymbol{v}) \rangle \tag{317}$$

represents the average effect of the pair interactions on a fluid particle at position $\boldsymbol{x}$.

We now define the mass density ρ, the velocity field $\boldsymbol{u}$, and the specific kinetic energy tensor $\boldsymbol{\Sigma}$ by

$$\rho(t, \boldsymbol{x}) = m \int d^3 v \, \langle f(t, \boldsymbol{x}, \boldsymbol{v}) \rangle, \tag{318a}$$

$$\rho(t, \boldsymbol{x}) \, \boldsymbol{u}(t, \boldsymbol{x}) = m \int d^3 v \, \langle f(t, \boldsymbol{x}, \boldsymbol{v}) \rangle \, \boldsymbol{v}. \tag{318b}$$

$$\rho(t, \boldsymbol{x}) \, \boldsymbol{\Sigma}(t, \boldsymbol{x}) = m \int d^3 v \, \langle f(t, \boldsymbol{x}, \boldsymbol{v}) \rangle \, \boldsymbol{v}\boldsymbol{v}. \tag{318c}$$

The tensor $\boldsymbol{\Sigma}$ is, by construction, symmetric as can be seen from the definition of its individual components

$$\rho(t, \boldsymbol{x}) \, \Sigma_{ij}(t, \boldsymbol{x}) = m \int d^3 v \, \langle f(t, \boldsymbol{x}, \boldsymbol{v}) \rangle \, v_i v_j,$$

and the trace of $\boldsymbol{\Sigma}$ defines the local *kinetic energy density*

$$\epsilon(t, \boldsymbol{x}) := \frac{1}{2} \mathrm{Tr}(\rho \boldsymbol{\Sigma}) = \frac{m}{2} \int d^3 v \, \langle f(t, \boldsymbol{x}, \boldsymbol{v}) \rangle \, |\boldsymbol{v}|^2. \tag{319}$$

Integrating Eq. (316) over $\boldsymbol{v}$, we get

$$\frac{\partial}{\partial t} \rho + \nabla \cdot (\rho \boldsymbol{u}) = -\int dv^3 \, \nabla_{\boldsymbol{v}} \cdot [\boldsymbol{G}(\boldsymbol{x}) \langle f \rangle + \boldsymbol{C}], \tag{320}$$

but the rhs. can be transformed into a surface integral (in velocity space) that vanishes since for physically reasonable interactions $[\boldsymbol{G}(\boldsymbol{x}) \langle f \rangle + \boldsymbol{C}] \to \boldsymbol{0}$ as $|\boldsymbol{v}| \to \infty$. We thus recover the mass conservation equation

$$\frac{\partial}{\partial t} \rho + \nabla \cdot (\rho \boldsymbol{u}) = 0. \tag{321}$$

To obtain the momentum conservation law, lets multiply (316) by $\boldsymbol{v}$ and subsequently integrate over $\boldsymbol{v}$,

$$\int dv^3 \, m \left(\frac{\partial}{\partial t} + \boldsymbol{v} \cdot \nabla \right) \langle f \rangle \boldsymbol{v} = -\int dv^3 \, \boldsymbol{v} \nabla_{\boldsymbol{v}} \cdot [\boldsymbol{G}(\boldsymbol{x}) \langle f \rangle + \boldsymbol{C}]. \tag{322}$$

The lhs. can be rewritten as

$$
\int dv^3\, m\left(\frac{\partial}{\partial t} + \boldsymbol{v}\cdot\nabla\right)\langle f\rangle \boldsymbol{v} \;=\; \frac{\partial}{\partial t}(\rho \boldsymbol{u}) + \nabla\cdot\int dv^3\, m\langle f\rangle \boldsymbol{v}\boldsymbol{v}
$$

$$
= \frac{\partial}{\partial t}(\rho \boldsymbol{u}) + \nabla\cdot(\rho\boldsymbol{\Sigma})
$$

$$
= \frac{\partial}{\partial t}(\rho \boldsymbol{u}) + \nabla\cdot(\rho\boldsymbol{u}\boldsymbol{u}) + \nabla\cdot[\rho(\boldsymbol{\Sigma}-\boldsymbol{u}\boldsymbol{u})]
$$

$$
= \rho\frac{\partial}{\partial t}\boldsymbol{u} + \boldsymbol{u}\frac{\partial}{\partial t}\rho + \boldsymbol{u}\nabla\cdot(\rho\boldsymbol{u}) + \rho\boldsymbol{u}\cdot\nabla\boldsymbol{u} + \nabla\cdot[\rho(\boldsymbol{\Sigma}-\boldsymbol{u}\boldsymbol{u})]
$$

$$
\overset{(321)}{=} \rho\left(\frac{\partial}{\partial t} + \boldsymbol{u}\cdot\nabla\right)\boldsymbol{u} + \nabla\cdot[\rho(\boldsymbol{\Sigma}-\boldsymbol{u}\boldsymbol{u})] \tag{323}
$$

The rhs. of (322) can be computed by partial integration, yielding

$$
-\int dv^3\, \boldsymbol{v}\nabla_{\boldsymbol{v}}\cdot[\boldsymbol{G}(\boldsymbol{x})\langle f\rangle + \boldsymbol{C}] \;=\; \int dv^3\, \cdot[\boldsymbol{G}(\boldsymbol{x})\langle f\rangle + \boldsymbol{C}]
$$

$$
= \rho\boldsymbol{g} + \boldsymbol{c}(t,\boldsymbol{x}), \tag{324}
$$

where $\boldsymbol{g}(\boldsymbol{x}) := \boldsymbol{G}(\boldsymbol{x})/m$ is the force per unit mass (acceleration) and the last term

$$
\boldsymbol{c}(t,\boldsymbol{x}) = \int dv^3 \boldsymbol{C} = \int dv^3 \sum_{\boldsymbol{x}_j\neq\boldsymbol{x}} \langle \boldsymbol{H}(\boldsymbol{x}-\boldsymbol{x}_j)f(t,\boldsymbol{x},\boldsymbol{v})\rangle \tag{325}
$$

encodes the mean pair interactions. Combining (323) and (324), we find

$$
\rho\left(\frac{\partial}{\partial t} + \boldsymbol{u}\cdot\nabla\right)\boldsymbol{u} \;=\; -\nabla\cdot[\rho(\boldsymbol{\Sigma}-\boldsymbol{u}\boldsymbol{u})] + \rho\boldsymbol{g}(\boldsymbol{x}) + \boldsymbol{c}(t,\boldsymbol{x}). \tag{326}
$$

The symmetric tensor

$$
\boldsymbol{\Pi} := \boldsymbol{\Sigma} - \boldsymbol{u}\boldsymbol{u} \tag{327}
$$

measures the covariance of the local velocity fluctuations of the molecules which can be related to their temperature. To estimate $\boldsymbol{c}$, let us assume that the pair interaction force $\boldsymbol{H}$ can be derived from a pair potential φ, which means that $\boldsymbol{H}(\boldsymbol{r}) = -\nabla_{\boldsymbol{r}}\varphi(\boldsymbol{r})$. Assuming further that $\boldsymbol{H}(\boldsymbol{0}) = \boldsymbol{0}$, we may write

$$
\boldsymbol{c}(t,\boldsymbol{x}) = -\int dv^3 \sum_{\boldsymbol{x}_j(t)} \langle [\nabla_{\boldsymbol{x}}\varphi(\boldsymbol{x}-\boldsymbol{x}_j)]f(t,\boldsymbol{x},\boldsymbol{v})\rangle \tag{328}
$$

Replacing for some function $\zeta(\boldsymbol{x})$ the sum over all particles by the integral

$$
\sum_{\boldsymbol{x}_j}\zeta(\boldsymbol{x}_j) \simeq \frac{1}{m}\int d^3y\, \rho(t,\boldsymbol{y})\,\zeta(\boldsymbol{y}) \tag{329}
$$

we have

$$
\boldsymbol{c}(t,\boldsymbol{x}) \;\simeq\; -\frac{1}{m}\int dv^3\int d^3y\, \rho(t,\boldsymbol{y})\,\langle [\nabla_{\boldsymbol{x}}\varphi(\boldsymbol{x}-\boldsymbol{y})]f(t,\boldsymbol{x},\boldsymbol{v})\rangle
$$

$$
= -\frac{1}{m}\int dv^3\int d^3y\, \rho(t,\boldsymbol{y})\,\langle [-\nabla_{\boldsymbol{y}}\varphi(\boldsymbol{x}-\boldsymbol{y})]f(t,\boldsymbol{x},\boldsymbol{v})\rangle
$$

$$
= -\frac{1}{m}\int dv^3\int d^3y\, [\nabla\rho(t,\boldsymbol{y})]\,\langle \varphi(\boldsymbol{x}-\boldsymbol{y})f(t,\boldsymbol{x},\boldsymbol{v})\rangle \tag{330}
$$

62

In general, it is impossible to simplify this further without some explicit assumptions about initial distribution $\mathbb{P}$ that determines the average $\langle \cdot \rangle$. There is however one exception, namely, the case when interactions are very short-range so that we can approximate the potential by a delta-function,

$$\varphi(\boldsymbol{r}) = \phi_0 a^3 \delta(\boldsymbol{r}), \tag{331}$$

where φ_0 is the interaction energy and a^3 the effective particle volume. In this case,

$$
\begin{aligned}
\boldsymbol{c}(t, \boldsymbol{x}) &= -\frac{\varphi_0 a^3}{m} \int dv^3 \int d^3 y \, [\nabla \rho(t, \boldsymbol{y})] \, \langle \delta(\boldsymbol{x} - \boldsymbol{y}) f(t, \boldsymbol{x}, \boldsymbol{v}) \rangle \\
&= -\frac{\varphi_0 a^3}{m} [\nabla \rho(t, \boldsymbol{x})] \int dv^3 \langle f(t, \boldsymbol{x}, \boldsymbol{v}) \rangle \\
&= -\frac{\varphi_0 a^3}{m^2} [\nabla \rho(t, \boldsymbol{x})] \rho(t, \boldsymbol{x}) \\
&= -\frac{\varphi_0 a^3}{2m^2} \nabla \rho(t, \boldsymbol{x})^2
\end{aligned}
\tag{332}
$$

Inserting this into (326), we have thus derived the following hydrodynamic equations

$$\frac{\partial}{\partial t}\rho + \nabla \cdot (\rho \boldsymbol{u}) = 0 \tag{333a}$$

$$\rho \left(\frac{\partial}{\partial t} + \boldsymbol{u} \cdot \nabla \right) \boldsymbol{u} = \nabla \cdot \boldsymbol{\Xi} + \rho \boldsymbol{g}(\boldsymbol{x}), \tag{333b}$$

where

$$\boldsymbol{\Xi} := -\left[\rho(\boldsymbol{\Sigma} - \boldsymbol{u}\boldsymbol{u}) + \frac{\varphi_0 a^3}{2m^2} \rho^2 \boldsymbol{I} \right] \tag{333c}$$

is the *stress tensor* with $\boldsymbol{I}$ denoting unit matrix.

Note that Eqs. (333) do not yet form a closed system, due to the appearance of the second-moment tensor $\boldsymbol{\Sigma}$. This is a manifestation of the well-known *hierarchy problem*, encountered in all[14] attempts to derive hydrodynamic equations from microscopic models. More precisely, the hierarchy problem means that the time evolution of the nth-moment depends on that of the higher moments. The standard approach to overcoming this obstacle is to postulate (guess) reasonable *ad-hoc closure conditions*, which essentially means that one tries to express higher moments, such as $\boldsymbol{\Sigma}$, in terms of the lower moments. For example, a commonly adopted closure condition is the ideal isotropic gas approximation

$$\boldsymbol{\Sigma} - \boldsymbol{u}\boldsymbol{u} = \frac{kT}{m}\boldsymbol{I}, \tag{334}$$

where T is the temperature and k the Boltzmann constant. For this closure condition, Eqs. (333a) and (333b) become to a closed system for ρ and $\boldsymbol{u}$.

Traditionally, and in most practical applications, one does not bother with microscopic derivations of $\boldsymbol{\Xi}$; instead one merely postulates that

$$\boldsymbol{\Xi} = -p\boldsymbol{I} + \mu(\nabla^\top \boldsymbol{u} + \nabla \boldsymbol{u}^\top) - \frac{2\mu}{3}(\nabla \cdot \boldsymbol{u}), \tag{335}$$

---

[14]Except, perhaps for very trivial examples.

where $p(t, \boldsymbol{x})$ is the pressure field and μ the dynamic viscosity, which can be a function of pressure, temperature etc. depending on the fluid. Equations (333a) and (333b) combined with the empirical ansatz (335) are the famous *Navier-Stokes equations.* The second summand in Eq. (335) contains the *rate-of-strain* tensor

$$\boldsymbol{E} = \frac{1}{2}(\nabla^\top \boldsymbol{u} + \nabla \boldsymbol{u}^\top) \tag{336}$$

and $(\nabla \cdot \boldsymbol{u})$ is the *rate-of-expansion* of the flow.

For incompressible flow, defined by $\rho = const.$, the Navier-Stokes equations simplify to

$$\nabla \cdot \boldsymbol{u} \;\; = \;\; 0 \tag{337a}$$

$$\rho\left(\frac{\partial}{\partial t} + \boldsymbol{u} \cdot \nabla\right)\boldsymbol{u} \;\; = \;\; -\nabla p + \mu \nabla^2 \boldsymbol{u} + \rho \boldsymbol{g}. \tag{337b}$$

In this case, one has to solve for $(p, \boldsymbol{u})$.

13   The Navier-Stokes Equations

In the previous section, we have seen how one can deduce the general structure of hydrodynamic equations from purely macroscopic considerations and and we also showed how one can derive macroscopic continuum equations from an underlying microscopic model. For the remainder of this course, we will return to the macroscopic viewpoint developed in Sec. 12.

13.1   Viscosity

A main insight from the discussion in the previous section is that the Euler equations, as given in Sec. 12.1, do not account for one final element needed to complete the macroscopic fluid equations: viscosity. Viscous stresses try to stop relative motion between nearby parts of the fluid. Another way of saying this is that wherever there is a rate of strain in the fluid, a stress acts to reduce the strain. As with pressure, viscosity has its origins in intermolecular forces and momentum transfer across a surface.

To understand more about viscosity, let's first have a general discussion of the stress acting on an infinitesimal fluid element. There are two kinds of stresses: normal stresses and tangential stresses. We anticipate that the viscous stresses act tangentially to the fluid element (as their role is to get rid of relative motion.) Our goal is to figure out the form of these tangential stresses. All of the information related to normal and tangential stresses within a fluid can be collected in the *stress tensor*. The stress tensor is a three by three matrix σ with components σ_{ij}, which has the property that the stress acting on a surface S with unit normal $\boldsymbol{n}$ is just $\sigma_{ij}n_j$. For an arbitrary fluid element, the net force arising from surface stresses is

$$\int_S \sigma \cdot \boldsymbol{n} \, dS = \int_V (\nabla \cdot \sigma) dV. \tag{338}$$

We must therefore determine the form of σ in order derive our equations of motion.

Firstly, suppose there were no tangential stresses on a fluid element. The normal stresses are just pressures. In this case the stress tensor would just be

$$\sigma = \begin{pmatrix} -p & 0 & 0 \\ 0 & -p & 0 \\ 0 & 0 & -p \end{pmatrix}. \tag{339}$$

The momentum equation for the component u_i of the velocity is then

$$\frac{Du_i}{Dt} = -\frac{\partial p}{\partial x_i}, \tag{340}$$

and this is Euler's equation, which we derived in the previous lecture.

Now let's think a little more about the tangential stresses acting on a fluid element. We argue that the net *torque* on an element must vanish. This means that σ_{12}, the stress in the x-direction on the face with normal in the y-direction must be equal to σ_{21}, the stress in the y-direction on the face with normal in the x-direction. If these do not exactly cancel, the forces will make the fluid element spin. The fact that the tangential stresses on the fluid element balance means that the stress tensor must be *symmetric*. We therefore deduce that the stress tensor is of the general form

$$\sigma = -pI + \begin{pmatrix} \sigma_{11} & \sigma_{12} & \sigma_{13} \\ \sigma_{12} & \sigma_{22} & \sigma_{23} \\ \sigma_{13} & \sigma_{23} & \sigma_{33} \end{pmatrix}, \tag{341}$$

where I is the identity matrix.

In determining the form of the viscous tangential stresses, we reason that these must arise from relative motion between fluid elements. Thus the stress should somehow depend on $\nabla \boldsymbol{u}$, which will only be nonzero if there are velocity gradients. Note that $\nabla \boldsymbol{u}$ is also a tensor, and can be written explicitly as

$$\nabla \boldsymbol{u} = \begin{pmatrix} \partial_x u_x & \partial_y u_x & \partial_z u_x \\ \partial_x u_y & \partial_y u_y & \partial_z u_y \\ \partial_x u_z & \partial_y u_z & \partial_z u_z \end{pmatrix}. \tag{342}$$

We immediately have a problem because the tensor is not symmetric, whilst we know that the stress tensor is necessarily symmetric. There is, however, a mathematical fact that says a general tensor can be expressed as the sum of a symmetric tensor and an antisymmetric tensor, i.e., if A is a tensor then

$$A_{ij} = A_{ij}^s + A_{ij}^a = \frac{1}{2}(A_{ij} + A_{ji}) + \frac{1}{2}(A_{ij} - A_{ji}). \tag{343}$$

The first part of the formula corresponds to a symmetric tensor and the second part to an antisymmetric tensor. Using this construction, the velocity gradient tensor can thus be divided into symmetric part

$$\nabla \boldsymbol{u}^s = \frac{1}{2}(\partial_i u_j + \partial_j u_i) \tag{344a}$$

and antisymmetric part

$$\nabla \boldsymbol{u}^a = \frac{1}{2}(\partial_i u_j - \partial_j u_i). \tag{344b}$$

Physically, the symmetric part $\nabla \boldsymbol{u}^s$ corresponds to the deformation of the fluid element and is called the *rate of strain tensor*. The antisymmetric part corresponds to rotation of the fluid element and is called the *vorticity tensor*. To see this, let's consider a flow that is rotating, but not deforming, and also a flow that is deforming, but not rotating. In two dimensions a rotating flow is $\boldsymbol{u} \propto (-y, x)$ and a deforming flow is $\boldsymbol{u} \propto (x, y)$. For the rotating flow it can be shown that the antisymmetric part $\nabla \boldsymbol{u}^a$ is non-zero, and for the deforming flow the symmetric part is non-zero $\nabla \boldsymbol{u}^s$.

The grand conclusion of this is that we expect the strain tensor σ to be a function of the rate of strain tensor i.e., $\sigma = \sigma(\nabla \boldsymbol{u}^s)$. The question now is, what function is it? This depends on the fluid and the situation is usually divided into two categories.

(i) *Newtonian fluids*: In Book II of the *Principia* Newton writes

'The resistance arising from the want of lubricity in the parts of a fluid is, other things being equal, proportional to the velocity with which the parts of the fluid are separated from one another.'

Thus Newton's guess, which corresponds to the simplest situation, was that the stress is a linear function of the strain,

$$\sigma = 2\mu \nabla \boldsymbol{u}^s. \tag{345}$$

(ii) *Non-Newtonian fluids*: This encompasses all other cases. That is, whenever the stress depends on the strain in a more complicated way, the fluid is called non-Newtonian.

Which of these two possibilities happens can only be determined experimentally for a particular fluid. In general, whether a fluid is non-Newtonian or not depends on how hard you are shearing it. Fortunately, it happens that most simple fluids are Newtonian under ordinary conditions. So for water, oil, air etc. it is often possible to approximate fluids as being Newtonian. Non-Newtonian also happens frequently in nature (e. g. liquid crystals) and gives rise to fascinating flow phenomena, but this is more specialised.

Now let's put everything together and write down the equations for Newtonian viscous flow. If we consider the equation for u_i, the ith component of the velocity, this is

$$
\begin{aligned}
\rho \frac{Du_i}{Dt} &= -\frac{\partial p}{\partial x_i} + 2\mu \sum \frac{\partial}{\partial x_j} \frac{1}{2}\left(\frac{\partial u_j}{\partial x_i} + \frac{\partial u_i}{\partial x_j}\right) \\
&= -\nabla_i p + \mu \nabla_i (\nabla \cdot \boldsymbol{u}) + \mu \nabla^2 u_i.
\end{aligned} \tag{346}
$$

When the fluid density doesn't change very much we have seen that $\nabla \cdot \boldsymbol{u} = 0$, and under these conditions the *Navier-Stokes equations* for fluid motion are

$$\rho \frac{D\boldsymbol{u}}{Dt} = -\nabla p + \mu \nabla^2 \boldsymbol{u}. \tag{347}$$

These form the basis for much of our studies, and it should be noted that the derivation relies crucially on the incompressibility of the flow. The equations are essentially a macroscopic description of microscopic laws, and were written down even before the notion of a molecule was fully understood.

The parameter μ is called the *coefficient of viscosity*, and since our derivation of the viscous force is phenomenological, it is both important and useful to make sure that all of the assumptions have been clearly stated. Is it true in general that only one number is sufficient to completely characterise the viscosity? Stated another way, the viscous effects in a fluid capture the macroscopic consequences of dissipative collisions between fluid particles. Is it obvious that only one number is sufficient to characterise this (enormously complicated!) process? Interestingly, one can show that if the fluid is both assumed to be both incompressible and isotropic (i.e., whichever way you look at the fluid it's macroscopic properties are the same) then the parameter μ is all that is needed.

13.2   Boundary conditions

Now we have the equations of motion governing a fluid, the basic claim is that all the phenomena of normal fluid motion are contained in the equations. Unfortunately, there is no general theory of obtaining solutions to the Navier-Stokes equations. In fact, so difficult can it be, that the challenge of proving the existence and smoothness of solutions has been named as one of the seven Millennium Prize Problems by the Clay Mathematics Institute (*www.claymath.org/prizeproblems/statement.htm*). All is not lost however, as one can turn to experiments to find new phenomena and, on the basis of this mathematicians can go looking for solutions. To become familiar with the equations we shall find some simple solutions to well known problems, but to directly compare solutions to experiments we first need to think a little about boundary conditions.

There are several types of boundaries that occur in practice, though the most common is simply the solid wall. The equations of motion for the fluid specify what happens everywhere except for the fluid element right next to the wall. At the wall, the forces between the wall and the fluid determine the dynamics.

To derive boundary conditions from first principles, it is necessary to take these interactions into account. Suffice to say that (a) in the nineteenth century there were vigorous debates between Maxwell, Stokes, etc. about what the correct conditions were, and (b) though today there is agreement for most situations, no decent derivation beginning with the microscopics has been given. From a purely mathematical point of view, it is necessary to check how many boundary conditions are allowed to still have unique solutions to the equations. If too many conditions are specified there might be no solutions of the equations which are consistent with them.

What are the boundary conditions? First, fluid cannot penetrate the boundary. That is, the component of the velocity normal to the solid boundary vanishes. What about the tangential component of the velocity? If the fluid has no viscosity, it is inconsistent to demand any relation on the tangential component of the velocity at the boundary. If there is viscosity then it is possible to demand another condition. The condition which is mostly accepted to be true is called the *no slip boundary condition* (there is important ongoing research which aims at determining if and when such a condition breaks down). The *no-slip*

condition says that dissipative processes are so strong that the tangential component of the velocity actually vanishes there! This is known to be true from experimental studies of the motion of fluid near walls. It is extremely important, however, to understand that this is a phenomenological observation, not derived from first principles.

13.3 Some simple solutions

As mentioned before, in different limits the Navier-Stokes equations contain all of the important classes of partial differential equations. Let's proceed to find an example which has within it a diffusion equation. We consider the following problem, at low Reynolds numbers (taken from Acheson, p.35). Consider a viscous fluid that is at rest in the region $0 < y < \infty$ and suppose that at $t = 0$ the rigid boundary at $y = 0$ is moved at constant speed U in the x-direction. What is the motion of the fluid?

Since the jerking motion is uniform in the x-direction, we expect the velocity to be of the form $(u, v, w) = (u(y, t), 0, 0)$. Moreover, there is no pressure variation across the system in the x-direction, so the pressure is uniform. Thus the equation of motion is just

$$\frac{\partial u}{\partial t} = \nu \frac{\partial^2 u}{\partial y^2}. \tag{348}$$

Note that the assumed form of the velocity automatically satisfies the incompressibility condition. Also, the nonlinear term has vanished because of the form of the velocity field. The equation is a diffusion equation for the velocity in which ν is the diffusion coefficient. The initial condition is that $u = 0$ in the upper half plane. The boundary conditions are that $u(0, t) = U$ for $t > 0$ (no-slip), and we expect that u will vanish as $y \to \infty$ (since it vanishes initially).

We look for a *similarity solution* of the form $u(y, t) = f(y/\sqrt{\nu t}) = f(\eta)$. The logic is the same as we employed in examining the diffusive spreading of a point cloud. That is, initially there are no characteristic scales in the solution. After time t the only scale is of order $\sqrt{t}$ because of the structure of the equations. The factor of ν is for convenience. Plugging this into the diffusion equation gives

$$f'' + \frac{1}{2}\eta f' = 0. \tag{349}$$

Integrating twice,

$$f = A + B \int_0^\eta e^{-s^2/4} ds, \tag{350}$$

where A and B are integration constants. The boundary conditions imply that $A + B \int_0^\infty exp(-s^2/4) ds = 0$ and $A = U$. Using the fact that

$$\int_0^\infty e^{-s^2/4} ds = \sqrt{\pi}, \tag{351}$$

we have the solution

$$u(y, t) = U \left(1 - \frac{1}{\sqrt{\pi}} \int_0^{y/\sqrt{\nu t}} e^{-s^2/4} ds \right). \tag{352}$$

The simple form of the initial and boundary conditions was essential to our finding this solution. We see that at different times the velocity profiles are all geometrically similar

i.e., the velocity is always the same function of $(y/\sqrt{\nu t})$. As time progresses, the velocity profile becomes stretched out and the effects of motion are largely confined to within a distance $\sqrt{\nu t}$ from the boundary.

The solution above would not have been so simple if, for instance, an upper boundary were present. In this case, a length-scale is imposed on the problem, this length-scale being the distance h between the plates. We can then no longer look for a similarity solution, and instead the solution is found by the method of separation of variables. The problem is described in detail in Acheson (p. 40-41). Without solving the problem in detail however, we can get a very good idea of what happens. We argue that after a large amount of time we expect the system to reach a steady state. This problem is easy to solve, as all we need to do is drop the time dependent term from equation (1) and solve subject to the boundary conditions $u(0,t) = U$ and $u(h,t) = 0$. The steady state solution is the linear profile

$$u(y) = U \left(1 - \frac{y}{h}\right). \tag{353}$$

The outstanding issue is to then ask, how long does it take for this profile to be realised. Well, we know that viscous diffusion is responsible for setting up the profile, and the dimensions of ν are L^2/T. Since the separation of the plates is h, then we obtain a timescale by forming the combination h^2/ν. This is roughly the time taken for viscous diffusion to act over the gap between the plates, and gives an order of magnitude estimate for the time taken to set up a steady profile. And we have obtained all this information, without having to do any difficult mathematics!

13.4   The Reynolds number

For an incompressible flow, we have established that the equations of motion are

$$\rho \frac{\partial \boldsymbol{u}}{\partial t} + \rho \boldsymbol{u} \cdot \nabla \boldsymbol{u} = -\nabla p + \mu \nabla^2 \boldsymbol{u} + \boldsymbol{f}_{ext}, \tag{354}$$

as well as incompressibility $\nabla \cdot \boldsymbol{u} = 0$. Now note that the equation has five terms in it. The first two have to do with inertia and the third is pressure gradient, the fourth is viscosity and the fifth is an external force. In many situations, all of these terms are not equally important. The most trivial situation is a *static* situation. Here all of the terms involving the velocity are zero, and the only nonzero terms are the pressure gradient and the external forces. There are many other possibilities. The most difficult part is to figure out in any particular situation which of the terms in the equation are large, and which are small. In different limits the Navier-Stokes equations contain all of the important classes of partial differential equations (i.e., diffusion equation, Laplace's equation, wave equations) which are usually considered. In the next lecture we shall find an example which has within it a diffusion equation.

An important parameter that indicates the relative importance of viscous and inertial forces in a given situation is the *Reynolds number*. Suppose we are looking at a problem where the characteristic velocity scale is U_0, and the characteristic length scale for variation of the velocity is L. Then the size of the terms in the equation are

$$\frac{\partial \boldsymbol{u}}{\partial t} \sim \frac{U_0^2}{L}, \qquad \boldsymbol{u} \cdot \nabla \boldsymbol{u} \sim \frac{U_0^2}{L}, \qquad \mu \nabla^2 \boldsymbol{u} \sim \frac{\mu U_0}{L^2}. \tag{355}$$

69

The ratio of the inertial terms to the viscous term is

$$\frac{\rho U_0^2/L}{\mu U_0/L^2} = \frac{\rho U_0 L}{\mu} = \text{Re}, \tag{356}$$

and this is called the Reynolds number, Re. When the Reynolds number is very high the flow is rather inviscid, and when the Reynolds number is low the flow is very viscous. Honey is at low Reynolds number and turbulence is at high Reynolds number. For low Reynolds number it may be possible to ignore the inertial terms in the Navier-Stokes equations and obtain the so-called *slow (or creeping) flow equations* for very viscous flow. At high Reynolds number one ends up with the Euler equations.

The Reynolds number can be varied by changing the viscosity of fluid. In practice, one distinguishes two types of viscosities.

Dynamic viscosity The SI physical unit of *dynamic* viscosity μ is the Pascal×second

$$[\mu] = 1\,\text{Pa} \cdot \text{s} = 1\,\text{kg}/(\text{m} \cdot \text{s}) \tag{357}$$

If a fluid with a viscosity $\mu = 1\,\text{Pa} \cdot \text{s}$ is placed between two plates, and one plate is pushed sideways with a shear stress of one pascal, it moves a distance equal to the thickness of the layer between the plates in one second. The dynamic viscosity of water ($T = 20\,^\circ\text{C}$) is $\mu = 1.0020 \times 10^{-3}\,\text{Pa} \cdot \text{s}$.

Kinematic viscosity When dealing with incompressible fluids of constant density, then it's often convenient to consider the *kinematic* viscosity ν, defined as

$$\nu = \frac{\mu}{\varrho}\,, \qquad [\nu] = \text{m}^2/\text{s} \tag{358}$$

which essentially enters into the Reynolds number of an object of given size L and speed U_0. The kinematic viscosity of water with mass density $\varrho = 1\,\text{g}/\text{cm}^3$ is $\nu = 10^{-6}\,\text{m}^2/\text{s} = 1\,\text{mm}^2/s = 1\,\text{cSt}$.

To conclude this section, let's put in some numbers. For example, for fish or humans swimming in water, we s finds:

$$L \simeq 1\,\text{m},\ U_0 \simeq 1\,\text{m/s} \qquad \Rightarrow \qquad \text{Re} \simeq 10^6,$$

whereas for bacteria:

$$L \simeq 1\,\mu\text{m},\ U_0 \simeq 10\,\mu\text{m/s} \qquad \Rightarrow \qquad \text{Re} \simeq 10^{-5}.$$

This is a huge difference and allows for considerable mathematical simplifications.

14   Low-Reynolds number limit

In this section, we look at the limit of $\text{Re} \to 0$ which is relevant to the construction of microfluidic devices and also governs the world of swimming microbes.

Bacteria and eukaryotic cells achieve locomotion in a fluid through a self-induced change of shape: *Escherichia coli* propel themselves by rotating a helically shaped bundle of flagella, much like a corkscrew penetrating into a cork. Sperm cells move by inducing a wave-like deformation in a thin flagellum or cilium, whereas algae and other organisms move by beating two or more cilia in a synchronized manner (see slides).

Because of their tiny size, these microswimmers operate at very low Reynolds number, i.e., inertial and turbulent effects are negligible[15]. In this regime, swimming mechanisms are very different from employed by humans and other animals. In particular, any micro-bial swimming strategy must involve time-irreversible motion. Whilst moving through the liquid, a swimmer modifies the flow of the surrounding liquid. This can lead to an effective hydrodynamic interactions between nearby organisms, which can be attractive or repulsive depending on the details of the swimming mechanism. In reality, such deterministic forces are usually perturbed by a considerable amount of thermal or intrinsic noise, but we will neglect such Brownian motion effects here.

14.1 Stokes equations

If the Reynolds number is very small, $\mathrm{Re} \ll 1$, the nonlinear NSEs (354) can be approximated by the linear *Stokes equations*[16]

$$
\begin{align}
0 &= \nabla \cdot \boldsymbol{u}, \tag{359a} \\
0 &= \mu \nabla^2 \boldsymbol{u} - \nabla p + \boldsymbol{f}. \tag{359b}
\end{align}
$$

The four equations (359) determine the four unknown functions $(\boldsymbol{u}, p)$. However, to uniquely identify such solutions, these equations must still be endowed with appropriate initial and boundary conditions, such as for example

$$
\begin{cases}
\boldsymbol{u}(t, \boldsymbol{x}) = 0, \\
p(t, \boldsymbol{x}) = p_\infty,
\end{cases} \qquad \text{as} \qquad |\boldsymbol{x}| \to \infty. \tag{360}
$$

Note that, by neglecting the explicit time-dependent inertial terms in NSEs, *the time-dependence of the flow is determined exclusively and instantaneously by the motion of the boundaries and/or time-dependent forces* as generated by the swimming objects.

14.2 Oseen's solution

Consider the Stokes equations (359) for a point-force

$$
\boldsymbol{f}(\boldsymbol{x}) = \boldsymbol{F}\, \delta(\boldsymbol{x}). \tag{361}
$$

---

[15]This is equivalent to larger animals swimming through a bath of treacle.

[16]More precisely, by replacing Eq. (354) with Eq. (359), it is assumed that for small Reynolds numbers $\tilde{\mathrm{Re}}(t, \boldsymbol{x}) := |\varrho(\boldsymbol{u} \cdot \nabla)\boldsymbol{u}| / (\mu \nabla^2 \boldsymbol{u}) \simeq UL(\varrho/\mu) \ll 1$ one can approximate

$$
\varrho \left[\partial_t \boldsymbol{u} + (\boldsymbol{u} \cdot \nabla)\boldsymbol{u} \right] - \mu \nabla^2 \boldsymbol{u} \simeq -\mu \nabla^2 \boldsymbol{u}
$$

The consistency of this approximation can be checked *a posteriori* by inserting the solution for $\boldsymbol{u}$ into the lhs. of Eq. (354) .

In this case, the solution with standard boundary conditions (360) reads[17]

$$u_i(\boldsymbol{x}) = G_{ij}(\boldsymbol{x}) \, F_j \, , \qquad p(\boldsymbol{x}) = \frac{F_j x_j}{4\pi|\boldsymbol{x}|^3} + p_\infty, \tag{362a}$$

where the Greens function G_{ij} is given by the Oseen tensor

$$G_{ij}(\boldsymbol{x}) = \frac{1}{8\pi\mu\,|\boldsymbol{x}|}\left(\delta_{ij} + \frac{x_i x_j}{|\boldsymbol{x}|^2}\right), \tag{362b}$$

which has the inverse

$$G_{jk}^{-1}(\boldsymbol{x}) = 8\pi\mu|\boldsymbol{x}|\left(\delta_{jk} - \frac{x_j x_k}{2|\boldsymbol{x}|^2}\right), \tag{363}$$

as can be seen from

$$\begin{aligned}
G_{ij}G_{jk}^{-1} &= \left(\delta_{ij} + \frac{x_i x_j}{|\boldsymbol{x}|^2}\right)\left(\delta_{jk} - \frac{x_j x_k}{2|\boldsymbol{x}|^2}\right) \\
&= \delta_{ik} - \frac{x_i x_k}{2|\boldsymbol{x}|^2} + \frac{x_i x_k}{|\boldsymbol{x}|^2} - \frac{x_i x_j}{|\boldsymbol{x}|^2}\frac{x_j x_k}{2|\boldsymbol{x}|^2} \\
&= \delta_{ik} - \frac{x_i x_k}{2|\boldsymbol{x}|^2} + \frac{x_i x_k}{2|\boldsymbol{x}|^2} \\
&= \delta_{ik}.
\end{aligned} \tag{364}$$

14.3 Stokes's solution (1851)

Consider a sphere of radius a, which at time t is located at the origin, $\boldsymbol{X}(t) = \boldsymbol{0}$, and moves at velocity $\boldsymbol{U}(t)$. The corresponding solution of the Stokes equation with standard boundary conditions (360) reads[18]

$$\begin{aligned}
u_i(t,\boldsymbol{x}) &= U_j\left[\frac{3}{4}\frac{a}{|\boldsymbol{x}|}\left(\delta_{ji} + \frac{x_j x_i}{|\boldsymbol{x}|^2}\right) + \frac{1}{4}\frac{a^3}{|\boldsymbol{x}|^3}\left(\delta_{ji} - 3\frac{x_j x_i}{|\boldsymbol{x}|^2}\right)\right], \tag{365a} \\
p(t,\boldsymbol{x}) &= \frac{3}{2}\mu a\frac{U_j x_j}{|\boldsymbol{x}|^3} + p_\infty. \tag{365b}
\end{aligned}$$

If the particle is located at $\boldsymbol{X}(t)$, one has to replace x_i by $x_i - X_i(t)$ on the rhs. of Eqs. (365). Parameterizing the surface of the sphere by

$$\boldsymbol{a} = a\sin\theta\,\cos\phi\,\boldsymbol{e}_x + a\sin\theta\,\sin\phi\,\boldsymbol{e}_y + a\cos\theta\,\boldsymbol{e}_z = a_i\boldsymbol{e}_i$$

where $\theta \in [0,\pi], \phi \in [0,2\pi)$, one finds that on this boundary

$$\begin{aligned}
\boldsymbol{u}(t,\boldsymbol{a}(\theta,\phi)) &= \boldsymbol{U}, \tag{366a} \\
p(t,\boldsymbol{a}(\theta,\phi)) &= \frac{3}{2}\frac{\mu}{a^2}U_j\,a_j(\theta,\phi) + p_\infty, \tag{366b}
\end{aligned}$$

---

[17]Proof by insertion.
[18]Proof by insertion.

corresponding to a no-slip boundary condition on the sphere's surface. The $\mathcal{O}(a/|\boldsymbol{x}|)$-contribution in (365a) coincides with the Oseen result (362), if we identify

$$\boldsymbol{F} = 6\pi\,\mu a\,\boldsymbol{U}. \tag{367}$$

The prefactor $\gamma = 6\pi\,\mu a$ is the well-known Stokes drag coefficient for a sphere.

The $\mathcal{O}[(a/|\boldsymbol{x}|)^3]$-part in (365a) corresponds to the finite-size correction, and defining the Stokes tensor by

$$S_{ij} = G_{ij} + \frac{1}{24\pi\mu}\frac{a^2}{|\boldsymbol{x}|^3}\left(\delta_{ji} - 3\frac{x_j x_i}{|\boldsymbol{x}|^2}\right), \tag{368}$$

we may rewrite (365a) as[19]

$$u_i(t, \boldsymbol{x}) = S_{ij}F_j. \tag{369}$$

14.4 Dimensionality

We saw above that, in 3D, the fundamental solution to the Stokes equations for a point force at the origin is given by the Oseen solution

$$u_i(\boldsymbol{x}) = G_{ij}(\boldsymbol{x})\,F_j\,, \qquad p(\boldsymbol{x}) = \frac{F_j x_j}{4\pi|\boldsymbol{x}|^3} + p_\infty, \tag{370a}$$

where

$$G_{ij}(\boldsymbol{x}) = \frac{1}{8\pi\mu\,|\boldsymbol{x}|}\left(\delta_{ij} + \frac{x_i x_j}{|\boldsymbol{x}|^2}\right), \tag{370b}$$

It is interesting to compare this result with corresponding 2D solution

$$u_i(\boldsymbol{x}) = J_{ij}(\boldsymbol{x})F_j\,, \qquad p = \frac{F_j x_j}{2\pi|\boldsymbol{x}|^2} + p_\infty\,, \qquad \boldsymbol{x} = (x, y) \tag{371a}$$

where

$$J_{ij}(\boldsymbol{x}) = \frac{1}{4\pi\mu}\left[-\delta_{ij}\ln\left(\frac{|\boldsymbol{x}|}{a}\right) + \frac{x_i x_j}{|\boldsymbol{x}|^2}\right] \tag{371b}$$

with a being an arbitrary constant fixed by some intermediate flow normalization condition. Note that (371) decays much more slowly than (370), implying that hydrodynamic interactions in 2D freestanding films are much stronger than in 3D bulk solutions.

To verify that (371) is indeed a solution of the 2D Stokes equations, we first note that generally

$$\partial_j|\boldsymbol{x}| \;=\; \partial_j(x_i x_i)^{1/2} = x_j(x_i x_i)^{-1/2} = \frac{x_j}{|\boldsymbol{x}|} \tag{372a}$$

$$\partial_j|\boldsymbol{x}|^{-n} \;=\; \partial_j(x_i x_i)^{-n/2} = -nx_j(x_i x_i)^{-(n+2)/2} = -n\frac{x_j}{|\boldsymbol{x}|^{n+2}}. \tag{372b}$$

---

[19]For arbitrary sphere positions $\boldsymbol{X}(t)$, replace $\boldsymbol{x} \to \boldsymbol{x} - \boldsymbol{X}(t)$.

From this, we find

$$\partial_i p = \frac{F_i}{2\pi|\boldsymbol{x}|^2} - 2\frac{F_j x_j x_i}{2\pi|\boldsymbol{x}|^4} = \frac{F_j}{2\pi|\boldsymbol{x}|^2}\left(\delta_{ij} - 2\frac{x_j x_i}{|\boldsymbol{x}|^2}\right) \tag{373}$$

and

$$
\begin{aligned}
\partial_k J_{ij} &= \frac{1}{4\pi\mu}\partial_k\left[-\delta_{ij}\ln\left(\frac{|\boldsymbol{x}|}{a}\right) + \frac{x_i x_j}{|\boldsymbol{x}|^2}\right] \\
&= \frac{1}{4\pi\mu}\left[-\delta_{ij}\frac{1}{|\boldsymbol{x}|}\partial_k|\boldsymbol{x}| + \partial_k\left(\frac{x_i x_j}{|\boldsymbol{x}|^2}\right)\right] \\
&= \frac{1}{4\pi\mu}\left[-\delta_{ij}\frac{x_k}{|\boldsymbol{x}|^2} + \left(\delta_{ik}\frac{x_j}{|\boldsymbol{x}|^2} + \delta_{jk}\frac{x_i}{|\boldsymbol{x}|^2} - 2\frac{x_i x_j x_k}{|\boldsymbol{x}|^4}\right)\right].
\end{aligned} \tag{374}
$$

To check the incompressibility condition, note that

$$
\begin{aligned}
\partial_i J_{ij} &= \frac{1}{4\pi\mu}\left[-\delta_{ij}\frac{x_i}{|\boldsymbol{x}|^2} + \left(\delta_{ii}\frac{x_j}{|\boldsymbol{x}|^2} + \delta_{ji}\frac{x_i}{|\boldsymbol{x}|^2} - \frac{x_i x_j x_i}{2|\boldsymbol{x}|^4}\right)\right] \\
&= \frac{1}{4\pi\mu}\left(-\frac{x_j}{|\boldsymbol{x}|^2} + 2\frac{x_j}{|\boldsymbol{x}|^2} + \frac{x_j}{|\boldsymbol{x}|^2} - 2\frac{x_j}{|\boldsymbol{x}|^2}\right) \\
&= 0,
\end{aligned} \tag{375}
$$

which confirms that the solution (371) satisfies the incompressibility condition $\nabla \cdot \boldsymbol{u} = 0$. Moreover, we find for the Laplacian

$$
\begin{aligned}
\partial_k \partial_k J_{ij} &= \frac{\partial_k}{4\pi\mu}\left[-\delta_{ij}\frac{x_k}{|\boldsymbol{x}|^2} + \delta_{ik}\frac{x_j}{|\boldsymbol{x}|^2} + \delta_{jk}\frac{x_i}{|\boldsymbol{x}|^2} - 2\frac{x_i x_j x_k}{|\boldsymbol{x}|^4}\right] \\
&= \frac{1}{4\pi\mu}\left[-\delta_{ij}\partial_k\left(\frac{x_k}{|\boldsymbol{x}|^2}\right) + \delta_{ik}\partial_k\left(\frac{x_j}{|\boldsymbol{x}|^2}\right) + \delta_{jk}\partial_k\left(\frac{x_i}{|\boldsymbol{x}|^2}\right) - 2\partial_k\left(\frac{x_i x_j x_k}{|\boldsymbol{x}|^4}\right)\right] \\
&= \frac{1}{4\pi\mu}\left[-\delta_{ij}\left(\frac{\delta_{kk}}{|\boldsymbol{x}|^2} - 2\frac{x_k x_k}{|\boldsymbol{x}|^4}\right) + \delta_{ik}\left(\frac{\delta_{jk}}{|\boldsymbol{x}|^2} - 2\frac{x_j x_k}{|\boldsymbol{x}|^4}\right) + \delta_{jk}\left(\frac{\delta_{ik}}{|\boldsymbol{x}|^2} - 2\frac{x_i x_k}{|\boldsymbol{x}|^4}\right) - \right. \\
&\qquad \left. 2\left(\frac{\delta_{ik} x_j x_k}{|\boldsymbol{x}|^4} + \frac{x_i \delta_{jk} x_k}{|\boldsymbol{x}|^4} + \frac{x_i x_j \delta_{kk}}{|\boldsymbol{x}|^4} - 4\frac{x_i x_j x_k x_k}{|\boldsymbol{x}|^6}\right)\right] \\
&= \frac{1}{4\pi\mu}\left[-\delta_{ij}\left(\frac{2}{|\boldsymbol{x}|^2} - 2\frac{1}{|\boldsymbol{x}|^2}\right) + \left(\frac{\delta_{ij}}{|\boldsymbol{x}|^2} - 2\frac{x_j x_i}{|\boldsymbol{x}|^4}\right) + \left(\frac{\delta_{ij}}{|\boldsymbol{x}|^2} - 2\frac{x_i x_j}{|\boldsymbol{x}|^4}\right) - \right. \\
&\qquad \left. 2\left(\frac{x_j x_i}{|\boldsymbol{x}|^4} + \frac{x_i x_j}{|\boldsymbol{x}|^4} + 2\frac{x_i x_j}{|\boldsymbol{x}|^4} - 4\frac{x_i x_j}{|\boldsymbol{x}|^4}\right)\right] \\
&= \frac{1}{2\pi\mu}\left(\frac{\delta_{ij}}{|\boldsymbol{x}|^2} - 2\frac{x_j x_i}{|\boldsymbol{x}|^4}\right) \tag{376}
\end{aligned}
$$

Hence, by comparing with (373), we see that indeed

$$-\partial_i p + \mu \partial_k \partial_k u_i = -\partial_i p + \mu \partial_k \partial_k J_{ij} F_j = 0. \tag{377}$$

The difference between 3D and 2D hydrodynamics has been confirmed experimentally for *Chlamydomonas* algae.

74

14.5   Force dipoles

In the absence of external forces, microswimmers must satisfy the force-free constraint. This simplest realization is a force-dipole flow, which provides a very good approximation for the mean flow field generated by an individual bacterium but not so much for a biflagellate alga.

To construct a force dipole, consider two opposite point-forces $\boldsymbol{F}^+ = -\boldsymbol{F}^- = F\boldsymbol{e}_x$ located at positions $\boldsymbol{x}^+ = \pm\ell\boldsymbol{e}_x$. Due to linearity of the Stokes equations the total flow at some point $\boldsymbol{x}$ is given by

$$
\begin{aligned}
u_i(\boldsymbol{x}) &= \Gamma_{ij}(\boldsymbol{x} - \boldsymbol{x}^+)\,F_j^+ + \Gamma_{ij}(\boldsymbol{x} - \boldsymbol{x}^-)\,F_j^- \\
&= \left[\Gamma_{ij}(\boldsymbol{x} - \boldsymbol{x}^+) - \Gamma_{ij}(\boldsymbol{x} - \boldsymbol{x}^-)\right]F_j^+ \\
&= \left[\Gamma_{ij}(\boldsymbol{x} - \ell\boldsymbol{e}_x) - \Gamma_{ij}(\boldsymbol{x} + \ell\boldsymbol{e}_x)\right]F_j^+
\end{aligned}
\tag{378}
$$

where $\Gamma_{ij} = J_{ij}$ in 2D and $\Gamma_{ij} = G_{ij}$ in 3D. If $|\boldsymbol{x}| \gg \ell$, we can Taylor expand Γ_{ij} near $\ell = 0$, and find to leading order

$$
\begin{aligned}
u_i(\boldsymbol{x}) &\simeq \left\{[\Gamma_{ij}(\boldsymbol{x}) - \Gamma_{ij}(\boldsymbol{x})] - \left[x_k^+\partial_k\Gamma_{ij}(\boldsymbol{x}) - x_k^-\partial_k\Gamma_{ij}(\boldsymbol{x})\right]\right\}F_j^+ \\
&= -2x_k^+\left[\partial_k\Gamma_{ij}(\boldsymbol{x})\right]F_j^+
\end{aligned}
\tag{379}
$$

2D case   Using our above result for $\partial_k J_{ij}$, and writing $\boldsymbol{x}^+ = \ell\boldsymbol{n}$ and $\boldsymbol{F}^+ = F\boldsymbol{n}$ with $|\boldsymbol{n}| = 1$, we find in 2D

$$
\begin{aligned}
u_i(\boldsymbol{x}) &= -\frac{x_k^+}{2\pi\mu}\left[-\delta_{ij}\frac{x_k}{|\boldsymbol{x}|^2} + \left(\delta_{ik}\frac{x_j}{|\boldsymbol{x}|^2} + \delta_{jk}\frac{x_i}{|\boldsymbol{x}|^2} - 2\frac{x_i x_j x_k}{|\boldsymbol{x}|^4}\right)\right]F_j^+ \\
&= -\frac{F\ell}{2\pi\mu}\left(-n_i\frac{x_k n_k}{|\boldsymbol{x}|^2} + n_i\frac{x_j n_j}{|\boldsymbol{x}|^2} + n_k n_k\frac{x_i}{|\boldsymbol{x}|^2} - 2\frac{n_k x_i x_j x_k n_j}{|\boldsymbol{x}|^4}\right)
\end{aligned}
$$

and, hence,

$$
\boldsymbol{u}(x) = \frac{F\ell}{2\pi\mu|\boldsymbol{x}|}\left[2(\boldsymbol{n}\cdot\hat{\boldsymbol{x}})^2 - 1\right]\hat{\boldsymbol{x}}
\tag{380}
$$

where $\hat{\boldsymbol{x}} = \boldsymbol{x}/|\boldsymbol{x}|$.

3D case   To compute the dipole flow field in 3D, we need to compute the partial derivatives of the Oseen tensor

$$
G_{ij}(\boldsymbol{x}) = \frac{1}{8\pi\mu|\boldsymbol{x}|}\left(1 + \hat{x}_i\hat{x}_j\right), \qquad \hat{x}_k = \frac{x_k}{|\boldsymbol{x}|}.
\tag{381}
$$

Defining the orthogonal projector (Π_{ik}) for $\hat{x}_k$ by

$$
\Pi_{ik} := \delta_{ik} - \hat{x}_i\hat{x}_k,
\tag{382}
$$

we have

$$\partial_k |\boldsymbol{x}| = \frac{x_k}{|\boldsymbol{x}|} = \hat{x}_k, \tag{383a}$$

$$\partial_k \hat{x}_i = \frac{\delta_{ik}}{|\boldsymbol{x}|} - \frac{x_k x_i}{|\boldsymbol{x}|^3} = \frac{\Pi_{ik}}{|\boldsymbol{x}|}, \tag{383b}$$

$$\partial_n \Pi_{ik} = -\frac{1}{|\boldsymbol{x}|} \left(\hat{x}_i \Pi_{nk} + \hat{x}_k \Pi_{ni} \right), \tag{383c}$$

and from this we find

$$\begin{aligned}
\partial_k G_{ij} &= -\frac{\hat{x}_k}{|\boldsymbol{x}|} G_{ij} + \frac{\kappa}{|\boldsymbol{x}|^2} \left(\Pi_{ik} \hat{x}_j + \Pi_{jk} \hat{x}_i \right) \\
&= \frac{\kappa}{|\boldsymbol{x}|^2} \left(-\hat{x}_k \delta_{ij} + \hat{x}_j \delta_{ik} + \hat{x}_i \delta_{jk} - 3\hat{x}_k \hat{x}_i \hat{x}_j \right).
\end{aligned} \tag{384}$$

Inserting this expression into (379), we obtain the far-field dipole flow in 3D

$$\boldsymbol{u}(\boldsymbol{x}) = \frac{F\ell}{4\pi\mu|\boldsymbol{x}|^2} \left[3(\boldsymbol{n} \cdot \hat{\boldsymbol{x}})^2 - 1 \right] \hat{\boldsymbol{x}}. \tag{385}$$

Experiments show that Eq. (385) agrees well with the mean flow-field of a bacterium.

Upon comparing Eqs. (380) and (385), it becomes evident that hydrodynamic interactions between bacteria in a free-standing 2D film are much longer-ranged than in a 3D bulk solution. This is a nice illustration of the fact that the number of available space dimensions can have profound effects on physical processes and interactions in biological systems.

14.6 Boundary effects

The results in the previous section assumed an quasi-infinte fluid. Yet, many swimming cells and microorganisms operate in the vicinity of solid boundaries that can substantially affect the self-propulsion and the hydrodynamic interactions of the organisms. Before tackling finite boundaries geometries it is useful to recall how the terms in the HD equations can be rewritten in cylindrical coordinates. The full Navier-Stokes equations are written out completely in Acheson's textbook for various coordinate systems. In the next part, we will summarize those terms that are most important for our further discussion of cylindrical confinements.

14.6.1 Reminder: Cartesian vs. cylindrical corodinates

Cartesian coordinates In a global orthornormal Cartesian frame $\{\boldsymbol{e}_x, \boldsymbol{e}_y, \boldsymbol{e}_z\}$, the position vector is given by $\boldsymbol{x} = x\boldsymbol{e}_x + y\boldsymbol{e}_y + z\boldsymbol{e}_z$, and accordingly the flow field $\boldsymbol{u}(\boldsymbol{x})$ can be represented in the form

$$\boldsymbol{u}(\boldsymbol{x}) = u_x(x, y, z)\, \boldsymbol{e}_x + u_y(x, y, z)\, \boldsymbol{e}_y + u_z(x, y, z)\, \boldsymbol{e}_z. \tag{386a}$$

The gradient vector is given by

$$\nabla = \boldsymbol{e}_x \partial_x + \boldsymbol{e}_y \partial_y + \boldsymbol{e}_z \partial_z, \tag{386b}$$

and, using the orthonormality $e_j \cdot e_k = \delta_{jk}$, the Laplacian is obtained as

$$\Delta = \nabla \cdot \nabla = \partial_x^2 + \partial_y^2 + \partial_z^2. \tag{386c}$$

One therefore finds for the vector-field divergence

$$\nabla \cdot \boldsymbol{u} \;=\; \partial_i u_i \;=\; \partial_x u_x + \partial_y u_y + \partial_z u_z \tag{386d}$$

and the vector-Laplacian

$$\Delta \boldsymbol{u} \;=\; \partial_i \partial_i \boldsymbol{u} \;=\; \begin{pmatrix} \partial_x^2 u_x + \partial_y^2 u_x + \partial_z^2 u_x \\ \partial_x^2 u_y + \partial_y^2 u_y + \partial_z^2 u_y \\ \partial_x^2 u_z + \partial_y^2 u_z + \partial_z^2 u_z \end{pmatrix}. \tag{386e}$$

Cylindrical coordinates   The local cylindrical basis vectors $\{e_r, e_\phi, e_z\}$ are defined by

$$e_r = \cos\phi\, e_x + \sin\phi\, e_y \,, \qquad e_\phi = -\sin\phi\, e_x + \cos\phi\, e_y \,, \qquad \phi \in [0, 2\pi) \tag{387a}$$

and they form a orthonormal system $e_j \cdot e_k = \delta_{jk}$, where now $i, j = r, \phi, z$. The volume element is given by

$$dV = r \, \sin\phi \, dr \, d\phi \, dz. \tag{387b}$$

In terms of cylindrical basis system, the position vector $\boldsymbol{x}$ can be expressed as

$$\boldsymbol{x} = r e_r + z e_z \,, \qquad r = \sqrt{x^2 + y^2} \tag{387c}$$

and the flow field $\boldsymbol{u}(\boldsymbol{x})$ can be decomposed in the form

$$\boldsymbol{u}(\boldsymbol{x}) = u_r(r, \phi, z)\, e_r + u_\phi(r, \phi, z)\, e_\phi + u_z(r, \phi, z)\, e_z. \tag{387d}$$

The gradient vector takes the form

$$\nabla = e_r \partial_r + e_\phi \frac{1}{r} \partial_\phi + e_z \partial_z, \tag{387e}$$

yielding the divergence

$$\nabla \cdot \boldsymbol{u} \;=\; \frac{1}{r} \partial_r (r u_r) + \frac{1}{r} \partial_\phi u_\phi + \partial_z u_z. \tag{387f}$$

The Laplacian of a scalar function $f(r, \phi, z)$ is given by

$$\nabla^2 f \;=\; \frac{1}{r} \partial_r (r \partial_r f) + \frac{1}{r^2} \partial_\phi^2 f + \partial_z^2 f \tag{387g}$$

and the Laplacian of a vector field $\boldsymbol{u}(r, \phi, z)$ by

$$\nabla^2 \boldsymbol{u} = L_r e_r + L_\phi e_\phi + L_z e_z \tag{387h}$$

where

$$L_r = \frac{1}{r}\partial_r(r\partial_r u_r) + \frac{1}{r^2}\partial_\phi^2 u_r + \partial_z^2 u_r - \frac{2}{r^2}\partial_\phi u_\phi - \frac{1}{r^2}u_r \qquad (387\text{i})$$

$$L_\phi = \frac{1}{r}\partial_r(r\partial_r u_\phi) + \frac{1}{r^2}\partial_\phi^2 u_\phi + \partial_z^2 u_\phi + \frac{2}{r^2}\partial_\phi u_r - \frac{1}{r^2}u_\phi \qquad (387\text{j})$$

$$L_z = \frac{1}{r}\partial_r(r\partial_r u_z) + \frac{1}{r^2}\partial_\phi^2 u_z + \partial_z^2 u_z \qquad (387\text{k})$$

Compared with the scalar Laplacian, the additional terms in the vector Laplacian arise from the coordinate dependence of the basis vectors.

Similarly, one finds that, the r-component of $(\boldsymbol{u}\cdot\nabla)\boldsymbol{u}$ is not simply $(\boldsymbol{u}\cdot\nabla)u_r$, but instead

$$e_r \cdot [(\boldsymbol{u} \cdot \nabla)\boldsymbol{u}] = (\boldsymbol{u} \cdot \nabla)u_r - \frac{1}{r}u_\phi^2. \qquad (388)$$

Physically, the term u_ϕ^2/r corresponds to the centrifugal force, and it arises because $\boldsymbol{u} = u_r\boldsymbol{e}_r + u_\phi\boldsymbol{e}_\phi + u_z\boldsymbol{e}_z$ and some of the unit vectors change with ϕ (e.g., $\partial_\phi\boldsymbol{e}_\phi = -\boldsymbol{e}_r$).

14.6.2 Hagen-Poiseuille flow

To illustrate the effects of no-slip boundaries on the fluid motion, let us consider pressure driven flow along a cylindrical pipe of radius R pointing along the z-axis. Assume that the flow is rotationally symmetric about the z-axis and constant in z-direction, $\boldsymbol{u} = u_z(r)\boldsymbol{e}_z$, where $r = \sqrt{x^2 + y^2}$ is the distance from the center. For such a flow, the incompressibility condition $\nabla \cdot \boldsymbol{u} = 0$ is automatically satisfied, and the Stokes equation in cylindrical coordinates (r, ϕ, z) reduces to

$$0 = -\partial_z p + \frac{\mu}{r}\partial_r(r\partial_r u_z). \qquad (389)$$

Integrating twice over r, the general solution u_z of this equation can be written as

$$u_z(r) = \frac{1}{4\mu}(\partial_z p)r^2 + c_1 \ln r + c_2, \qquad (390)$$

where c_1 and c_2 are constants to be determined by the boundary conditions. For a no-slip boundary with $u_z(R) = 0$ and finite flow speed at $r = 0$, one then finds

$$u_z(r) = -\frac{1}{4\mu}(\partial_z p)(R^2 - r^2). \qquad (391)$$

If we assume a linear pressure difference $\Delta P = P(L) - P(0)$ over a length L, then simply

$$p(z) = [P(L) - P(0)]\frac{z}{L} \qquad \Rightarrow \qquad \partial_z p = -\frac{P(0) - P(L)}{L}. \qquad (392)$$

The flow speed is maximal at center of the pipe

$$u_z^+ = \frac{P(0) - P(L)}{4\mu L}R^2 \qquad (393)$$

and the average transport velocity is

$$\overline{u}_z = \frac{1}{\pi R^2} \int_0^R u_z(r)\, 2\pi r dr = 0.5 u_z^+.$$ (394)

Note that, for fixed pressure difference and channel length, the transport velocity $\overline{u}_z$ decreases quadratically with the channel radius, signaling that the presence of boundaries can substantially suppress hydrodynamic flows. To illustrate this further, we next consider a useful approximation that can help to speed up numerical simulations through an effective reduction from 3D to 2D flow.

14.6.3   Hele-Shaw flow

Consider two quasi-infinite parallel walls located at $z = 0$ and $z = H$. This setting is commonly encountered in experiments that study microbial swimming in flat microfluidic chambers. Looking for a 2D approximation of the Stokes equation, we may assume constant pressure along the z-direction, $p = P(x, y)$, and neglect possible flow components in the vertical direction, $u_z = 0$. Furthermore, using the above results for Hagen-Poiseuille flow as guidance, we can make the ansatz

$$\boldsymbol{u}(x, y, z) = \frac{6z(H-z)}{H^2} \left[U_x(x, y)\boldsymbol{e}_x + U_x(x, y)\boldsymbol{e}_y \right] \equiv \frac{6z(H-z)}{H^2} \boldsymbol{U}(x, y),$$ (395)

corresponding to a parabolic flow profile in the vertical direction that accounts for no-slip boundaries at the walls; in particular, in the mid-plane

$$\boldsymbol{u}(x, y, H/2) = \frac{3}{2}\boldsymbol{U}(x, y).$$ (396)

We would like to obtain an effective equation for the effective 2D flow $\boldsymbol{U}(x, y)$. This can be achieved by inserting ansatz (395) into the Stokes equations and subsequently averaging along the z-direction[20], yielding

$$0 = \nabla \cdot \boldsymbol{U}\,, \qquad 0 = -\nabla P + \mu \nabla^2 \boldsymbol{U} - \kappa \boldsymbol{U}$$ (397)

where $\kappa = 12\mu/H^2$ and ∇ is now the 2D gradient operator. Note that compared with unconfined 2D flow in a free film, the appearance of the κ-term leads to an exponential damping of hydrodynamic excitations. This is analogous to the exponential damping in the Yukawa-potential (mediated by massive bosons) compared to a Coloumb potential (mediated by massless photons). That ist, due to the presence of the no-slip boundaries, effective 2D hydrodynamic excitations acquire an effective mass $\propto 1/H^2$.

15   The coffee cup

Let's try and apply our knowledge of fluid dynamics to a real observation, to test whether the theory actually works. We shall consider a question you will encounter in the last problem

---

[20]That is, by taking the integral $(1/H)\int_0^H dz$ of both sides.

set[21]: how long does it take a cup of coffee (or glass of water) to spin down if you start by stirring it vigorously? To proceed, we need a model of a coffee cup. For mathematical simplicity, let's just take it to be an infinite cylinder occupying $r \leq R$. Suppose that at $t = 0$ the fluid and cylinder are spinning at an angular frequency ω, and then the cylinder is suddenly brought to rest. Assuming constant density, we expect the solution to be cylindrically symmetric

$$p(\boldsymbol{x}, t) = p(r, t) , \qquad \boldsymbol{u}(\boldsymbol{x}, t) = u_\phi(r, t)\boldsymbol{e}_\phi, \tag{398}$$

with only a component of velocity in the angular direction $\boldsymbol{e}_\phi$. This component will only depend on r, not the angular coordinate or the distance along the axis of the cylinder (because the cylinder is assumed to be infinite).

We shall just plug the assumed functional form into the Navier-Stokes equations and see what comes out. Let's put our ansatz $p = p(r, t)$ and $\boldsymbol{u} = (0, u_\phi(r, t), 0)$, which satisfies $\nabla \cdot \boldsymbol{u} = 0$, into the cylindrical Navier-Stokes equations. The radial equation for $\boldsymbol{e}_r$-component becomes

$$\frac{u_\phi^2}{r} = \frac{\partial p}{\partial r}. \tag{399a}$$

Physically this represents the balance between pressure and centrifugal force. The angular equation to be satisfied by the $\boldsymbol{e}_\phi$-component is

$$\frac{\partial u_\phi}{\partial t} = \nu \left(\frac{\partial^2 u_\phi}{\partial r^2} + \frac{1}{r}\frac{\partial u_\phi}{\partial r} - \frac{u_\phi}{r^2} \right), \tag{399b}$$

and the vertical equation is

$$0 = \frac{1}{\rho}\frac{\partial p}{\partial z}. \tag{399c}$$

The last equation of these three is directly satisfied by our solution ansatz, and the first equation can be used to compute p by simple integration over r once we have found u_ϕ.

We want to solve these equation (399a) and (399b) with the initial condition

$$u_\phi(r, 0) = \omega r, \tag{400a}$$

and the boundary conditions that

$$u_\phi(0, t) = 0 , \qquad u_\phi(R, t) = 0 \qquad \forall t > 0. \tag{400b}$$

This is done using *separation of variables*. Since the lhs. of Eq. (399b) features a first-order time derivative, which usually suggests exponential growth or damping, let's guess a solution of the form

$$u_\phi = e^{-k^2 t} F(r). \tag{401}$$

Putting this into the governing equation (399b) gives the ODE

$$-k^2 F = \nu \left(F'' + \frac{F'}{r} - \frac{F}{r^2} \right) \tag{402}$$

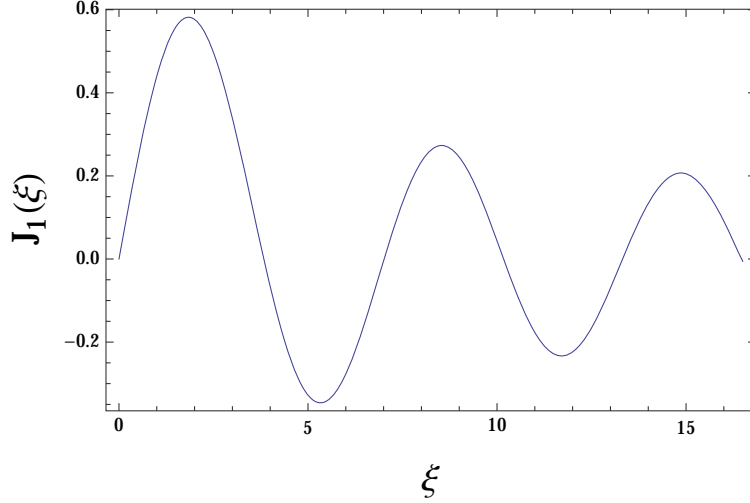[21]See Acheson, *Elementary Fluid Dynamics*, pp. 42-46

Figure 3: The Bessel function of the first order $J_1(\xi)$.

This equation looks complicated. However, note that if the factors of r weren't in this equation we would declare victory. The equation would just be $F'' + k^2/\nu F = 0$, which has solutions that are sines and cosines. The general solution would be $A\sin(k/\sqrt{\nu}r) + B\cos(k/\sqrt{\nu}r)$. We would then proceed by requiring that (a) the boundary conditions were satisfied, and (b) the initial conditions were satisfied.

We rewrite the above equation as

$$r^2 F'' + rF' + \left(\frac{k^2}{\nu}r^2 - 1\right) F = 0, \tag{403}$$

and make a change of variable,

$$\xi = kr/\sqrt{\nu}.$$

The equation becomes

$$\xi^2 F'' + \xi F' + \left(\xi^2 - 1\right) F = 0. \tag{404}$$

Even with the factors of ξ included, this problem is not more conceptually difficult, though it does require knowing solutions to the equation. It turns out that the solutions are called *Bessel Functions*. You should think of them as more complicated versions of sines and cosines. There exists a closed form of the solutions in terms of elementary functions. However, people usually denote the solution to the Eq. (404) as $J_1(\xi)$, named the *Bessel function of first order*[22]. This function is plotted in Fig. 3, satisfies the inner boundary conditions $J_1(0) = 0$. For more information, see for example the book *Elementary Applied Partial Differential Equations*, by Haberman (pp. 218-224). Now let's satisfy the boundary

---

[22]Bessel functions $J_\alpha(x)$ of order α are solutions of

$$x^2 J'' + xJ' + \left(x^2 - \alpha\right) J = 0$$

condition $u_\phi(R, t) = 0$. Since we have that

$$u_\phi = AJ_1(\xi) = AJ_1(kr/\sqrt{\nu}), \tag{405}$$

this implies that $AJ_1(kR/\sqrt{\nu}) = 0$. We can't have $A = 0$ since then we would have nothing left. Thus it must be that $J_1(kR/\sqrt{\nu}) = 0$. In other words, $kR/\sqrt{\nu} = \lambda_n$, where λ_n is the nth zero of J_1 (morally, J_1 is very much like a sine function, and so has a countably infinite number of zeros.) Our solution is therefore

$$u_\phi(r, t) = \sum_{n=1}^{\infty} A_n e^{-\nu \lambda_n^2 t / R^2} J_1(\lambda_n r/R). \tag{406}$$

To determine the A_n's we require that the initial conditions are satisfied. The initial condition is that

$$u_\phi(r) = \omega r. \tag{407}$$

Again, we now think about what we would do if the above sum had sines and cosines instead of J_1's. We would simply multiply by sine and integrate over a wavelength. Here, we do the same thing. We multiply by $rJ_1(\lambda_m r/R)$ and integrate from 0 to R. This gives the formula

$$A_n \int_0^R rJ_1(\lambda_n r/R)J_1(\lambda_m r/R) \, dr = \int_0^R \omega r^2 J_1(\lambda_m r/R)dr. \tag{408}$$

Using the identities

$$\int_0^R rJ_1(\lambda_n r/R)J_1(\lambda_m r/R) \, dr = \frac{R^2}{2} J_2(\lambda_n)^2 \delta_{nm}, \tag{409}$$

and

$$\int_0^R \omega r^2 J_1(\lambda_m r/R)dr = \frac{\omega R^3}{\lambda_m} J_2(\lambda_m), \tag{410}$$

we get

$$A_n = -\frac{2\omega R}{\lambda_n J_0(\lambda_n)}, \tag{411}$$

where we have used the identity $J_0(\lambda_n) = -J_2(\lambda_n)$. Our final solution is therefore

$$u_\phi(r, t) = -\sum_{n=1}^{\infty} \frac{2\omega R}{\lambda_n J_0(\lambda_n)} e^{-\nu \lambda_n^2 t / R^2} J_1(\lambda_n r/R). \tag{412}$$

Okay, so this is the answer. Now lets see how long it should take for the spin down to occur. Each of the terms in the sum is decreasing exponentially in time. The smallest value of λ_n decreases the slowest. It turns out that this value is $\lambda_1 = 3.83$. Thus the spin down time should be when the argument of the exponential is of order unity, or

$$t \sim \frac{R^2}{\nu \lambda_1^2}. \tag{413}$$

This is our main result, and we should test its various predictions. For example, this says that if we increase the radius of the cylinder by 4, the spin down time increases by a factor of 16. If we increase the kinematic viscosity ν by a factor of 100 (roughly the difference between water and motor oil) then it will take roughly a factor of 100 shorter to spin down. Note that for these predictions to be accurate, one must start with the *same angular velocity* for each case.

In your problem set you are asked to look at the spin down of a coffee cup. From our theory we have a rough estimate of the spin down time, which you can compare with your experiment. Do you get agreement between the two?

16 Singular perturbations

The *singular perturbation* is the bogeyman of applied mathematics. The fundamental problem is to ask: when can you neglect a term in a continuous equation? The answer is not always obvious and, amongst other things, this was the reason why early attempts to understand the theory of flight failed so dramatically. Before progressing towards this, we shall begin with a few examples of singular perturbations.

16.1 Magnetization

A magnet is composed of atoms, each of which has a molecular spin. The energetics of the interaction between the spins is that each spin produces a magnetic field which tries to align the neighboring spins. A popular microscopic model for a magnet imagines the spins confined to a regular lattice, and then ascribes an energy

$$U = \sum_{i \sim j} J_{ij} \boldsymbol{s}_i \cdot \boldsymbol{s}_j \tag{414}$$

where $i \sim j$ indicates a summation over nearest neighbors. A typical approximation is to take the sum over only the nearest neighbors of a given spin and to take the interaction constants J_{ij} to be a constant.

If one assumes that the local spins vary on a length scale much longer than a lattice spacing, then it is possible to derive a *macroscopic* analogue of the above energy. A complete derivation of this includes the effect of random thermal fluctuations and is beyond the scope of this course. For simplicity we consider just a one dimensional array of atoms for which the energy is

$$U[M(x)] = \int \left[\nu \left(\frac{dM}{dx} \right)^2 + f(M) \right] dx, \tag{415a}$$

where M is the magnitude of the local magnetization, which depends on the average spin in a small region, and

$$f(M) = -bM^2 + cM^4. \tag{415b}$$

Physically, ν punishes gradients in magnetization. If $b < 0$ then we have a *paramagnet*, with $M = 0$ being the minimum energy configuration. Otherwise if $b > 0$ then we have a *ferromagnet*, with minima at $\pm\sqrt{b/(2c)}$.

Using the calculus of variations the function $M(x)$ that minimises the energy satisfies

$$\nu \frac{d^2 M}{dx^2} - bM + 2cM^3 = 0. \tag{416}$$

We already know that

$$M = 0, \pm\sqrt{\frac{b}{2c}} \tag{417}$$

are three constant solutions. Now if $\nu = 0$ there is no penalty for orientation change throughout the system, and for $b > 0$ the entire system has magnetization $\pm\sqrt{\frac{b}{2c}}$ with any orientation. If the system has boundaries then the magnetization must match the boundary conditions, but is otherwise free to be orientated however it wants.

What happens, however, if $\nu \neq 0$? If we multiply both sides of (3) by M', then the equilibrium condition can be integrated to give

$$\frac{dM}{dx} = \frac{1}{\nu}\sqrt{bM^2 - cM^4 + k}, \tag{418}$$

where k is a constant. Rearranging this one obtains

$$\int \frac{\nu \, dM}{\sqrt{bM^2 - cM^4 + k}} = \int dx. \tag{419}$$

Solving this, subject to the appropriate boundary conditions, one finds that *domain boundaries* arise. These are transition regions in which the magnetization flips from the value imposed at one boundary to that at the other boundary. In the limit of $\nu \to 0$, these domain boundaries become infinitely sharp.

So now you start to get an idea of the problem. If $\nu = 0$ then the orientation of the spins throughout the system is arbitrary, except at the boundaries, which are fixed. However, even for extremely small non-zero ν (e.g., 10^{-100}), we have completely different behaviour and obtain extended regions of uniform magnetization separated by a sharp domain boundary. The different behaviour arises because if ν is nonzero the entire system is forced to match the imposed boundary conditions at the edges. Setting $\nu = 0$ is therefore called a singular perturbation.

16.2 An elementary algebraic equation

As another example of a singular perturbation, consider the solution of the algebraic equation

$$bx + c = 0. \tag{420}$$

The solution is simply $x = -c/b$. Now we make a small change, and consider the equation

$$\epsilon x^2 + bx + c = 0, \tag{421}$$

Using the quadratic formula,

$$x = \frac{-b \pm \sqrt{b^2 - 4\epsilon c}}{2\epsilon}. \tag{422}$$

In the limit $\epsilon \to 0$

$$x \approx -\frac{c}{b}, -\frac{2b - 2\epsilon c}{2\epsilon}. \tag{423}$$

and the latter solution can be further approximated as $-b/\epsilon$ if ϵ is very small. If this term has some physical significance then you are in trouble. You cannot simply neglect the term ϵx^2 in the original problem.

16.3 An elementary differential equation

Let's consider the differential equation[23]

$$\epsilon \frac{d^2 u}{dx^2} + \frac{du}{dx} = 1. \tag{424}$$

If ϵ is very small we might argue that we can neglect this term, the solution therefore being

$$u = x + C. \tag{425}$$

Alternatively, if we consider the full problem the solution is

$$u = A + x + Be^{-x/\epsilon}. \tag{426}$$

Imposing the boundary conditions $u(0) = 0, u(1) = 2$, for the full problem we determine A and B, and find that

$$u = x + \frac{1 - e^{-x/\epsilon}}{1 - e^{-1/\epsilon}} \tag{427}$$

is the exact solution. We cannot apply both these boundary conditions to our approximate solution (as it is a first order equation), so we choose the 'outer' condition $u(1) = 2$. The approximate solution satisfying the outer condition is therefore

$$u = x + 1. \tag{428}$$

In the outer region the approximate solution and the true solution are very close. However, in a region close to $x = 0$ they differ greatly. We call this the *boundary layer*. It arises because the small parameter ϵ multiplies the highest derivative in the equation, and by ignoring this term we lower the order of the system and are unable to satisfy both boundary conditions.

We need to find an approximate 'inner' solution that matches the boundary condition at $x = 0$. To do so, we change the independent variable to

$$X = \frac{x}{\epsilon}. \tag{429}$$

This enables us to zoom in on the boundary layer. With this scaling the original equation becomes

$$\frac{1}{\epsilon} \frac{d^2 u}{dX^2} + \frac{1}{\epsilon} \frac{du}{dX} = 1, \tag{430}$$

---

[23]See Acheson, pp. 269-271

so that to a first approximation the 'inner' solution satisfies

$$\frac{d^2u}{dX^2} + \frac{du}{dX} = 0. \tag{431}$$

Imposing the boundary condition at $X = 0$ gives

$$u = A(1 - e^{-X}) = A(1 - e^{-\frac{x}{\epsilon}}). \tag{432}$$

Finally, we require that as $X \to \infty$ the inner solution matches the outer solution in the limit $x \to 0$, so that $A = 1$.

We have thus been able to approximate the full solution in two parts, an inner and outer solution. Although we could solve for the full solution analytically, often this is not possible and we must resort to approximations like those used here. The inner solution is valid within a boundary layer of thickness ϵ and matches to the outer solution. Once again we see that ignoring the term multiplied by ϵ in the original problem is a *singular perturbation*; no matter how small ϵ is, there exists a region in which it has a significant affect on the solution. This idea was due to Prandtl, who first discovered it within the context of airplane flight. We will now take a bit of a digression to justify the concept of a boundary layer in fluid dynamics.

17   Towards airplane flight

There are two forces, lift and drag, experienced when an airplane wing moves through the air. At the start of the 20th century, however, fluid dynamicists were unable to correctly predict them. In fact, the lift and drag were determined to be identically zero, for all wing shapes (despite the fact that the Wright brothers had successfully built airplanes!). To proceed further into airplane flight, and how this problem was resolved, we shall first need some fluid mechanical preliminaries.

17.1   High-Reynolds number limit

We have already derived the Navier-Stokes equations

$$\frac{\partial \boldsymbol{u}}{\partial t} + \boldsymbol{u} \cdot \nabla \boldsymbol{u} = -\frac{\nabla p}{\rho} + \nu \nabla^2 \boldsymbol{u} , \qquad \nabla \cdot \boldsymbol{u} = 0. \tag{433}$$

The ratio of the viscous forces to inertial forces is

$$\frac{\nu \nabla^2 \boldsymbol{u}}{\boldsymbol{u} \cdot \nabla \boldsymbol{u}} \sim \frac{\nu U/L^2}{U^2/L} = \frac{\nu}{UL} = \frac{1}{\mathrm{Re}} \tag{434}$$

where Re is the *Reynolds number*. For an airplane typical values are U=400mph, L=5m and ν=0.1cm^2/s, giving $Re = 10^8$. Thus, the inertial forces are eight orders of magnitude larger than viscous forces, so it is seems very reasonable that we can neglect them. Doing so, we are left with the *Euler equations* for an inviscid fluid:

$$\frac{\partial \boldsymbol{u}}{\partial t} + \boldsymbol{u} \cdot \nabla \boldsymbol{u} = -\frac{\nabla p}{\rho} , \qquad \nabla \cdot \boldsymbol{u} = 0. \tag{435}$$

We shall first convince ourselves that these equations predict both the lift force (F_l) and the drag force (F_d) to be zero, independent of the shape of the wing.

The Euler equations can be written in an interesting form using the vector identity

$$\boldsymbol{u} \cdot \nabla \boldsymbol{u} = (\nabla \times \boldsymbol{u}) \times \boldsymbol{u} + \frac{\nabla(u^2)}{2} \tag{436}$$

as

$$\frac{\partial \boldsymbol{u}}{\partial t} + (\nabla \times \boldsymbol{u}) \times \boldsymbol{u} = -\nabla \left(\frac{p}{\rho} + \frac{u^2}{2} \right). \tag{437}$$

where u is the magnitude of $\boldsymbol{u}$. The quantity

$$\boldsymbol{\omega} = \nabla \times \boldsymbol{u} \tag{438}$$

is called the *vorticity*. In 2D it represents the average angular velocity of the fluid around any point, and has little to do with global rotations of the fluid (e.g., shear flows have non-zero vorticity). If the flow is steady ($\partial \boldsymbol{u}/\partial t = \boldsymbol{0}$) and *irrotational* ($\boldsymbol{\omega} = \boldsymbol{0}$) then we have *Bernoulli's law*:

$$H = \frac{p}{\rho} + \frac{u^2}{2} = constant. \tag{439}$$

The constancy of H in irrotational flow is a famous result, and has many simple qualitative consequences. It requires that the pressure in a fluid is smaller when the velocity is larger, and is a statement of conservation of energy when viscous dissipation can safely be ignored.

What are the consequences of $\boldsymbol{\omega} = \boldsymbol{0}$? The most important is that we can look for solutions $\boldsymbol{u}$ of the Euler equation that can be derived from velocity potential:

$$\boldsymbol{u} = \nabla \phi. \tag{440}$$

Now the wonderful thing is that if the flow is also incompressible, then from $\nabla \cdot \boldsymbol{u} = 0$ we obtain

$$\nabla^2 \phi = 0, \tag{441}$$

and we have reduced the problem to solving Laplace's equation. We can determine the pressure from the *Bernoulli relation*

$$\frac{p}{\rho} = H - \frac{(\nabla \phi)^2}{2}. \tag{442}$$

Solutions of these equations are typically called *ideal flows*, because viscosity has been neglected.

17.2 Kelvin's Theorem

When a plane is at rest we can reasonably argue that flow is initially irrotational ($\boldsymbol{\omega} = \boldsymbol{0}$). When the system becomes non-steady, and the plane accelerates, what happens? To answer this, consider the *circulation* around a closed loop moving with the flow:

$$\Gamma = \int_{C(t)} \boldsymbol{u} \cdot dl. \tag{443a}$$

By Stoke's theorem

$$\Gamma(t) = \int \boldsymbol{\omega} \cdot \boldsymbol{n} dA. \tag{443b}$$

Thus if $\boldsymbol{\omega} = \boldsymbol{0}$, $\Gamma = 0$. What is the time evolution of Γ? We know that

$$\frac{D\Gamma}{Dt} = \frac{d}{dt} \int_{C(t)} \boldsymbol{u} \cdot d\boldsymbol{l} = \int \left[\frac{D\boldsymbol{u}}{Dt} \cdot d\boldsymbol{l} + \boldsymbol{u} \cdot \frac{D(d\boldsymbol{l})}{Dt} \right]. \tag{444}$$

The first term concerns changes in the velocity field and is identically zero since

$$\int \frac{D\boldsymbol{u}}{Dt} \cdot d\boldsymbol{l} = \frac{1}{\rho} \int -\nabla p \cdot d\boldsymbol{l} = \frac{1}{\rho} \int (\nabla \times \nabla p) \cdot \boldsymbol{n} dA = 0. \tag{445}$$

The second term relates to stretching of the loop and is zero for essentially geometric reasons. One has that

$$\frac{D(d\boldsymbol{l})}{Dt} = d\boldsymbol{u} \tag{446}$$

since one end of the spatial vector $d\boldsymbol{l}$ moves with velocity $\boldsymbol{u}$ and the other with velocity $\boldsymbol{u} + d\boldsymbol{u}$. Thus

$$\int \boldsymbol{u} \cdot \frac{D(d\boldsymbol{l})}{Dt} = \int \boldsymbol{u} \cdot d\boldsymbol{u} = \int \frac{d(u^2)}{2} = 0, \tag{447}$$

because the integration is around a closed loop and u^2 has the same value at the start and end of it. But this implies

$$\frac{D\Gamma}{Dt} = 0, \tag{448}$$

so the circulation around a loop remains constant. If it is initially zero then it remains zero for all subsequent times. We should keep in mind, however, that our derivations of this result relied on the assumption that the fluid is inviscid and incompressible[24]

One of the most interesting things about this theorem is its historical origin: Kelvin viewed it as the basis of his vortex theory of the atom.[25]

18 Euler equations: basic solutions and forces

In the limit where the flow is irrotational, we just need to find solutions to Laplace's equation to obtain solutions to the Euler equations. Let's write down a couple of these to gain some intuition: our aim being to acquire techniques to begin to think about airplane flight.

18.1 Point source

We know from electrostatics that a solution of Laplace's equation is just

$$\phi = -\frac{c}{4\pi r}, \tag{449}$$

---

[24]More generally, $D\Gamma/Dt = 0$ still holds for barotropic ideal fluids with conservative body forces.
[25]Read Acheson (p. 168) for an interesting discussion of this.

where c would be the charge in an electrostatic problem. What does this solution correspond to for us? The velocity field

$$\boldsymbol{u} = \frac{c}{4\pi r^3}\boldsymbol{r} \tag{450}$$

is a radial source or sink of fluid.

18.2 Uniform flow

Another trivial solution is simply uniform flow

$$\phi = \boldsymbol{U}\cdot\boldsymbol{r}, \tag{451}$$

which works for any constant velocity vector $\boldsymbol{U}$.

18.3 Vortex solutions

We can also guess solutions by separation of variables $\phi = f(\theta)g(r)$, where θ and r denote cylindrical coordinates. Laplace's equation in cylindrical coordinates is

$$\frac{1}{r}\frac{\partial}{\partial r}\left(r\frac{\partial\phi}{\partial r}\right) + \frac{1}{r^2}\frac{\partial^2\phi}{\partial\theta^2} = 0. \tag{452}$$

Plugging this Ansatz into the equation gives that

$$\frac{r}{g}\frac{d}{dr}\left(r\frac{dg}{dr}\right) + \frac{1}{f}\frac{d^2f}{d\theta^2} = 0. \tag{453}$$

Each term in (453) must be a constant, i.e.

$$\frac{d^2f}{d\theta^2} = -fk^2, \tag{454a}$$

$$r\frac{d}{dr}\left(r\frac{dg}{dr}\right) = gk^2. \tag{454b}$$

For $k \neq 0$,

$$f = C\sin(k\theta) + D\cos(k\theta), \tag{455a}$$

with continuity of $\boldsymbol{u}$ requiring k to be an integer. Turning to the radial part we guess that $g = r^\alpha$. The radial equation then requires that $\alpha = \pm k$, giving

$$g(r) = Ar^k + Br^{-k}. \tag{455b}$$

However, if $k = 0$ then

$$f = C + D\theta. \tag{455c}$$

and the radial part is given by

$$g(r) = A + B\ln r. \tag{456}$$

89

So, the most general solution is

$$\phi(r, \theta) = (A_0 + B_0 \ln r)(C_0 + D_0 \theta) + \sum_{k=1}^{\infty} (C_k \sin k\theta + D_k \cos k\theta)(A_k r^k + B_k r^{-k}) \quad (457)$$

The corresponding velocity field is

$$\boldsymbol{u} = \nabla\phi = \frac{\partial\phi}{\partial r}\hat{\mathbf{r}} + \frac{1}{r}\frac{\partial\phi}{\partial\theta}\hat{\boldsymbol{\theta}}. \quad (458)$$

Putting in our general solution with $k = 0$, we get

$$\boldsymbol{u} = \frac{B_0(C_0 + D_0\theta)}{r}\hat{\mathbf{r}} + \frac{D_0}{r}(A_0 + B_0\ln r)\hat{\boldsymbol{\theta}} \quad (459)$$

Setting $B_0 = 0$ to obtain a continuous flow field, we get a flow with no radial component, and angular component

$$u_\theta = \frac{D}{r}, \quad (460)$$

which is irrotational by virtue of its construction. This is called a *point vortex* solution. If we consider the circulation about a loop containing the origin

$$\int \boldsymbol{u} \cdot d\mathbf{l} = \int_0^{2\pi} u_\theta r d\theta = 2\pi D = \Gamma \quad (461)$$

Thus $D = \Gamma/2\pi$, where Γ is the circulation about the point vortex.

18.4   Flow around a cylindrical wing

Okay, so this isn't the true shape of an airplane wing, but it's a good place to start. Let's see if we can calculate the lift and drag on a wing of length ℓ and radius $R \ll \ell$ moving with velocity u_0. In the frame of reference of the wing, the boundary conditions are

$$\phi \to u_0 x \quad \text{as} \quad r \to \infty, \quad (462\text{a})$$

$$\frac{\partial\phi}{\partial r} = 0 \quad \text{at} \quad r = R. \quad (462\text{b})$$

Using the general solution found above, the first boundary condition requires that

$$\phi = \left(u_0 r + \frac{D_1 B_1}{r}\right)\cos\theta + A_0(C_0 + D_0\theta). \quad (463)$$

The second boundary condition gives us

$$\phi = D_0\theta + u_0 \cos\theta \left(r + \frac{R^2}{r}\right), \quad (464)$$

where we have set $C_0 = 0$ since $\nabla\phi$ is all that matters. Physically we can see that $D_0 = \Gamma/2\pi$, where Γ is the circulation about the wing (check this by integrating around a circular loop containing the wing).

18.5   Forces on the circular wing

The lift and drag forces on the wing (length ℓ) are respectively given by

$$F_L = \ell \int_0^{2\pi} p(R, \theta) \ R \sin\theta d\theta, \tag{465a}$$

$$F_D = \ell \int_0^{2\pi} p(R, \theta) \ R \cos\theta d\theta. \tag{465b}$$

We can determine the pressure distribution from Bernoulli's Law

$$p = p_0 - \frac{\rho}{2}(\nabla\phi)^2\big|_{r=R} = p_0 - \frac{\rho}{2}\left(2u_0 \sin\theta - \frac{\Gamma}{2\pi R}\right)^2. \tag{466}$$

Putting this into the above relations we find that

$$F_D = 0. \tag{467}$$

This result is known as *D'Alembert's paradox*, contracting the well-known fact that drag is acting on a moving body even in in low viscosity fluids.

Furthermore, the lift on the wing is linearly proportional to the circulation about the wing;

$$F_L = \Gamma \rho \, u_0 \, \ell. \tag{468}$$

Thus, the lift on the cylindrical wing is zero (unless it is spinning, so that $\Gamma \neq 0$!). The lift force due to rotation is also known as Magnus force.

Our earlier discussion of singular perturbations suggests that *D'Alembert's paradox* for inviscid flows arises as a consequence of the fact that we have neglected viscosity in the Euler equations. Historically, this was first realized by Prandtl. Another shortcoming of our above calculations is that wings are not circular and, maybe, if we consider an alternative shape we would find lift. This will be our next avenue of investigation. We could also be worried about the fact that our problem is 2D. However, given that the aspect ratio of a wing is roughly 10:1, it is acceptable to consider 2D flow. In the next part, we will study how things change if we alter the shape of the wing. To do so will require *conformal mapping*.

19   Stream functions and conformal maps

There is a useful device for thinking about two dimensional flows, called the *stream function* of the flow. The stream function $\psi(x, y)$ is defined as follows

$$\boldsymbol{u} = (u, v) = \left(\frac{\partial\psi}{\partial y}, -\frac{\partial\psi}{\partial x}\right). \tag{469}$$

The velocity field described by ψ automatically satisfies the incompressibility condition, and it should be noted that

$$\boldsymbol{u} \cdot \nabla\psi = u\frac{\partial\psi}{\partial x} + v\frac{\partial\psi}{\partial y} = 0. \tag{470}$$

Thus ψ is constant along streamlines of the flow. Besides it's physical convenience, another great thing about the stream function is the following. By definition

$$u = \frac{\partial \psi}{\partial y} = \frac{\partial \phi}{\partial x}, \tag{471a}$$

$$v = -\frac{\partial \psi}{\partial x} = \frac{\partial \phi}{\partial y}, \tag{471b}$$

where ϕ is the velocity potential for an irrotational flow. Thus, both ϕ and ψ obey the well known *Cauchy-Riemann* equations of complex analysis.

19.1 The Cauchy-Riemann equations

In complex analysis you work with the complex variable $z = x + iy$. Thus, if you have some complex function $f(z)$ what is df/dz? Well, $f(z)$ can be separated into a real part $u(x, y)$ and an imaginary part $v(x, y)$, where u and v are real functions, i.e.:

$$f(z) = f(x + iy) = u(x, y) + iv(x, y). \tag{472}$$

For example, if $f(z) = z^2$ then $u = x^2 - y^2$ and $v = 2xy$. What then is df/dz? Since we are now in two-dimensions we can approach a particular point z from the x-direction or the y-direction (or any other direction, for that matter). On one hand we could define

$$\frac{df}{dz} = \frac{\partial f}{\partial x} = \frac{\partial u}{\partial x} + i\frac{\partial v}{\partial x}. \tag{473a}$$

Or, alternatively

$$\frac{df}{dz} = \frac{\partial f}{\partial(iy)} = -i\frac{\partial f}{\partial y} = -i\frac{\partial u}{\partial y} + \frac{\partial v}{\partial y}. \tag{473b}$$

For the definition of the derivative to make sense requires $\partial u/\partial x = \partial v/\partial y$ and $-\partial u/\partial y = \partial v/\partial x$, the Cauchy-Riemann equations. If this is true then $f(z)$ is said to be analytic and we can simply differentiate with respect to z in the usual manner. For our simple example $f(z) = z^2$ we have that $df/dz = 2z$ (confirm for yourself that z^2 is analytic as there are many functions that are not, e.g., $|z|$ is not an analytic function.)

19.2 Conformal mapping

We can now use the power of complex analysis to think about two dimensional potential flow problems. Since ϕ and ψ obey the Cauchy-Riemann equations, this implies that $w = \phi + i\psi$ is an analytic function of the complex variable $z = x + iy$. We call w the *complex potential*. Another important property of 2D incompressible flow is that both ϕ and ψ satisfy Laplace's equation. For example, using the Cauchy-Riemann equations we see that

$$\frac{\partial \psi}{\partial x^2} + \frac{\partial \psi}{\partial y^2} = -\frac{\partial^2 \psi}{\partial x \partial y} + \frac{\partial^2 \psi}{\partial y \partial x} = 0. \tag{474}$$

The same proof can be used for ϕ. We can therefore consider any analytic function (e.g., $\sin z, z^4,...$), calculate the real and imaginary parts and both of them satisfy Laplace's equation.

The velocity components u and v are directly related to dw/dz, which is conveniently calculated as follows:

$$\frac{dw}{dz} = \frac{\partial \phi}{\partial x} + i\frac{\partial \psi}{\partial x} = u - iv. \tag{475}$$

As a simple example consider uniform flow at an angle α to the x-axis. The corresponding complex potential is $w = u_0 z e^{-i\alpha}$. In this case $dw/dz = u_0 e^{-i\alpha}$. Using the above relation, this tells us that $u = u_0 \cos\alpha$ and $v = u_0 \sin\alpha$.

We can also determine the complex potential for flow past a cylinder since we know that

$$\phi = u_0\left(r + \frac{R^2}{r}\right)\cos\theta, \tag{476}$$

and this is just the real part of the complex potential

$$w = u_0\left(z + \frac{R^2}{z}\right). \tag{477}$$

Check this by substituting in $z = re^{i\theta}$. What is the corresponding stream function? Also $w(z) = -i\ln z$ is the complex potential for a point vortex since

$$Re\left(w(z)\right) = Re\left(-i\ln(re^{i\theta})\right) = \theta, \tag{478}$$

and we know that $\phi = \theta$ is the real potential for a point vortex. Thus

$$w(z) = u_0\left(z + \frac{R^2}{z}\right) - \frac{i\Gamma}{2\pi}\ln z \tag{479}$$

is the complex potential for flow past a cylinder with circulation Γ.

So let's assume that the only problem we know how to solve is flow past a cylinder, when really we want to know how to solve for flow past an aerofoil. The idea is to now consider two complex planes (x, y) and (X, Y). In the first plane we have the complex variable $z = x + iy$ and in the latter we have $Z = X + iY$. If we construct a mapping $Z = F(z)$ which is analytic, with an inverse $z = F^{-1}(Z)$, then $W(Z) = w(F^{-1}(Z))$ is also analytic, and may be considered a complex potential in the new co-ordinate system. Because $W(Z)$ and $w(z)$ take the same value at corresponding points of the two planes it follows that Ψ and ψ are the same at corresponding points. Thus streamlines are mapped into streamlines. In particular a solid boundary in the z-plane, which is necessarily a streamline, gets mapped into a streamline in the Z-plane, which could accordingly be viewed as a rigid boundary. Thus all we have done is distort the streamlines and the boundary leaving us with the key question: Given flow past a circular cylinder in the z-plane can we choose a mapping so as to obtain in the Z-plane uniform flow past a more wing-like shape? (Note that we have brushed passed some technical details here, such as the requirement that $dF/dz \neq 0$ at any point, as this would cause a blow-up of the velocity).

19.3 Simple conformal maps

The simplest map is

$$Z = F(z) = z + b, \tag{480}$$

which corresponds to a translation. Then there is

$$Z = F(z) = ze^{i\alpha}, \tag{481}$$

which corresponds to a rotation through angle α. In this case, the complex potential for uniform flow past a cylinder making angle α with the stream is

$$W(Z) = u_0 \left(Ze^{-i\alpha} + \frac{R^2}{Z}e^{i\alpha} \right) - \frac{i\Gamma}{2\pi} \ln Z. \tag{482}$$

Note, that this expression could also include the term $\ln e^{i\alpha} = i\alpha$ which I have neglected. This is just a constant however and doesn't change the velocity.

Finally there is the non-trivial *Joukowski transformation*,

$$Z = F(z) = z + \frac{c^2}{z}. \tag{483}$$

What does this do to the circle? Well, $z = ae^{i\theta}$ becomes

$$Z = ae^{i\theta} + \frac{c^2}{a}e^{-i\theta} = (a + \frac{c^2}{a})\cos\theta + i(a - \frac{c^2}{a})\sin\theta. \tag{484}$$

Defining $X = Re(Z)$, $Y = Im(Z)$, it is easily shown that

$$\left(\frac{X}{a + \frac{c^2}{a}} \right)^2 + \left(\frac{Y}{a - \frac{c^2}{a}} \right)^2 = 1, \tag{485}$$

which is the equation of an ellipse, provided $c < a$.

20 Classical aerofoil theory

We now know that through conformal mapping it is possible to transform a circular wing into a more realistic shape, with the bonus of also getting the corresponding inviscid, irrotational flow field. Let's consider some more realistic shapes and see what we get.

20.1 An elliptical wing

First let's rotate our cylinder by an angle α. The complex potential becomes

$$w(z) = u_0 \left(ze^{-i\alpha} + \frac{R^2}{z}e^{i\alpha} \right) - \frac{i\Gamma}{2\pi} \ln z. \tag{486}$$

Now, using the Joukowski transformation we want to turn our circular wing into an elliptical wing. The transformation stipulates that $Z = z + c^2/z$, so that

$$z_\pm(Z) = \frac{Z}{2} \pm \sqrt{\frac{Z^2}{4} - c^2}. \tag{487}$$

Considering $z_+(Z)$

$$w(z) = u_0 \left[z_+(Z)e^{-i\alpha} + \frac{R^2}{z_+(Z)}e^{i\alpha} \right] - \frac{i\Gamma}{2\pi} \ln z_+(Z). \tag{488}$$

If we choose $c = R$, then the ellipse collapses to a flat plate. The velocity components in the Z plane are

$$U - iV = \frac{dW}{dZ} = u_0 \cos\alpha - \frac{i(\Gamma + 2\pi u_0 Z \sin\alpha)}{2\pi\sqrt{Z^2 - 4R^2}}, \tag{489}$$

which can also be written as

$$U - iV = \frac{dw/dz}{dZ/dz} = \frac{u_0\left(e^{-i\alpha} - \frac{e^{i\alpha}R^2}{z^2}\right) - \frac{i\Gamma}{2\pi z}}{1 - R^2/z^2} \tag{490}$$

On the surface of the body we have $z = Re^{i\theta}$, so the velocities become

$$U - iV = \frac{u_0\left(e^{-i\alpha} - e^{-2i\theta}e^{i\alpha}\right) - \frac{i\Gamma e^{-i\theta}}{2\pi R}}{1 - e^{-2i\theta}}. \tag{491}$$

At $\theta = 0$ and $\theta = \pi$ we are in trouble because the velocities are infinite. Notably, however, this problem can be removed at $\theta = 0$ if the circulation is chosen so that the numerator vanishes

$$U - iV = \frac{e^{-i\theta}\left[u_0(e^{i(\theta-\alpha)} - e^{-i(\theta-\alpha)}) - \frac{i\Gamma}{2\pi R}\right]}{1 - e^{-2i\theta}}. \tag{492}$$

Thus for a finite velocity at $\theta = 0$ we require

$$u_0(e^{-i\alpha} - e^{i\alpha}) - \frac{i\Gamma}{2\pi R} = 0, \tag{493}$$

giving

$$\Gamma = -4\pi u_0 R \sin\alpha. \tag{494}$$

In this case flow leaves the trailing edge smoothly and parallel to the plate. Note that it is not possible to cancel out singularities at both ends simultaneously, as we have to rotate in the opposite direction to cancel out the singularity at $\theta = \pi$.

20.2 Flow past an aerofoil

What if we could now construct a mapping with a singularity just on one side ? This we can do by considering a shifted circle, that passes through $z = R$ but encloses $z = -R$. In this case we obtain an aerofoil with a rounded nose but a sharp trailing edge. The boundary of the appropriate circle is prescribed by

$$z = -\lambda + (a + \lambda)e^{i\theta}, \tag{495}$$

where θ is a parameter. First we must modify the complex potential for flow past a cylinder to take account of this new geometry. We have that

$$w(z) = u_0\left[(z + \lambda)e^{-i\alpha} + \frac{(R + \lambda)^2}{(z + \lambda)^2}e^{i\alpha}\right] - \frac{i\Gamma}{2\pi}\ln(z + \lambda). \tag{496}$$

To find the complex potential for the aerofoil one must then substitute in $z = Z/2 + \sqrt{Z^2/4 - R^2}$. Determining the velocities as before we find that

$$u - iv = \frac{dW}{dZ} = \frac{dw/dz}{dZ/dz} = u_0 \frac{e^{-i\alpha} - \left(\frac{R+\lambda}{z+\lambda}\right)^2 - \frac{i\Gamma}{2\pi(z+\lambda)}}{1 - \frac{R^2}{z^2}}. \tag{497}$$

The value of Γ that makes the numerator zero at the trailing edge is

$$\Gamma = -4\pi u_0 (R + \lambda) \sin \alpha. \tag{498}$$

The flow is then smooth and free of singularities everywhere (because we have successfully trapped the rogue singularity inside the wing), and this is an example of the *Kutta-Joukowski condition* at work.

Our goal in the reminder of this part is to show that our earlier results $F_L = \rho \ell u_0 \Gamma$ and $F_D = 0$ are unaffected by the wing shape. To this end, we first derive Blasius' lemma and then the Kutta-Joukowski theorem.

20.3 Blasius' lemma

To derive Blasius' lemma, we consider the force acting per unit length on the wing, $\boldsymbol{f} = \boldsymbol{F}/\ell = (f_x, f_y)$, which is obtained by integrating the pressure over the (now arbitrary) surface contour ∂S

$$\boldsymbol{f} = -\oint_{\partial S} p\,\boldsymbol{n}\,ds \tag{499}$$

where $\boldsymbol{n}$ is the outward surface normal vector and ds the arc length. Denote by $dz = dx + idy$ a small change along the curve ∂S. In complex notation, the normal element $\boldsymbol{n}\,ds$ can then be expressed as

$$-i\,dz = dy - i\,dx, \tag{500}$$

and Eq. (499) can be rewritten as

$$f := f_x + if_y = i\oint p\,dz. \tag{501}$$

From Bernoulli we have that $p = p_0 - \rho|v|^2/2$, where

$$v = v_x - iv_y = \frac{dw}{dz}, \qquad |v|^2 = v\bar{v} = v_x^2 + v_y^2 = \left|\frac{dw}{dz}\right|^2. \tag{502}$$

Thus, we find

$$f = i\oint \left(p_0 - \frac{\rho}{2}|v|^2\right)\,dz = -i\frac{\rho}{2}\oint |v|^2\,dz \tag{503}$$

Taking the complex conjugate, we have

$$\bar{f} = f_x - if_y = i\frac{\rho}{2}\oint |v|^2\,d\bar{z}. \tag{504}$$

96

Furthermore, since v is parallel to z on boundary (which is a stream line), we may use

$$0 = v_x dy - v_y dx \tag{505}$$

to rewrite

$$
\begin{aligned}
v^2\, dz &= (v_x - iv_y)^2(dx + idy) \\
&= (v_x^2 - v_y^2 - 2iv_x v_y)(dx + idy) \\
&= v_x^2 dx - v_y^2 dx - 2iv_x v_y dx + v_x^2 idy - v_y^2 idy + 2v_x v_y dy \\
&= v_x^2 dx - v_y^2 dx - 2iv_x^2 dy + v_x^2 idy - v_y^2 idy + 2v_y^2 dx \\
&= v_x^2 dx + v_y^2 dx - v_x^2 idy - v_y^2 idy \\
&= (v_x^2 + v_y^2)dx - (v_x^2 + v_y^2)idy \\
&= (v_x^2 + v_y^2)(dx - idy) \\
&= |v|^2\, d\bar{z} \tag{506}
\end{aligned}
$$

Hence,

$$\bar{f} = i\frac{\rho}{2}\oint v^2\, dz = i\frac{\rho}{2}\oint \left(\frac{dw}{dz}\right)^2 dz \tag{507}$$

which is the statement of the Blasius lemma.

20.4   Kutta-Joukowski theorem

We now use Blasius' lemma to prove the Kutta-Joukowski lift theorem. For flow around a plane wing we can expand the complex potential in a *Laurent series*, and it must be of the form

$$\frac{dw}{dz} = a_0 + \frac{a_{-1}}{z} + \frac{a_{-2}}{z^2} + \dots \tag{508}$$

Higher powers of z cannot appear if the flow remains finite at $|z| \to \infty$ and, in this case, we can identify

$$a_0 = v_x(\infty) - iv_y(\infty). \tag{509}$$

In particular, if the wing moves along the x-axis and surrounding gas is at rest, then simply $a_0 = v_x(\infty)$.

To obtain the physical meaning of a_{-1}, we note that by virtue of the residues theorem[26]

$$a_{-1} = \frac{1}{2\pi i}\oint \frac{dw}{dz}\, dz \tag{510}$$

---

[26]Let's assume some otherwise analytic function $f(z)$ has a pole at $z = 0$. The residue is the coefficient a_{-1} of the Laurent series $f(z) = \sum_{k=-\infty}^{\infty} a_k z^k$. The residue theorem states that for a positively oriented simple closed curve γ around $z = 0$

$$\oint_\gamma f(z)dz = 2\pi i\, a_{-1}.$$

Computing the integral on the rhs. gives

$$
\begin{aligned}
\oint \frac{dw}{dz}\, dz &= \oint (v_x - iv_y)(dx + idy) \\
&= \oint (v_x dx + v_y dy) + i \oint (v_x dy - v_y dx)
\end{aligned}
\tag{511}
$$

The last integral vanishes as the boundary is stream line, see Eq. (505), so that

$$
a_{-1} = \frac{1}{2\pi i} \oint \boldsymbol{v} \cdot d\boldsymbol{x} = \frac{\Gamma}{2\pi i}.
\tag{512}
$$

where Γ is the circulation defined above.

To evaluate the rhs. in Eq. (507), we note that to leading order

$$
\left(\frac{dw}{dz}\right)^2 \simeq a_0 + 2\frac{a_0 a_{-1}}{z} = a_0 + \frac{a_0 \Gamma}{\pi i z}
\tag{513}
$$

Thus, using the residue theorem, we find

$$
\bar{f} = f_x - if_y = i\frac{\rho}{2}\left(2\pi i \frac{a_0 \Gamma}{\pi i}\right) = i\rho \Gamma a_0 = \rho \Gamma v_y(\infty) + i\rho \Gamma v_x(\infty).
\tag{514}
$$

Recall that $F_D = \ell f_x$ and $F_L = \ell f_y$, this is indeed the generalization of our earlier results for drag and lift on a cylinder, if we identify $v_y(\infty) = 0$ and $v_x(\infty) = -u_0$. Note that the results $F_D = 0$ is again a manifestation of d'Alembert's paradox (now for arbitrarily shaped wings), which can be traced back to the fact that we neglected the viscosity terms in the Navier-Stokes equations.

21 Rotating flows

In our above discussion of airfoils, we have neglected viscosity which led to d'Alembert's paradox. To illustrate further the importance of boundary layers, we will consider one more example of substantial geophysical importance, where the dynamics of laminar flows is completely controlled by the boundary layer. In the process of deriving this result we will also learn about a rather remarkable phenomenon in rotating fluid dynamics.[27]

21.1 The Taylor-Proudman theorem

Consider a fluid rotating with angular velocity Ω. The equation of motion in the frame of reference rotating with the fluid is

$$
\frac{\partial \boldsymbol{u}}{\partial t} + \boldsymbol{u} \cdot \nabla \boldsymbol{u} + \Omega \times (\Omega \times \boldsymbol{r}) = -\frac{1}{\rho}\nabla p_\Omega + \nu \nabla^2 \boldsymbol{u} - 2\Omega \times \boldsymbol{u},
\tag{515a}
$$

$$
\nabla \cdot \boldsymbol{u} = 0.
\tag{515b}
$$

---

[27]See Acheson, pp. 278-287

There are two additional terms: the first $\Omega \times (\Omega \times \boldsymbol{r})$ is the centrifugal acceleration, which can be thought of as an augmentation to the pressure distribution, using the identity

$$\Omega \times (\Omega \times \boldsymbol{r}) = -\frac{1}{2}\nabla(\Omega \times \boldsymbol{r})^2. \tag{516}$$

Henceforth, we will simply absorb this into the pressure by writing

$$p = p_\Omega - \frac{\rho}{2}(\Omega \times \boldsymbol{r})^2. \tag{517}$$

For the rotating earth, the effect of this force is to simply distort the shape of the object from a sphere into an oblate ellipsoid. The second term is the *Coriolis acceleration* which is velocity dependent. Hopefully you have heard about it in classical mechanics.

We are going to be interested in flows which are much weaker than the rotation of the system. If U is a characteristic velocity scale and L is a characteristic length scale, then the advective term is of order U^2/L whereas the coriolis force is of order ΩU. We will assume that $\Omega U \gg U^2/L$ so that the equation of motion is effectively

$$\frac{\partial \boldsymbol{u}}{\partial t} = -\frac{1}{\rho}\nabla p + \nu \nabla^2 \boldsymbol{u} - 2\Omega \times \boldsymbol{u}, \tag{518a}$$

$$\nabla \cdot \boldsymbol{u} = 0. \tag{518b}$$

21.2 Steady, inviscid flow

Now let's consider flow at high Reynolds number. The Reynolds number is now $\Omega L^2/\nu$ within this framework. As usual, the first step is to write down the inviscid equations (since the viscosity is small), and then the next step is to correct them with boundary layers.

Following Acheson, let's write the flow velocity as $\boldsymbol{u} = (u_I, v_I, w_I)$ and $\boldsymbol{\Omega} = (0, 0, \Omega)$. The steady, inviscid flow satisfies

$$2\Omega v_I = \frac{1}{\rho}\frac{\partial p_I}{\partial x}, \tag{519a}$$

$$2\Omega u_I = -\frac{1}{\rho}\frac{\partial p_I}{\partial y}, \tag{519b}$$

$$0 = \frac{1}{\rho}\frac{\partial p_I}{\partial z}, \tag{519c}$$

$$\frac{\partial u_I}{\partial x} + \frac{\partial v_I}{\partial y} + \frac{\partial w_I}{\partial z} = 0. \tag{519d}$$

The third equation says that the pressure is independent of z. Hence, the first two equations say that u_I and v_I are independent of z. Then the last equation says that w_I is independent of z. Thus, *the entire fluid velocity is independent of z!* This result, which is remarkable, is called the *Taylor-Proudman theorem*. Proudman discovered the theorem, but Taylor discovered what is perhaps its most remarkable consequence.

21.3 Taylor columns

In his paper "Experiments on the motion of solid bodies in rotating fluids", Taylor posed the simple question: given the above fact that slow steady motions of a rotating liquid must be two-dimensional, what happens if one attempts to make a three dimensional motion by, for example, pushing a three dimensional object through the flow with a small uniform velocity? At the beginning of his paper he points out three possibilities:

1. The motion in the liquid is never steady.

2. The motion is steady, but our assumption that u_I is small relative to the rotation velocity breaks down near the object.

3. The motion is steady and two dimensional.

He remarks that the first possibility is unlikely, since it must settle down eventually. The realistic possibilities are (2) and (3). His paper, which can be downloaded from the course page, demonstrates that actually what happens is possibility (3). This is really rather remarkable (as Taylor notes) because there is only one way that it can really happen: An entire column of fluid must move atop the object.

21.4 More on rotating flows

Above, we wrote the equations of a rotating fluid assuming that the rotation frequency dominated the characteristic hydrodynamic flows in the problem. In other words, if Ω is the characteristic rotation frequency, L is a horizontal lengthscale, and U is a typical velocity in the rotating frame, we assumed that

$$\mathrm{Ro} = \frac{U}{\Omega L} \ll 1. \tag{520}$$

This dimensionless number is called the *Rossby number*. The equations were

$$\frac{\partial \boldsymbol{u}}{\partial t} = -\frac{1}{\rho}\nabla p + \nu\nabla^2\boldsymbol{u} - 2\Omega \times \boldsymbol{u}, \tag{521a}$$
$$\nabla \cdot \boldsymbol{u} = 0. \tag{521b}$$

We will use these ideas to revisit the famous problem of the spin-down of a coffee cup that we discussed at the very beginning of class. You might recall that the problem we had was that our simple theory of how the spin-down occurred turned out to be entirely false. We shall now construct the correct theory, while learning a bit of atmospheric and oceanic physics along the way.

21.5 More on the Taylor-Proudman theorem

Let's consider the Taylor-Proudman theorem again, this time using another method. We consider the viscosity to be small so that we can use the limit of a stationary, inviscid fluid. More precisely, we consider the ratio

$$\mathrm{E_k} = \frac{\nu\nabla^2\boldsymbol{u}}{\Omega \times \boldsymbol{u}} = \frac{\nu}{\Omega L^2} \ll 1. \tag{522}$$

This dimensionless number is called the *Ekman number.* The flow is then strictly two-dimensional, and the Navier-Stokes equation simplifies to

$$-\frac{1}{\rho}\nabla p = 2\boldsymbol{\Omega} \times \boldsymbol{u}. \tag{523}$$

Taking the curl of both sides, we find

$$\nabla \times (\boldsymbol{\Omega} \times \boldsymbol{u}) = \boldsymbol{\Omega}\nabla \cdot \boldsymbol{u} - \boldsymbol{u}\nabla \cdot \boldsymbol{\Omega} + \boldsymbol{u} \cdot \nabla\boldsymbol{\Omega} - \boldsymbol{\Omega} \cdot \nabla\boldsymbol{u} = -\Omega\frac{\partial \boldsymbol{u}}{\partial z}. \tag{524}$$

Here, we have used the fact that the fluid velocity is divergence free. Hence we have that $\partial \boldsymbol{u}/\partial z$=0, or that the fluid velocity is independent of z. A major consequence of this (Taylor columns) was discussed above.

Before leaving this topic, let's make one more remark. Taking the dot product of the equations of inviscid flow with $\boldsymbol{u}$, we get

$$\boldsymbol{u} \cdot \nabla p = -\rho\boldsymbol{u} \cdot (2\Omega \times \boldsymbol{u}) = 0. \tag{525}$$

This formula states that *the velocity field moves perpendicular to the pressure gradient,* which is somewhat against one's intuition. Hence, the fluid actually moves along lines of constant pressure. Pressure work is not performed either on the fluid or by the fluid. Geophysicists call this fact the *geostrophic balance.*

There is an entertaining fact that one can deduce about atmospheric flows. For an atmospheric flow, the analogue of Ω is not the earth's rotation speed $\hat{\omega}$, but instead $\Omega = \hat{\omega}\sin\phi$, where ϕ is the longitude. Now, this shows that the effective Ω changes sign in the northern and southern hemisphere. What does this imply for the dynamics? When $\Omega > 0$ the velocity moves with the high pressure on the right. Conversely in the southern hemisphere, the velocity moves with the high pressure on the left. It is also true that because of this change in sign, Naval warships have to adjust their range finding when crossing over the equator. However, the myth about the bathtub vortex does not hold because one cannot throw out inertial and viscous terms in solving this problem. The Coriolis force is only important on large scales.

22 The Ekman layer

We would now like to return to our coffee cup problem, to get the right answer. To do so, we shall consider the effect of walls on the inviscid flow we calculated in the previous lecture. For starters, lets consider a jar with the top moving at angular velocity Ω_T and the bottom moving at angular velocity Ω_B. Clearly, if $\Omega_T = \Omega_B$ then our inviscid solution applies. Let's try and figure out what happens when Ω_T becomes different from Ω_B.

22.1 A small deviation

Suppose Ω_T=Ω and $\Omega_B = \Omega + \epsilon$. Now there is no way to satisfy the no slip condition on both the top and bottom while having the whole flow spin at angular velocity Ω. Let's move first to the rotating frame, and try to compute the secondary flow that is induced. Clearly,

without viscosity it is impossible to solve this problem because the Taylor-Proudman theorem states that inviscid flow is two dimensional (and so no gradient in Ω across the cylinder axis is possible). We therefore anticipate that even though the Rossby number is small, there will be boundary layers. Let's divide the flow into three regions: (1) A boundary layer at the top plate; (2) a boundary layer at the bottom plate; and (3) a central inviscid region.

In the inviscid region we would expect that the solution is (u_I, v_I, w_I), where

$$-2\Omega v_I = -\frac{1}{\rho}\frac{\partial p_I}{\partial x}, \tag{526a}$$

$$2\Omega u_I = -\frac{1}{\rho}\frac{\partial p_I}{\partial y}, \tag{526b}$$

$$0 = \frac{1}{\rho}\frac{\partial p_I}{\partial z}. \tag{526c}$$

In the same way as before, we expect the pressure gradient of the outer flow to force the boundary layer at the rotating wall. Let's consider the structure of the boundary layer at the bottom wall, $z = 0$. There the equations are

$$-2\Omega v = -\frac{1}{\rho}\frac{\partial p_I}{\partial x} + \nu\frac{\partial^2 u}{\partial z^2}, \tag{527a}$$

$$2\Omega u = -\frac{1}{\rho}\frac{\partial p_I}{\partial y} + \nu\frac{\partial^2 v}{\partial z^2}, \tag{527b}$$

$$0 = \frac{1}{\rho}\frac{\partial p_I}{\partial z} + \nu\frac{\partial^2 w}{\partial z^2}, \tag{527c}$$

$$\nabla \cdot \boldsymbol{u} = 0. \tag{527d}$$

Here we have made the boundary layer approximation that $\partial/\partial z \gg \partial/\partial x, \partial/\partial y$.

From the continuity equation we deduce that w is much smaller than the velocity components parallel to the boundary so that $\partial p_I/\partial z = 0$, and the equations become

$$-2\Omega(v - v_I) = \nu\frac{\partial^2 u}{\partial z^2}, \tag{528a}$$

$$2\Omega(u - u_I) = \nu\frac{\partial^2 v}{\partial z^2}. \tag{528b}$$

These are the equations we must solve. Acheson has a good trick. Multiplying the second equation by i and adding the two yields

$$\nu\frac{\partial^2 f}{\partial z^2} = 2\Omega i f, \tag{529a}$$

where

$$f = u - u_I + i(v - v_I). \tag{529b}$$

The solution is obtained by guessing $f \sim e^{\alpha z}$, which yields $\alpha^2 = 2\Omega i/\nu$. Hence,

$$f = Ae^{(1+i)z^*} + Be^{-(1+i)z^*}, \qquad z^* = z\sqrt{\Omega/\nu}. \tag{530}$$

We require that as $z^* \to \infty$, $f \to 0$. This implies that $A = 0$. We are in the frame of reference moving with the bottom plate, so the no slip boundary condition at $z = 0$ requires that $f(z = 0) = -u_I - iv_I$. Splitting f into its real an imaginary parts implies

$$u = u_I - e^{-z^*}(u_I \cos(z/\delta) + v_I \sin(z/\delta)), \tag{531}$$

$$v = v_I - e^{-z^*}(v_I \cos(z/\delta) - u_I \sin(z/\delta)). \tag{532}$$

This is the velocity profile in the boundary layer.

What about the z-component? From the divergence free condition, we have

$$\left(\frac{\Omega}{\nu}\right)^{1/2} \frac{\partial w}{\partial z^*} = \frac{\partial w}{\partial z} = -\frac{\partial u}{\partial x} - \frac{\partial v}{\partial y} = \left(\frac{\partial v_I}{\partial x} - \frac{\partial u_I}{\partial y}\right) e^{-z^*} \sin z^*. \tag{533}$$

Integrating from $z^* = 0$ to ∞ gives

$$w = \frac{1}{2}\left(\frac{\Omega}{\nu}\right)^{-1/2}\left(\frac{\partial v_I}{\partial x} - \frac{\partial u_I}{\partial y}\right) = \frac{\hat{\omega}_I}{2}\sqrt{\frac{\nu}{\Omega}}, \tag{534}$$

where $\hat{\omega}_I$ is the vorticity in the inviscid flow. Thus, if $\hat{\omega}_I > 0$ (i.e., the bottom boundary is moving slower than the main body of fluid) then there is flow from the boundary layer into the fluid.

22.2   Matching

Now we have these Ekman layers at the top and the bottom. What we just assumed was that the boundary is moving at frequency Ω. If it is not, but instead moving at an angular frequency Ω_B relative to the rotating frame, then we need to change the boundary conditions a little in the rotating frame. In this case

$$w = \left(\frac{\nu}{\Omega_B}\right)^{1/2}\left(\frac{\hat{\omega}_I}{2} - \Omega_B\right). \tag{535a}$$

We could derive this, but it is intuitive since $(\hat{\omega}_I - 2\Omega_B)$ is the vorticity of the interior flow relative to the moving lower boundary. Similarly, if Ω_T denotes the angular velocity of the rigid upper boundary relative to the rotating frame, then there is a small z-component of velocity up into the boundary layer

$$w = \left(\frac{\nu}{\Omega_T}\right)^{1/2}\left(\Omega_T - \frac{\hat{\omega}_I}{2}\right). \tag{535b}$$

Now in our container both are happening. Since u_I, v_I and w_I are all independent of z then so is $\hat{\omega}_I$. Thus, the only way the experiment could work is if the induced value of $\hat{\omega}_I$ from both cases matches. This implies that

$$\hat{\omega}_I = \Omega_T + \Omega_B. \tag{536}$$

With $\Omega_B = 0$ and $\Omega_T = \epsilon$ we have that $\hat{\omega}_I = \epsilon$. Thus, the flow in the inner region has a velocity which is entirely set by the boundary layers. Note that there is no viscosity in this formula, but viscosity plays a role in determining the flow. We have completely different behaviour for $\nu = 0$ and in the limit $\nu \to 0$.

22.3 Spin-down of this apparatus

We now want to finally solve the spin-down of our coffee cup. To do so we assume the coffee cup to be a cylinder with a top and a bottom both rotating with angular velocity $\Omega + \epsilon$. At $t = 0$ the angular velocity of the boundaries is reduced to Ω. How long does it take to reach a steady state?

We use the time-dependent formula

$$\frac{\partial u_I}{\partial t} - 2\Omega v_I = -\frac{1}{\rho}\frac{\partial p_I}{\partial x}, \tag{537a}$$

$$\frac{\partial v_I}{\partial t} + 2\Omega u_I = -\frac{1}{\rho}\frac{\partial p_I}{\partial y}. \tag{537b}$$

Then differentiate the first equation with respect to y and the second with respect to x. Subtracting the latter from the former, and using the continuity equation, we obtain the vorticity equation

$$\frac{\partial \hat{\omega}_I}{\partial t} = 2\Omega\frac{\partial w_I}{\partial z}. \tag{538}$$

Now $\hat{\omega}_I$ is independent of z, so

$$\int_0^L \frac{\partial \hat{\omega}_I}{\partial t}dz = L\frac{\partial \hat{\omega}_I}{\partial t} = 2\Omega[w(L) - w(0)]. \tag{539}$$

The velocity is equal and opposite at the two boundaries (flow is leaving both boundary layers), and has magnitude $(\nu/\Omega)^{1/2}\hat{\omega}_I/2$. Thus

$$\frac{\partial \hat{\omega}_I}{\partial t} = -\frac{2\sqrt{\Omega\nu}}{L}\,\hat{\omega}_I, \tag{540}$$

implying that vorticity is decreasing in the interior with a characteristic decay time $L/2\sqrt{\Omega\nu}$. For the coffee cup this gives us a much more realistic spin down time compared to our experiments. In real life we should note that diffusion of the no-slip condition also will play a role, and there will be competition between the two depending on the particular shape of your coffee cup. If you go look at the corresponding flow in Acheson, you can now also understand the deep reason why coffee grounds end up at the centre of your cup.

23 Water waves

If you look out onto the River Charles, the waves that are immediately apparent are surface waves on the water. However, there are many different types of waves in the rivers and oceans, which have profound effects on our surroundings. The most dramatic example is a Tsunami, which is a wave train generated by earthquakes and volcanoes. Before considering these, however, let's begin by considering the motion of a disturbance on the surface of water.

23.1   Deep water waves

The flow is assumed to be inviscid, and as it is initially irrotational it must remain so. Fluid motion is therefore described by the velocity potential $(u, v) = \nabla\phi$, and satisfies Laplace's equation (incompressibility condition)

$$\nabla^2\phi = 0. \tag{541a}$$

The momentum equation becomes

$$\frac{\partial\nabla\phi}{\partial t} + \frac{1}{2}\nabla(\nabla\phi)^2 = -\frac{1}{\rho}\nabla p - \nabla\chi, \tag{541b}$$

where χ is the gravitational potential such that $\mathbf{g} = -\nabla\chi$. This can be integrated to give the unsteady Bernoulli relation

$$\frac{\partial\phi}{\partial t} + \frac{1}{2}(\nabla\phi)^2 + \frac{p}{\rho} + \chi = C(t). \tag{542}$$

Here, $C(t)$ is a time dependent constant that does not affect the flow, which is related to ϕ only through spatial gradients. The surface is $h(x, t)$ and we have the kinematic condition

$$\frac{\partial h}{\partial t} + u\frac{\partial h}{\partial x} = v \tag{543}$$

on $y = h(x, t)$. This simply states that if you choose an element of fluid on the surface, the rate at which that part of the surface rises or falls is, by definition, the vertical velocity. Finally, we require that the pressure be atmospheric, p_0 at the surface. From the unsteady Bernoulli relation we get

$$\frac{\partial\phi}{\partial t} + \frac{1}{2}(u^2 + v^2) + gh = 0 \tag{544}$$

on $h(x, t)$, where we have chosen the constant $C(t)$ appropriately to simplify things.

The equations we have derived so far take account of the effect of gravity on the free surface. We have ignored one important factor, however, which is *surface tension*. It costs energy to create waves, as they have greater surface area than a flat surface. From our earlier work we know that a pressure jump exists across a distorted interface. If p_0 is atmospheric pressure, then the pressure at the fluid surface is

$$p = p_0 - \gamma\frac{\partial^2 h(x, t)}{\partial x^2}. \tag{545}$$

Including surface tension in our pressure condition at the surface, we have that

$$\frac{\partial\phi}{\partial t} + \frac{1}{2}(u^2 + v^2) + gh - \frac{\gamma}{\rho}\frac{\partial^2 h}{\partial x^2} = 0 \tag{546}$$

at $y = h(x, t)$.

We now follow the same procedure as in the last lecture and assume all the variables to be small, so that we can linearise the equations. The linearised system of equations consists of Laplace's equation and the boundary conditions at $y = 0$:

$$\nabla^2 \phi = 0 \tag{547a}$$

$$\frac{\partial h}{\partial t} = \frac{\partial \phi}{\partial y}(x, 0, t), \tag{547b}$$

$$\frac{\partial \phi}{\partial t} = -gh + \frac{\gamma}{\rho}\frac{\partial^2 h}{\partial x^2}, \tag{547c}$$

These conditions arise because we have Taylor expanded terms such as

$$v(x, h, t) = v(x, 0, t) + hv_y(x, 0, t), \tag{548}$$

and then ignored nonlinear terms. We guess solutions of the form

$$\phi = Ae^{ky}\sin(kx - \omega t) \,, \qquad h = \epsilon e^{ky}\cos(kx - \omega t), \tag{549}$$

knowing that these satisfy Laplace's equation (we have ignored terms of the form e^{-ky}, as the surface is at $y = 0$ and we need all terms to disappear as $y \to -\infty$). Putting these into the surface boundary conditions (8) and (9) gives

$$\omega\epsilon = Ak, \tag{550a}$$

$$\omega A = g\epsilon + \frac{\gamma k^2 \epsilon}{\rho}. \tag{550b}$$

Eliminating A we get the dispersion relation

$$\omega^2 = gk + \frac{\gamma k^3}{\rho}. \tag{551}$$

What are the consequences of this relation? On the simplest level we know that the *phase speed*, c, of a disturbance is given by the relation $c = \omega/k$. Thus

$$c^2 = \frac{g}{k} + \frac{\gamma k}{\rho}. \tag{552}$$

The relative importance of surface tension and gravity in determining wave motion is given by the *Bond number* $B_o = \gamma k^2/\rho g$. If $B_o < 1$ then we have *gravity waves*, for which longer wavelengths travel faster. If $B_o > 1$ then we have *capillary waves*, for which shorter wavelengths travel faster. For water, the Bond number becomes unity for wavelengths of about 2 cm, and this accounts for the different ring patterns you can observe when a stone and a raindrop fall into water.

23.2   Properties of the dispersion relation

When a group of waves travels across the surface of water each particular wave crest moves faster than the group as a whole, i.e., if you look closely then wave crests within the disturbance appear to move through it. Why is this? The answer is that different Fourier

components of the disturbance move at different speeds. Such a system is said to be *dispersive*.

If we consider a stone thrown into a pond, and we take the Fourier transform of the disturbance it creates, then that disturbance is described by

$$h(x,t) = \int_{-\infty}^{\infty} \hat{h}_k e^{i[kx - \omega(k)t]} dk. \tag{553}$$

Now the dominant wavelength in the disturbance corresponds to the diameter of the rock d. We shall call the corresponding wavenumber $k_0 = 2\pi/d$. Other wavenumbers will also be excited but we argue that $\hat{h}_k$ will be very small except when k is very near to k_0. Near k_0 we have that

$$\omega(k) \approx \omega(k_0) + \omega'(k_0)(k - k_0). \tag{554}$$

where $\omega' = \partial \omega / \partial k$. Thus

$$h(x,t) = e^{i[k_0 x - \omega(k_0)t]} \int_{-\infty}^{\infty} \hat{h}_k e^{i(k-k_0)[x - \omega'(k_0)t]} dk. \tag{555}$$

The first term of this expression is a travelling wave moving with *p*hase velocity

$$c_p = \frac{\omega(k_0)}{k_0} \tag{556a}$$

The second term is a function only of $[x - \omega'(k_0)t]$. It corresponds to an envelope moving with the *g*roup velocity

$$c_g = \omega'(k_0) \tag{556b}$$

that encloses the travelling wave describes. Thus, the wave packet as a whole moves with c_g. It is a simple step to recognise that if $\omega(k) \neq ck$ then $c_g \neq c_p$. For gravity waves in deep water, we have

$$c_g = \frac{d}{dk}(gk)^{\frac{1}{2}} = \frac{1}{2} c_p. \tag{557a}$$

Alternatively for capillary waves

$$c_g = \frac{d}{dk}(\gamma k^3/\rho)^{\frac{1}{2}} = \frac{3}{2} c_p. \tag{557b}$$

For comparison, the dispersion relation for sound waves, $\omega = ck$, tells us that

$$h(x,t) = \int_{-\infty}^{+\infty} b_k e^{ik(x \pm ct)} dk. \tag{558}$$

So we start with an arbitrary disturbance, and this perturbation just moves without changing shape (although in three dimensions there would be a decay in amplitude due to power conservation).

This is not so for water waves, which have a different dispersion relation, and we can highlight the difference between these two cases by considering the wakes behind an airplane and a boat.

23.3 The wake of an airplane

The equation governing the propagation of a 2D disturbance in air is the wave equation

$$\frac{\partial^2 \phi}{\partial t^2} = c^2 \nabla^2 \phi = c^2 \left(\frac{\partial^2 \phi}{\partial x^2} + \frac{\partial^2 \phi}{\partial y^2} \right), \tag{559}$$

where ϕ is some scalar quantity representing the disturbance (e.g., the velocity potential, the density or the pressure). For an airplane moving through the air we anticipate a solution that is constant in the frame of reference of the plane. Thus

$$\phi(x, y, t) = \tilde{\phi}(x - Ut, y), \tag{560}$$

and we have

$$U^2 \frac{\partial^2 \tilde{\phi}}{\partial x^2} = c^2 \left(\frac{\partial^2 \tilde{\phi}}{\partial x^2} + \frac{\partial^2 \tilde{\phi}}{\partial y^2} \right). \tag{561}$$

Defining the *Mach number* $M = U^2/c^2$, the above equation becomes

$$(1 - M^2) \frac{\partial^2 \tilde{\phi}}{\partial x^2} + \frac{\partial^2 \tilde{\phi}}{\partial y^2} = 0. \tag{562}$$

If $M < 1$ we can make a simple change of variables $X = x/\sqrt{1 - M^2}$ and regain Laplace's equation. Thus everything can be solved using our conformal mapping techniques. However, if $M > 1$ then the original equation now looks like a wave equation, with y replacing t, yielding solutions of the form

$$\tilde{\phi}(x, y) = \Phi(x - y\sqrt{M^2 - 1}) \tag{563}$$

Thus disturbances are confined to a wake whose half angle is given by

$$\tan \theta = \frac{1}{\sqrt{M^2 - 1}}. \tag{564}$$

Only a narrow region behind the plane knows it exists, and the air ahead doesn't know what's coming!

23.4 Flow created by a 1D 'boat'

We now consider a boat moving at constant speed across the surface of water. The motion of the boat generates a disturbance at point (x', t'). The total disturbance generated as the boat progresses is the sum of the individual contributions

$$h(x, t | x', t') = \int dk \, \hat{h}_k e^{i[k(x - x') - \omega(k)(t - t')]} e^{-\Gamma_k (t - t')} \, \Theta(t - t'), \tag{565}$$

where Γ_k describes the attenuation of the disturbance in time. Let us assume the boat's trajectory is given by $x' = Ut'$, corresponding the boat moving from left to right. In this

case, the sum over the history of the boat positions is given by

$$
\begin{aligned}
h(x,t) \;\; &\propto \;\; \int dx' \int dt' \, h(x,t|x',t') \, \delta(x' - Ut') \\
&= \;\; \int dk \, \hat{h}_k e^{i[kx - \omega(k)t] - \Gamma_k t} \int dx' \int dt' \, \hat{h}_k e^{i[-kx' + \omega(k)t']} e^{\Gamma_k t'} \, \Theta(t - t') \, \delta(x' - Ut') \\
&= \;\; \int dk \, \hat{h}_k e^{i[kx - \omega(k)t] - \Gamma_k t} \int_{-\infty}^{Ut} dx' \, \hat{h}_k e^{\{-i[(k - \omega(k)/U] + (\Gamma/U)\}x'} \quad\quad (566)
\end{aligned}
$$

To simplify things a bit, let's focus on spatial perturbations at time $t = 0$

$$
\begin{aligned}
h(x,0) \;\; &\propto \;\; \int_{-\infty}^{\infty} dk \, \hat{h}_k e^{ikx} \int_{-\infty}^{0} dx' \, e^{\{-i[(k - \omega(k)/U] + (\Gamma/U)\}x'} \\
&= \;\; U \int_{-\infty}^{\infty} dk \, \frac{e^{ikx}}{-i[kU - \omega(k)] + \Gamma_k}. \quad\quad (567)
\end{aligned}
$$

Now this integral is dominated by Fourier components for which $kU - \omega(k)$ is close to zero. Thus the biggest contribution comes from the component whose phase velocity matches that of the boat. Let's write

$$
k = k_0 + \delta k , \qquad \omega(k) = \omega(k_0) + \omega'(k_0)\delta k.
$$

To further simplify matters we will assume that $\hat{h}_k$ and Γ_k are well approximated by constants $\hat{h}_{k_0}$ and Γ_{k_0} over the range for which the denominator is small. Then, to a good approximation our integral may be expressed as an integral over δk with infinite limits

$$
\begin{aligned}
h(x,0) \;\; &\propto \;\; U\hat{h}_{k_0} e^{ik_0 x} \int_{-\infty}^{\infty} d(\delta k) \, \frac{e^{i(\delta k)x}}{-iU_0\delta k + \Gamma_{k_0}} \\
&= \;\; i\frac{U}{U_0} h_{k_0} e^{ik_0 x} \oint_C d(\delta k) \, \frac{e^{i(\delta k)x}}{\delta k + i\Gamma_{k_0}/U_0}, \quad\quad (568)
\end{aligned}
$$

where $U_0 = U - \omega'(k_0)$ is the difference between the boat velocity and the group velocity of the Fourier component, and the contour C includes the real k-axis with other contributions vanishing. If we are considering gravity waves, then U_0 is a positive quantity. The integral has to be evaluated around a contour C in the complex plane. For $x > 0$ there is no pole inside the semicircle and the integral is zero. For $x < 0$, in the lower half of the complex plane there is a pole at $\delta k = i\Gamma_{k_0}/U_0$, and it follows that

$$
h(x,0) \propto 2\pi \frac{U}{U_0} \, \hat{h}_{k_0} \, e^{ik_0 x} e^{\Gamma_{k_0} x/U_0} \, \Theta(-x). \quad\quad (569)
$$

Thus we see that the boat is trailed by a wave travelling in the same direction, whose wavelength is such that the boat and wave stay in step (i.e., the phase velocity of the wave matches the boat velocity). In front of the boat the amplitude of the wave is zero.

Note that if we had considered the motion of an insect across the water then we would be considering capillary waves. Then the group velocity is faster than the phase velocity. Thus U_0 would be a negative quantity and our complex integration would have revealed a

wave that *precedes* the insect, with no disturbance behind it. As mentioned at the start, this analysis is applicable to the steady flow past an obstacle. In this case, if U is the steady stream velocity we can now understand why we see a steady pattern of capillary waves upstream from the object and a steady pattern of gravity waves downstream from the object.

Finally, on open water, the waves created by a boat can move in two dimensions. To describe this, our 1D treatment needs to be extended to account for the V-shaped wake behind a boat, also known as the *Kelvin wedge*. In 2D, the disturbance generated by the boat is

$$h(\boldsymbol{x}, t | \boldsymbol{x}', t') = \int d\boldsymbol{k} \; \hat{h}(\boldsymbol{k}) e^{i\boldsymbol{k}(\boldsymbol{x}-\boldsymbol{x}')} e^{i\omega(\boldsymbol{k})(t-t')} e^{\Gamma_k(t-t')}. \tag{570}$$

As before, the only waves that contribute significantly are those whose phase velocity in the direction of motion of the boat matches the speed of the boat. If the waves are gravity waves, then the relevant $\boldsymbol{k}$-vectors are those with inclination α and magnitude k_α satisfying

$$k_\alpha = \frac{g}{U^2 \sin^2 \alpha}. \tag{571}$$

Turning back to our dispersion relation for water waves, it can readily be shown that the minimum phase velocity is

$$c = \left(\frac{4g\gamma}{\rho} \right)^{1/2}, \tag{572}$$

and this occurs for the wavenumber $k = \sqrt{\rho g/\gamma}$.

24 Solitons

In the previous section, we considered *dispersive* waves characterized by time-dependent change (e.g., spreading) of the wave form. Now, we will study another interesting class of *non-dispersive* waves called *solitons*.

24.1 History

The occurrence of solitons were first reported by the Scottish engineer and naval architect John Scott Russell, who described his observation as follows:

"I was observing the motion of a boat which was rapidly drawn along a narrow channel by a pair of horses, when the boat suddenly stopped –not so the mass of water in the channel which it had put in motion; it accumulated round the prow of the vessel in a state of violent agitation, then suddenly leaving it behind, rolled forward with great velocity, assuming the form of a large solitary elevation, a rounded, smooth and well-defined heap of water, which continued its course along the channel apparently without change of form or diminution of speed. I followed it on horseback, and overtook it still rolling on at a rate of some eight or nine miles an hour [14km/h], preserving its original figure some thirty feet [9m] long and a foot to a foot and a half [30-45cm] in height. Its height gradually diminished, and after a chase of one or two miles I lost it in the windings of the channel. Such, in the month of August 1834, was my first chance interview with that singular and beautiful phenomenon which I have called the Wave of Translation."

Intrigued by his observation, Russell built an smaller-cases channel in his backyard and performed the first systematic studies of solitary water waves.

Another class of solitons was discovered by Enrico Fermi, John Pasta, Stanislaw Ulam (FPU) and Mary Tsingou in 1953. FPU had formulated as simple nonlinear chain model to understand better the thermalization processes (dispersion of energy) in solids. Their model was implemented numerically by Tsingou in what can be considered the first application of computers tin physics. Remarkably, instead of showing the expected thermalization, the numerical results predicted the existence long-lived non-dispersive excitations, illustrating a previously unknown transport mode.

Since then, solutions have been intensely studied as models of elementary particles and they have also been utilized in electronics and fibre optics.

24.2 Korteweg-de Vries (KdV) equation

A continuum model for solitary waves in water was first introduced by Boussinesq in 1871. The theory was developed further by Lord Rayleigh in 1876 and by Korteweg and de Vries (KdV) in 1895. According to their theory, the spatio-temporal evolution of weakly nonlinear shallow water waves is described by

$$\partial_t h = \frac{3}{2}\sqrt{\frac{g}{l}}\,\partial_x \left(\frac{h^2}{2} + \frac{2}{3}h + \frac{\sigma}{3}\partial_x^2 h \right) \tag{573}$$

where $h(t,x)$ is the surface profile of the wave and

$$\sigma = \frac{\ell^3}{3} - \frac{\gamma\ell}{\rho g} \tag{574}$$

with ℓ the channel height, γ the surface tension, g the gravitational acceleration and ρ the mass density.

Mathematical studies of the KdV-solitons typically focus on the rescaled version

$$\partial_t \phi + \partial_x^3 \phi + 6\phi\partial_x\phi = 0. \tag{575}$$

To find an exact solution, we make the ansatz

$$\phi(t,x) = f(x - ct - a) = f(X). \tag{576}$$

Insertion then gives

$$-cf' + f''' + 3(f^2)' = 0. \tag{577}$$

where $f' = df/dX$. We next integrate once to obtain

$$-cf + f'' + 3f^2 = A. \tag{578}$$

This equation can be rewritten in the Newtonian form

$$\frac{d^2 f}{dX^2} = -\frac{d\Phi}{df} \tag{579a}$$

111

with potential

$$V(f) = -Af - \frac{c}{2}f^2 + f^3. \tag{579b}$$

This equation possesses an explicit solution with $f(X) = 0$ as $X \to \pm\infty$, given by

$$\phi(t,x) = \frac{c}{2}\text{sech}^2\left[\frac{\sqrt{c}}{2}(x - ct - a)\right]. \tag{580}$$

This solution describes a right-moving solitary wave-front of speed c.

In 1965, Zabesky and Kruskal showed how one can derive this equation in the continuum limit from the FPU model. They argued that two KdV solitons could collide and penetrate each other without exchanging energy. This explains intuitively why the FPU chain model does not lead to thermalization. Miura *et al.*[28] provided a general rigorous argument by showing that the KdV equation possesses an infinite number of non-trivial integrals of motion.

---

[28]Journal of Mathematical Physics 9:1204-1209, 1968

18.354J / 1.062J / 12.207J Nonlinear Dynamics II: Continuum Systems
Spring 2015